

ERRATUM: PAIR PRODUCTION AND BREMSSTRAHLUNG OF CHARGED LEPTONS*

[Rev. Mod. Phys. 46, 815 (1974)]

Yung-Su Tsai

Stanford Linear Accelerator Center
Stanford University, Stanford, California 94305

- Page 820: Eq. (3.3), $n(n^2+z)$ should read $1/[n(n^2+z)]$.
Eq. (3.5), $-\frac{4lx(1-x)}{(1+l)^4}$ should read $+\frac{4lx(1-x)}{(1+l)^4}$.
- Page 822: Eq. (3.18), $(1/6)(1+B^2)^2$ should read $(1/6)/(1+B^2)^2$.
Eq. (3.19), $-4B^2 \ln(1+B^2) + (4/3)(1+B^2) - (1/6)(1+B^2)^2$
should read
 $-4B^{-2} \ln(1+B^2) + (4/3)/(1+B^2) - (1/6)/(1+B^2)^2$.
Eq. (3.25), $(1/6)(1+C^{-2})$ should read $(1/6)/(1+C^{-2})$.
- Page 826: Table III.5, $\sigma(\infty)$ for H should read 20.56 mb instead
of 20.73 mb.
- Page 829: Eq. (3.76), $\left(1 + \frac{b}{c}\right)$ should read $\left(1 - \frac{b}{c}\right)$.
- Page 834: Eq. (4.12), $\frac{1}{k} \frac{\dots}{k[\dots]}$ should read $\frac{1}{k} \frac{\dots}{[\dots]}$.
- Page 838/839: Table V.1 (C) and (D), the entries in the first column
are momentum p in GeV not $p\theta/m$.
- Page 848: 5. Sample atomic form factors should read
5. Simple atomic form factors
- Page 849: Eq. (B55), Q should read Q^2 .

Programming error: In the computer program for evaluating the contribution from the inelastic excitation of the proton, the integration routine with respect

*Work supported by the Energy Research and Development Administration.

to m_f^2 in Eq. (2.7) was inadvertently carried out in such a way that finer mesh was used for larger m_f^2 instead of the other way. This results in underestimating the cross sections in all the entries labeled "proton inelastic" in Tables V.1, V.2, V.3, V.4, and V.5. The corrected versions for these entries are given below.

I would like to thank Allen Eisner of UCSB, Hobey DeStaebler of SLAC, Jack Smith of Stony Brook, and C. M. Hoffman of Los Alamos Scientific Laboratory for kindly pointing out some of the above errors.

TABLE V. 1. $d\sigma/d\Omega dp$ for photoproduction of muon ($\text{cm}^3/\text{GeV}/\text{sr}$).

$p\theta/m$	Proton Inelastic	Proton Inelastic	$p(\text{GeV})$	Proton Inelastic	$p(\text{GeV})$	Proton Inelastic
(A) $k=20, m=0.1056$	(B) $k=200, m=0.1056$	(C) $k=20, m=0.1056$	(D) $k=200, m=0.1056$			
	P=4.0	P=40.0		$\theta=0.0$	$\theta=0.0$	
0	1.138D-31	1.331D-30	2	2.842D-32	20	3.277D-31
0.5	8.348D-32	9.853D-31	4	1.138D-31	40	1.331D-30
1.0	4.559D-32	5.500D-31	6	2.488D-31	60	3.004D-30
2.0	1.456D-32	1.925D-31	8	4.278D-31	80	5.373D-30
4.0	2.473D-33	4.311D-32	10	6.461D-31	100	8.502D-30
7.0	3.090D-34	8.377D-33	12	8.966D-31	120	1.249D-29
10.0	4.996D-35	2.271D-33	14	1.161D-30	140	1.741D-29
15.0	2.193D-36	4.020D-34	16	1.383D-30	160	2.314D-29
20.0	2.002D-38	1.010D-34	18	1.356D-30	180	2.828D-29
	P=8.0	P=80.0		$\theta=0.1$	$\theta=0.1$	
0	4.278D-31	5.373D-30	2	4.118D-33	20	2.423D-35
0.5	3.028D-31	3.828D-30	4	2.928D-33	40	2.141D-36
1.0	1.593D-31	2.032D-30	6	1.733D-33	60	2.215D-37
2.0	5.196D-32	7.014D-31	8	1.020D-33	80	6.204D-39
4.0	9.707D-33	1.610D-31	10	6.120D-34	100	0.0
7.0	1.412D-33	3.180D-32	12	3.576D-34	120	0.0
10.0	2.804D-34	8.859D-33	14	1.756D-34	140	0.0
15.0	2.372D-35	1.689D-33	16	4.363D-35	160	0.0
20.0	1.477D-36	4.636D-34	18	0.0		
	P=12.0	P=120.0		$\theta=0.2$	$\theta=0.2$	
0	8.966D-31	1.249D-29	2	6.618D-34	20	1.078D-37
0.5	6.363D-31	8.911D-30	4	2.160D-34	40	0.0
1.0	3.378D-31	4.756D-30	6	6.896D-35	60	0.0
2.0	1.129D-31	1.655D-30	8	2.208D-35	80	0.0
4.0	2.193D-32	3.764D-31	10	5.569D-36	100	0.0
7.0	3.357D-33	7.400D-32	12	5.355D-37	120	0.0
10.0	6.952D-34	2.093D-32	14	0.0		
15.0	6.158D-35	4.121D-33	16	0.0		
20.0	3.935D-36	1.161D-33	18	0.0		
	P=16.0	P=160.00				
0	1.383D-30	2.314D-29				
0.5	1.024D-30	1.721D-29				
1.0	5.759D-31	9.726D-30				
2.0	1.977D-31	3.445D-30				
4.0	3.769D-32	7.509D-31				
7.0	5.396D-33	1.450D-31				
10.0	9.682D-34	4.086D-32				
15.0	4.810D-35	7.867D-33				
20.0	4.932D-37	2.121D-33				

TABLE V.2. $d\sigma/d\Omega dp$ for photoproduction of heavy leptons ($\text{cm}^2/\text{GeV}/\text{sr}$).

$p\theta/m$	Proton Inelastic		Proton Inelastic
(A) $k=200, m=4.0$			(B) $k=200, m=6.0$
P=40 GeV			
0	8.458D-37		7.255D-39
0.2	7.509D-37		4.991D-39
0.4	5.206D-37		1.400D-39
0.6	2.762D-37		8.436D-41
0.8	1.084D-37		0.0
1.0	2.906D-38		0.0
P=80 GeV			
0	4.827D-36		1.771D-37
0.2	4.476D-36		1.507D-37
0.4	3.509D-36		8.756D-38
0.6	2.275D-36		3.022D-38
0.8	1.215D-36		4.847D-39
1.0	5.353D-37		1.856D-40
P=120 GeV			
0	1.029D-35		3.545D-37
0.2	9.529D-36		3.000D-37
0.4	7.452D-36		1.716D-37
0.6	4.813D-36		5.758D-38
0.8	2.558D-36		8.702D-39
1.0	1.118D-36		2.689D-40
P=160 GeV			
0	1.011D-35		4.488D-38
0.2	8.925D-36		2.826D-38
0.4	6.081D-36		5.347D-39
0.6	3.128D-36		6.358D-42
0.8	1.166D-36		0.0
1.0	2.859D-37		0.0

TABLE V.3. $d\sigma/dp$ (cm^2/GeV).

p(GeV)	Proton Inelastic	p(GeV)	Proton Inelastic	p(GeV)	Proton Inelastic	p(GeV)	Proton Inelastic
m=0.1056 GeV k=20 GeV		m=0.1056 GeV k=200 GeV		m=4.0 GeV k=200 GeV		m=6.0 GeV k=200 GeV	
	10^{-34}		10^{-35}		10^{-38}		10^{-40}
1.99	5.049	20.0	7.024	19.5	0.079	19.2	0.0
5.97	4.832	60.0	6.514	58.5	1.407	57.5	3.029
9.95	4.479	100.0	6.370	97.5	1.811	95.8	7.211
13.93	4.410	140.0	7.031	136.5	1.326	134.2	3.359
17.90	3.524	180.0	7.657	175.5	0.098	172.5	0.0

TABLE V.4. Total heavy lepton production cross section (cm^2).

k	Proton Inelastic	Be total
m=0.105	10^{-32}	10^{-30}
20	0.849	1.795
40	1.060	2.276
100	1.271	2.817
200	1.349	3.026
m=0.5	10^{-33}	10^{-32}
20	0.430	1.733
40	0.764	3.190
100	1.274	5.668
200	1.638	7.764
m=1.0	10^{-34}	10^{-32}
20	0.322	0.087
40	0.959	0.247
100	2.327	0.646
200	3.598	1.080
m=2.0	10^{-35}	10^{-34}
40	0.267	0.644
100	2.002	3.986
200	4.627	9.600
m=4.0	10^{-36}	10^{-35}
100	0.169	0.400
200	1.886	3.415
m=6.0	10^{-38}	10^{-36}
100	0	0
200	5.123	1.138

TABLE V.5. Total heavy lepton production cross section (cm^2) from proton.

Photon Energy GeV	Proton Elastic	Proton Inelastic	Proton Total
m=5			
500	4.043D-36	3.208D-36	7.251D-36
1000	9.592D-36	7.577D-36	1.733D-35
1500	1.404D-35	1.078D-35	2.482D-35
2000	1.767D-35	1.324D-35	3.091D-35
m=10			
500	2.111D-38	1.241D-38	3.352D-38
1000	2.702D-37	2.184D-37	4.886D-37
1500	6.325D-37	5.361D-37	1.169D-36
2000	1.014D-36	8.625D-37	1.877D-36
m=15			
1000	4.563D-39	2.801D-39	7.364D-39
1500	3.528D-38	2.658D-38	6.186D-38
2000	8.860D-38	7.163D-38	1.602D-37
m=20			
1000	4.860D-43	1.608D-43	6.468D-43
1500	6.616D-40	3.855D-40	1.047D-39
2000	5.328D-39	3.705D-39	9.033D-39

PAIR PRODUCTION AND BREMSSTRAHLUNG OF CHARGED LEPTONS*†

Yung-Su Tsai

Stanford Linear Accelerator Center
Stanford University, Stanford, Calif. 94305

ABSTRACT

Photo pair productions of electrons, muons and heavy leptons and bremsstrahlung of electrons and muons are reviewed. Atomic and nuclear form factors necessary for these calculations are discussed. Straggling of electrons in matter and other effects due to finite target thickness are considered. Tables of radiation lengths of all materials and the energy dependence of photon absorption coefficients of many materials presented. Problems associated with production of particles by photon and electron beams discussed.

(Submitted to Rev. of Mod. Physics)

* Work supported by the U. S. Atomic Energy Commission

† This paper supersedes SLAC-PUB-1105, "Photoproduction of Electrons, Muons and Heavy Leptons," Kwang Je Kim and Yung-Su Tsai, Sept. 1972.

TABLE OF CONTENTS

- I. Introduction
- II. Pair Production Cross Section by Born Approximation
- III. Approximate Expressions
 - A. Electron Pair Production
 - 1. Arbitrary Form Factors
 - 2. Hydrogen and Helium Atoms
 - 3. Checking the Accuracy of Bethe's Approximations
 - 4. Thomas-Fermi Atoms
 - 5. Total Pair Production Cross Section
 - B. Radiation Length of Materials
 - C. Muon Pair Production
 - D. Energy-Angle Distribution of Bremsstrahlung
 - E. Bremsstrahlung in Colliding Beam Experiment
 - F. $e^+ + e^- \rightarrow 2\gamma, 3\gamma$
 - G. Muon Bremsstrahlung
- IV. Effects Due to Finite Target Thickness
 - A. Straggling of an Electron due to Bremsstrahlung
 - B. Thin Target Bremsstrahlung
 - C. Approximate Expression for Thick Target Bremsstrahlung
 - D. Production of Particles Using a Photon Beam
 - E. Production of Particles Using an Electron Beam
 - F. Production by Virtual Photons
- V. Production of Heavy Leptons and Muons (Numerical Examples)
 - A. Kinematics
 - B. Energy-Angle Distribution $d\sigma/d\Omega dp$

C. Energy Distribution $d\sigma/dp$

D. Total Cross Sections

VI. Acknowledgments

Appendix A. Minimum Momentum Transfer

Appendix B. Atomic and Nuclear Form Factors

1. Atomic Form Factors

A. Hydrogen Atom ($Z = 1$)

B. Helium Atom ($Z = 2$)

C. Light Z elements ($Z = 3$ to $Z = 7$)

D. Thomas Fermi Model ($Z \geq 5$)

E. Simple Atomic Form Factors

2. Elastic Form Factors of Nucleons

3. Elastic Form Factors of Nuclei

4. Inelastic Nuclear Form Factors

5. Inelastic Nucleon Form Factors

I. INTRODUCTION

The work on this paper started about ten years ago when Stanford Linear Accelerator Center was still under construction. At that time like any other new high energy physics laboratory, people were concerned with problems such as what would be the yields of muons, pions, K mesons, antiprotons etc. and also whether any new particles such as W bosons and heavy leptons could be discovered by the new machine. In the electron machine these particles are produced by the bremsstrahlung beam which in turn is produced by the electron. Hence one has to know accurately the properties of the bremsstrahlung beam in a fairly thick target. The pair production is related to the bremsstrahlung problem by a substitution rule, thus the electron pair production cross section can be calculated trivially once we know how to calculate the bremsstrahlung by electrons. Muon and heavy lepton pair productions were also estimated at that time. For production near the forward angle, the electron pair production involves only the atomic form factors, whereas in the muon and heavy lepton productions, nuclear form factors must be taken into consideration. As the laboratory began to operate and experiments became more precise, many of these calculations also became more refined and efficient. For example in order to do precise measurements in the photoproduction experiments, it is desirable to know the photon spectrum to within 1 percent level. Also in order to do inelastic electron scattering accurately, one likes to know the straggling function of the electron in the target to within 1%. These will be discussed in Section IV.

Heavy lepton has never been discovered. Recently the interest in the possible existence of heavy lepton gained a new impetus, because in some versions of the gauge theory, the heavy leptons are required to make unified

theory of weak and electromagnetic interactions finite. (Georgi and Glashow¹ 1972 , Bjorken and Llewellyn Smith² 1972). These gauge theories do not affect the calculation of heavy lepton production by pair production. The decay modes of heavy leptons have been considered by many authors. The most complete pre-gauge theory version was given by Tsai³ (1971) and the post gauge theory version was given by Bjorken and Llewellyn Smith² (1972). The two versions are essentially identical except that in the latter, there is a possibility that heavy neutrinos also exist in nature and if the mass of the heavy neutrino is lighter than that of charged heavy leptons, additional decay modes into these heavy neutrinos must be included. The readers should refer to these two papers and also a review paper by M. Perl⁴(1972) for details of the present status, both experimental and theoretical, concerning heavy leptons.

The objectives of this paper are two: (1) to put together in one place all the useful formulas pertaining to the bremsstrahlung and the pair production of electrons and muons and the associated phenomena of electromagnetic shower theory useful in high energy physics experiments. (2) To obtain the production cross section of heavy leptons to assist in the discovery of these new particles. The underlying physical principles involved in this paper are not controversial and to a large extent well known. However this paper is strictly speaking not a review paper, because rather than reviewing the existing literature, we have concentrated in making the contents of this paper self-contained and whenever possible we have tried to present new results which are either more accurate or simpler to handle than what exist in the literature.

The table of contents shows the materials to be discussed in this paper. They are arranged in order to give a logical development of the theory. However from practical point of view, the subject matter can be divided into three

obvious parts: 1. Electron, 2. Muon and 3. Heavy lepton. Let us describe briefly the major topics discussed in each part:

1. Electron The part dealing with bremsstrahlung and pair production of electron is of the greatest practical importance because an electron loses its energy so easily by bremsstrahlung in passing through a medium and also at high energies a photon gets absorbed in a medium mainly by pair production of electrons. This part is useful to those experimentalists who have to deal with high energy electrons or photons in any part of their experiment. For this purpose we give a). Table of radiation lengths of all materials (Table III. 4), b). Energy dependence of total pair production cross sections for many commonly used materials (Table III. 3), c). Energy-angle distribution, $d\sigma/d\Omega dp$, energy distribution $d\sigma/dp$ for pair production from hydrogen and helium atoms (Section III A 2), from Li and Be atoms [Eqs. (III. 44) through (III. 49)], and for all atoms heavier than Be [Eqs. (III. 38) through (III. 41)], Eqs. (III. 79), (III. 80) and (III. 82). d). The bremsstrahlung spectrum from a target of finite thickness is given by Eqs. (IV. 11) and (IV. 12). These expressions are useful for photo-production experiments when ordinary bremsstrahlung beam is used. e). Formulas for production of particles using an electron beam directly on the target are considered in Sections IV E and IV F. f). The photons from the annihilation of the positron by an atomic electron, $e^+ e^- \rightarrow 2\gamma, 3\gamma$, are discussed in Section III F. g). Bremsstrahlung in the colliding beam experiment $e + e \rightarrow e + e + \gamma$ is treated in Section III E. h). Straggling of an electron in medium due to bremsstrahlung is given in Section IV A, which is very important in the external photon correction to the electron scattering experiment or any other experiment in which an electron is involved. i). Production of particles using a photon beam is discussed in Section IV D.

2. Muon This part is useful for those people who want to estimate the muon flux from an electron machine near the target. In the proton machine the muon flux comes mainly from the decay of pions which are produced by the proton impinging on a target. In the electron machine, usable muon source comes mostly from photopair production. Even in the electron machine, there are more pions produced than muons (see SLAC Users Handbook⁵ Section C), hence at a distance of one decay length from the target, there will be more muons from pion decay than photo pair produced muons. Numerical examples of angular distributions $d\sigma/d\Omega dp$, momentum distributions $d\sigma/dp$ and the total cross sections σ are given in Section V. To obtain the yield of muon flux per incident electron on a target of T radiation lengths, one may use Eq. (IV.13) and the appropriate expression for $d\sigma/d\Omega dp$. For small angles, the process is dominated by the coherent production, hence $d\sigma/d\Omega dp$ given by Eq. (III.5) with X given by Eq. (III.76) may be used. For large angles incoherent production from nucleons in the nucleus as well as the production accompanied by meson production must be included. Energy loss due to muon bremsstrahlung is discussed in Section III G.

3. Heavy Lepton In Section V, we give numerical examples of the energy angle distribution $d\sigma/d\Omega dp$, the energy distribution $d\sigma/dp$ and, the total cross section σ for the production of heavy leptons. We hope these numerical examples will help experimentalists in designing experiments to discover the existence of heavy leptons.

Since we are dealing with one photon exchange processes, the cross section is dominated by the kinematical region where the momentum transfer is small. Expressions for the minimum momentum transfer for various processes are derived in Appendix A. Appendix B deals with atomic form factors, nuclear form factors and meson production form factors used in our calculation.

History

Even though we know now that the pair production and the bremsstrahlung processes are theoretically closely related, the bremsstrahlung process was recognized and studied much earlier than the pair production process. This is because the bremsstrahlung process can be qualitatively understood using only the classical Maxwell equations (see for example, Panofsky and Phillips⁶, 1955), whereas for the pair production process it is necessary to use the Dirac equation. The bremsstrahlung process was studied as early as 1923 (Kramers⁷). The Dirac equation was invented in 1928 (Dirac⁸). The positron was discovered in 1932 (Anderson⁹). The first calculations on the pair production were by Nishina and Tomonaga¹⁰ (1933), Oppenheimer and Plesset¹¹ (1933), and Heitler and Sauter¹² (1933). Bethe and Heitler¹³ (1934) treated both the bremsstrahlung and the pair production relativistically using the Born approximation, in which the screening of the nuclear coulomb field was properly taken into account. Wheeler and Lamb¹⁴ (1939, 1956) treated the same phenomena in the field of atomic electrons. Experimentally, the productions in the nuclear coulomb field and the electron field always occur together, hence two effects must be combined in order to make comparison with experiments. When the atomic number Z is large, the correction to the one photon exchange mechanism must be included and this was done by Bethe and Maximon¹⁵ (1954), Davies, Bethe and Maximon¹⁶ (1954), and Olsen¹⁷ (1955). It should be noted that in Bethe and Maximon,¹⁵ it was erroneously stated that the Coulomb correction affects only the pair production but not the bremsstrahlung. This error was corrected by Olsen¹⁷ (1955). The radiative corrections to bremsstrahlung and pair production were treated by Mork and Olsen¹⁸ (1965) and an experiment was carried out by Schulz and Lutz¹⁹ (1968) to confirm their calculations. The polarizations of electrons and

photons in the pair production and bremsstrahlung of electrons were calculated by Olsen and Maximom²⁰ (1959). There are many review papers on the subject of pair production and bremsstrahlung of electrons. The most useful ones are Rossi²¹ (1952), Bethe and Ashkin²² (1952), Motz, Olsen and Koch²³ (1959, 1969).

Despite the abundance of literatures available on the pair production and the bremsstrahlung of electrons, we have included these subjects in this paper for the following reasons: 1. The original papers of Bethe-Heitler¹³ (1934) and Wheeler and Lamb¹⁴ (1939) were written when there was no electronic computer, hence the atomic form factors and integrations with respect to them were treated crudely and the results were presented only in graphic forms which are difficult to read accurately. Also in Bethe-Heitler only the Thomas-Fermi atom was treated which is not applicable to low Z elements. 2. In practice, pair production and bremsstrahlung take place in a medium of finite thickness (except in the colliding beam experiments), the effect of which must be taken into account in actual applications of the theory.

The muon was discovered not as the result of a single observation, but rather the conclusion of a long series of experimental and theoretical investigations in the cosmic rays. A high energy muon is characterised by its deep penetrating power. Unlike electrons and photons, it does not produce electromagnetic shower because of its heavy mass. Also unlike all hadrons it does not have strong interactions, hence its energy loss is practically all due to ionizations only. As early as 1932 (Rossi²⁴ 1932), this deep penetrating component was seen in the cosmic ray experiment. The definitive identification of muon came in 1937 from the observations of Neddermeyer and Anderson²⁵ (1937) and those of Street and Stevenson²⁶ (1937). The $\mu \rightarrow e$ decay was discovered by Williams and Roberts²⁷ (1940) and the $\pi \rightarrow \mu$ decay was discovered by Lattes, Occhialini and Powell²⁸ (1947). The photoproduction of muon pair was observed much later. In 1956,

Masek and Panofsky²⁹ succeeded in separating one member of the pair from a large background of pions and electrons in the photoproduction. In 1962 Aberigi-Quaranta et al³⁰ observed muon pair in coincidence and confirmed the Bethe-Heitler formula within 5% accuracy.

The most accurate test of quantum electrodynamics using the electron pair production was carried out by Ashbury et al³¹ (1967) and the muon pair production by Hayes et al (1970). The results of these experiments show that the Bethe-Heitler formula is correct even when the lepton propagators are far off the mass shell in the space like region. The test of QED using the wide angle bremsstrahlung of an electron was carried out by Sieman et al³³ (1969) and that of a muon by Liberman et al³⁴ (1969). Neither of these two experiments saw any deviation from the Bethe-Heitler formula. The results of these experiments can be regarded as indicating the absence of the kind of heavy leptons which decays into an electron and a photon or a muon and a photon. If such heavy leptons exist, they must show up in the lepton propagator, thus altering the prediction of Bethe-Heitler theory (Low³⁵ 1965). For this reason we shall assume that heavy leptons, if they exist, will not decay into $\gamma + e$ or $\gamma + \mu$, but decay weakly into $e + \nu + \bar{\nu}$, $\mu + \nu + \bar{\nu}$, $\pi + \nu$, $k + \nu$, $p + \nu$ etc. (Tsai³ 1972).

The existence of an electron is essential for all the chemical bindings and chemical interactions. The existence of pions is essential for nuclear bindings (Yukawa³⁶ 1935). The existence of muon was not predicted before its discovery and nobody knew why it should exist, in particular nobody has an explanation why its mass is $m_{\mu} \sim 207 m_e$, which is slightly less than the lightest hadron, pion. Since nobody understands why muon should exist, there have been speculations that there might be other similar particles in nature yet to be discovered (Zel'dovich³⁷ 1962). Everytime a new high energy accelerator is built, the

discovery of heavy lepton is usually one of its hoped for objectives. As mentioned previously, recently the search for the existence of heavy lepton received a new impetus because their existence may be required to unify the weak and electromagnetic interactions and also make the higher order weak interaction finite.

Heavy leptons, if they exist, can be produced in many ways besides the pair production. Which way is the most advantageous depends upon the quantum number and the mass of the heavy lepton as well as the energy and the intensity of various beams available from accelerators. These problems are reviewed by Perl⁴ (1972) hence we shall not go into detail here. Since μe coincidence will probably be the most direct proof of heavy lepton pair (or W^\pm pair) production, there is some practical reason why we have treated pair productions of electron, muon and heavy lepton in a single paper.

II. PAIR PRODUCTION CROSS SECTION BY BORN APPROXIMATION

In this section, we give the cross section for $\gamma + Z \rightarrow \ell^+ \ell^- + \text{anything}$ via the Bethe-Heitler mechanism shown in Fig.II.1. The cross sections for the bremsstrahlung emission can be obtained from those for the pair production and this is done in Section III D. We use the symbol k to represent the four momentum of the incident photon and also the energy of the photon in the laboratory system. Whenever it appears in the dot product it represents a four momentum, otherwise it is the energy in the laboratory system. The symbol p represents the four momentum of ℓ^- and also the absolute value of its three dimensional momentum in the laboratory system. E is the energy of ℓ^- in the laboratory system. p_+ is the four momentum of ℓ^+ and E_+ is its energy in the laboratory system. m is the mass of ℓ^+ or ℓ^- . p_i and m_i are the four momentum and the mass respectively of the initial target system and p_f and m_f are corresponding quantities for the final state of the target. The four momentum transfer

to the target system is denoted by $q \equiv k - p - p_+ = p_f - p_i$. Bethe and Heitler¹³ (1934) treated a special case in which the target particle is an infinitely heavy point-like and spinless nucleus whose coulomb field is screened by atomic electrons. They did not include the atomic excitation of the target which was later considered by Wheeler and Lamb (1939).¹⁴ While these treatments by Bethe and Heitler¹³ combined with the work of Wheeler and Lamb¹⁴ adequately describe the pair production of electrons at high energies and small angles, they are not adequate to describe the pair production of particles with mass of muons or heavier, because the effects of nuclear form factors and the recoil of the target system must be included when heavy particles are produced. Even in the electron pair production the nuclear form factors and the recoil must be taken into account if the production angle is large. In fact when the transverse momentum of the particle produced is much larger than the mass, the cross section is nearly independent of the mass of the particle produced. Drell and Walecka (1964)³⁸ generalized the result of Bethe and Heitler to deal with a target of arbitrary mass, spin and form factors and arbitrary final states. This generalization was made possible by an earlier observation due to Bjorken (1960) and others³⁹ that in any space-like one photon exchange process, as long as the target particle is unpolarized and the final state of the target system is left unmeasured, the only things one has to know about the target system are the structure functions $W_1(q^2, \nu)$ and $W_2(q^2, \nu)$ of the electron scattering defined by

$$\begin{aligned}
 W_{\mu\nu} &\equiv M_i^{-2} (p_{i\mu} - q_\nu (p_i \cdot q) / q^2) (p_{i\nu} - q_\mu (p_i \cdot q) / q^2) W_2 \\
 &\quad - (q_{\mu\nu} - q_\mu q_\nu / q^2) W_1 \\
 &\equiv \sum_f \langle p_i | j_\mu(0) | f \rangle \langle f | j_\nu(0) | p_i \rangle (2\pi)^3 \delta^4(q + p_i - p_f) e^{-2},
 \end{aligned}$$

where the spin average over the initial state p_i is assumed. The state $|p_i\rangle$ is normalized such that the factor $(m/E)^{1/2} (2\pi)^{-3/2}$ has been taken out from the matrix elements. With this normalization, the matrix element, the phase space and the incident flux are all separately covariant. The cross section for $\gamma + Z \rightarrow \ell^+ \ell^- + \text{anything from the mechanism shown in Fig. II. 1}$ can then be written as

$$d\sigma = e^6 \frac{m_i}{4(k \cdot p_i)} \frac{d^3 p}{E} \frac{d^3 p_+}{E_+} \frac{1}{(2\pi)^5} \frac{1}{q} (L^{\mu\nu} W_{\mu\nu}) \quad (\text{II. 1})$$

where

$$L^{\mu\nu} = - \sum_{\substack{\text{photon} \\ \text{polarization}}} \frac{\text{Tr}}{4} (-\not{p}_+ + m) \left(\not{\epsilon} \frac{1}{-\not{p}_+ + \not{k} - m} \gamma^\mu + \gamma^\mu \frac{1}{\not{p} - \not{k} - m} \not{\epsilon} \right) \\ \times (\not{p} + m) \left(\not{\epsilon} \frac{1}{\not{p} - \not{k} - m} \gamma^\nu + \gamma^\nu \frac{1}{-\not{p}_+ + \not{k} - m} \not{\epsilon} \right) \quad (\text{II. 2})$$

After taking the trace and contracting the tensors, we obtain

$$- L^{\mu\nu} W_{\mu\nu} = W_2(q^2, m_f^2) \left[\frac{H}{(p_+ \cdot k)^2} + \frac{B}{(p_+ \cdot k)} + C + D(p_+ \cdot k) \right] \\ + W_1(q^2, m_f^2) \left[\frac{H'}{(p_+ \cdot k)^2} + \frac{B'}{(p_+ \cdot k)} + C' + D'(p_+ \cdot k) \right], \quad (\text{II. 3})$$

where

$$H = -m^2 \left\{ \frac{1}{2} q^2 (1 - 2E/m_i) + 2E^2 + 2E\Delta \right\}, \\ B = -\frac{2}{k \cdot p} \left\{ (m^2 - q^2/2) \left[2E(E - k) + \frac{1}{2} q^2 ((k - 2E)/m_i + 1) + (2E - k) \Delta \right] \right. \\ \left. - \frac{1}{2} q^2 k^2 \right\} + (q^2/m_i) (m_i + E - k - \frac{1}{2} q^2/m_i) - 2\Delta(\Delta - k + E - q^2/m_i) + k \cdot p,$$

$$C = - \frac{m^2}{(k \cdot p)^2} \left\{ 2(k - E - \Delta + q^2/2m_i)(k - E) + q^2/2 \right\} \\ + \frac{1}{k \cdot p} \left\{ q^2(1 - E/m_i) + 2E\Delta \right\} ,$$

$$D = 1/(k \cdot p) ,$$

$$H' = m^2(2m^2 + q^2) ,$$

$$B' = - \left[(q^4 - 4m^2)/k \cdot p + 2q^2 + 2k \cdot p + 4m^2 \right] ,$$

$$C' = m^2(2m^2 + q^2)/(k \cdot p)^2 - 2(2m^2 + q^2)/(k \cdot p) ,$$

$$D' = -2/(k \cdot p) ,$$

$$\Delta = (m_f^2 - m_i^2)/(2m_i) \quad \text{and} \quad q^2 = (k - p - p_+)^2 .$$

k and E are the laboratory energies of the incident photon and ℓ_- respectively.

In order to obtain $d\sigma/dp d\Omega$ we have to integrate with respect to d^3p_+ . It is convenient to do this in the coordinate system where $U = p_+ + p_f$ is at rest and $\vec{k} - \vec{p}$ is the z axis and both \vec{k} and \vec{p} are in the xz plane as shown in Fig. II.2. In this frame only $(p_+ \cdot k)$ in Eq. (II.3) is a function of φ , and the magnitude of p_+ is independent of θ_+ . It is convenient to define a pure time like vector

$$U = p_+ + p_f = k + p_i - p .$$

We have

$$U^2 = m^2 + m_i^2 + 2m_i(k - E) - 2k \cdot p . \quad (\text{II.4})$$

Hereafter we use the symbol U as $U = (U^2)^{1/2}$ when it does not appear in the dot product. All the quantities in the special frame, denoted by a subscript s , can

be written in terms of U . The energy of the photon in the special frame is

$$\vec{k}_s = [km_i - (k \cdot p)] / U.$$

The energy and momentum of p_+ are respectively

$$E_{+s} = (U^2 + m^2 - m_f^2) / (2U) \quad (\text{II.5})$$

and

$$p_{+s} = (E_{+s}^2 - m^2)^{1/2}.$$

The momentum of the target particle is

$$p_{is} = m_i (k^2 + p^2 - 2pk \cos \theta)^{1/2} / U$$

The energy of p is

$$E_s = [(p \cdot k) - m^2 + Em_i] / U.$$

The angle θ_k in Fig. 2 is

$$\cos \theta_k = (k_s - E_s) / p_{is} + (k \cdot p) / (k_s p_{is}).$$

q^2 can be written as

$$q^2 = 2m^2 - 2(k \cdot p) - 2E_{+s}(k_s - E_s) + 2p_{+s}p_{is} \cos \theta_+. \quad (\text{II.6})$$

The integration with respect to φ can be carried out readily, we obtain

$$\frac{1}{2\pi} \int_0^{2\pi} d\varphi (p_+ \cdot k)^{-2} = W / (Y^3 k_s^2),$$

$$\frac{1}{2\pi} \int_0^{2\pi} d\varphi (p_+ \cdot k)^{-1} = 1 / (Yk_s),$$

and

$$\frac{1}{2\pi} \int_0^{2\pi} d\varphi (\mathbf{p}_+ \cdot \mathbf{k}) = Wk_s,$$

where

$$W = E_{+s} - p_{+s} \cos \theta_+ \cos \theta_k,$$

and

$$Y = \left[m^2 \sin^2 \theta_k + (p_{+s} \cos \theta_+ - E_{+s} \cos \theta_k)^2 \right]^{1/2}.$$

The cross section for detecting only the lepton p can be written as (in $\text{cm}^2/\text{sr}/\text{GeV}$)

$$\begin{aligned} \frac{d\sigma}{d\Omega dp} = & - \frac{\alpha^3}{2\pi} (0.19732)^2 \times 10^{-26} \int_{-1}^1 d\cos \theta_+ \int_{m_i^2}^{(U-m)^2} dm_f^2 \\ & \frac{p^2}{UkE} \frac{p_{+s}}{q^4} \left[W_2(q^2, m_f^2) \left(\frac{HW}{Y^3 k_s^2} + \frac{B}{Yk_s} + C + Dk_s W \right) \right. \\ & \left. + W_1(q^2, m_f^2) \left(\frac{H'W}{Y^3 k_s^2} + \frac{B'}{Yk_s} + C' + D'k_s W \right) \right]. \end{aligned} \quad (\text{II. 7})$$

Using Eq. (II. 6), the integration with respect to $\cos \theta_+$ can be replaced by the integration with respect to $t \equiv -q^2$:

$$\int_{-1}^1 d\cos \theta_+ = \int_{t_{\min}}^{t_{\max}} \frac{dt}{2p_{is} p_{+s}}, \quad (\text{II. 8})$$

where t_{\min} and t_{\max} can be obtained from Eq. (II. 6) by setting $\cos \theta_+ = 1$ and $\cos \theta_+ = -1$ respectively:

$$t_{\max} = -2m^2 + 2(k \cdot p) + 2E_{+s}(k_s - E_s) \pm 2p_{+s} p_{is}. \quad (\text{II. 9})$$

The target form factors $W_1(q^2, m_f^2)$ and $W_2(q^2, m_f^2)$ needed in our calculations as well as an approximate expression for t_{\min} are given in Appendix B.

Equation (II.1) can be used to calculate any cross section in which ℓ^+ and ℓ^- are detected in coincidence, whereas Eq. (II.7) gives the cross section where only ℓ^- or ℓ^+ is detected. The numerical results of (II.7) for the production of muon and heavy leptons are given in Section V. In the next section, we derive various approximate expressions based on Eq. (II.7). The Coulomb correction will also be included in the next section.

III. APPROXIMATE EXPRESSIONS

Equations (II.1) and (II.7) are exact expressions to order α^3 for pair production. However, they are too complicated for many of the practical applications. Since electrons and muons are very common particles in the laboratory it is desirable to have simple and yet reliable expressions to represent their energy-angle distributions. Bremsstrahlung by electron and muon will also be discussed because they are related to the pair production of these particles by the substitution rule. Relatively simple expressions for the energy-angle distribution for pair production $d\sigma/d\Omega dp$ and bremsstrahlung $d\sigma_b/d\Omega_k dk$ can be obtained when the angle is small and leptons are all extremely relativistic. More explicitly, we shall assume the kinematical conditions specified by (B.4) in the derivation of approximate expressions.

A. Electron Pair Production

For the electron pair production near the forward angle, we need to take into account the atomic screening. Of course at large angles, the nuclear form factor must also be considered even for the electron production. When $t_{\min} r_{\text{nucleus}}^2$ is comparable to unity, we have to include the effect due to nuclear form factors. In this subsection we limit our discussion to small angle production

so that the nuclear form factors can be ignored. The atomic form factors, elastic and inelastic, for various atoms are discussed in Appendix B. Since t_{\min} is very small compared with the electron mass squared, the recoil of the target system can be ignored even when the target is an atomic electron. Thus we expect that our equation (II.7) should yield the same approximate formula as the Bethe-Heitler formula¹³ which is much simpler to handle than ours. This can be shown explicitly using the simple atomic form factors given by (B.38) and (B.39) into (II.7) and carrying out the integration with respect to t . The results can then be expanded in powers of m^2/E^2 , $k \cdot p/E^2$, $m^2/(k-E)^2$ and $(k \cdot p)/(k-E)^2$, etc. After extremely tedious algebra, one finds that a fantastic number of cancellations occurs among the leading terms, leaving a relatively simple formula in the end, which is identical to the formula obtained by Schiff⁴⁰ (1952) who started from the Bethe-Heitler formula. This exercise shows that Eq. (II.7) is indeed identical to the Bethe-Heitler formula when recoil is ignored and also that the effect of the target recoil is negligible when kinematical conditions specified by (B.4) are satisfied.

1. Arbitrary Atomic Form Factors

Both elastic and inelastic atomic form factors, $G_2^{\text{el}}(t)$ and $G_2^{\text{inel}}(t)$ defined by (B.5) and (B.9) respectively, are characterized by the facts that they are zero when $t = 0$ and become constants, Z^2 and Z respectively, when $t \geq m_e^2$. The t dependence of the atomic form factors is thus opposite to that of nuclear form factors. It can be shown that for form factors with this general behavior, we have

$$\begin{aligned} \frac{d\sigma}{d\Omega dp} &= \frac{d\sigma}{d\Omega dp} \text{ (no screening)} \\ &- \frac{2\alpha^3}{\pi k} \left(\frac{E^2}{m^4} \right) \left[\frac{2x^2 - 2x + 1}{(1+l)^2} + \frac{4x(1-x)l}{(1+l)^4} \right] \int_{t'_{\min}}^{\infty} [G_2^{(\infty)} - G_2(t)] \frac{t-t'_{\min}}{t^2} dt, \end{aligned} \quad (\text{III.1})$$

where

$$x = E/k, \quad l = E^2 \theta^2 / m^2, \quad t'_{\min} = \left[\frac{m^2(1+l)}{2kx(1-x)} \right]^2, \quad G_2(t) = G_2^{\text{el}}(t) + G_2^{\text{inel}}(t),$$

and

$$\begin{aligned} \frac{d\sigma}{d\Omega dp} \text{ (no screening)} &= \frac{2\alpha^3}{\pi k} \left(\frac{E^2}{m^4} \right) \left((Z^2 + Z) \left\{ \frac{2x(1-x)}{(1+l)^2} - \frac{12lx(1-x)}{(1+l)^4} \right\} \right. \\ &+ \left. \left\{ \frac{2x^2 - 2x + 1}{(1+l)^2} + \frac{4x(1-x)l}{(1+l)^4} \right\} \left\{ Z^2 \left[\ln \frac{m^2(1+l)^2}{t'_{\min}} - 1 - 2f((\alpha z)^2) \right] \right. \right. \\ &\left. \left. + Z \left[\ln \frac{m^2(1+l)^2}{t'_{\min}} - 1 \right] \right\} \right) \quad (\text{III. 2}) \end{aligned}$$

The function $f((\alpha z)^2)$ in (III. 2) is the Coulomb correction to the one photon exchange approximation worked out by Bethe and Maximon¹⁵ (1954) and is given by

$$f(z) = z \sum_{n=1}^{\infty} \frac{1}{n(n^2+z)} \approx 1.202z - 1.0369z^2 + 1.008z^3/(1+z), \quad (\text{III. 3})$$

where

$$z = (Z/137)^2.$$

Except for the Coulomb correction term, Eqs. (III. 1) and (III. 2) can be derived from our Eq. (III. 7). They summarize the work of many people. The expression for $d\sigma/d\Omega dp$ (no screening), except for the Coulomb correction and the terms proportional to Z , was first derived by Sommerfeld (1939).⁴¹ The terms proportional to Z^2 in (III. 1) and (III. 2) are equivalent to the formulae given by Davis-Bethe-Maximom¹⁶ (1953) and Olsen-Maximom (1959).⁴¹ The terms proportional to Z come from $G_2^{\text{inel}}(t)$ and they are usually ignored (they should not be!).

It will be convenient for our later discussions to write Eq. (III. 1) in a slightly different form. We notice first that the logarithmic terms in (III. 2)

can be written as

$$\ln \frac{m^2(1+l)^2}{t'_{\min}} - 1 \approx \int_{t'_{\min}}^{m^2(1+l)^2} \frac{(t-t'_{\min})}{t^2} dt. \quad (\text{III. 4})$$

Using the simple form factors given by (B. 38) and (B. 39) we can convince ourselves that the upper limit of the integration in (III. 1) can be replaced by $m^2(1+l)^2$.

Thus (III. 1) and (III. 2) can be combined to give

$$\begin{aligned} \frac{d\sigma}{d\Omega dp} = & \frac{2\alpha^3}{\pi k} \left(\frac{E^2}{m^4} \right) \left\{ \left[\frac{2x(1-x)}{(1+l)^2} - \frac{12lx(1-x)}{(1+l)^4} \right] G_2^{(\infty)} \right. \\ & \left. + \left[\frac{2x^2 - 2x + 1}{(1+l)^2} - \frac{4lx(1-x)}{(1+l)^4} \right] \left[X - 2Z^2 f((\alpha Z)^2) \right] \right\}, \quad (\text{III. 5}) \end{aligned}$$

where

$$G_2^{(\infty)} = G_2^{\text{el}(\infty)} + G_2^{\text{inel}(\infty)} = Z^2 + Z,$$

and

$$X = X^{\text{el}} + X^{\text{inel}} = \int_{t'_{\min}}^{m^2(1+l)^2} \left[G_2^{\text{el}}(t) + G_2^{\text{inel}}(t) \right] \frac{(t-t'_{\min})}{t^2} dt. \quad (\text{III. 6})$$

Integrating (III. 5) with respect to the solid angle, we see that the coefficients of $G_2^{(\infty)}$ cancel each other, hence

$$\frac{d\sigma}{dp} = \frac{2\alpha r_0^2}{k} \int_0^\infty dl \left[\frac{2x^2 - 2x + 1}{(1+l)^2} + \frac{4lx(1-x)}{(1+l)^4} \right] (X - 2Z^2 f). \quad (\text{III. 7})$$

Let us make several comments about (III. 5), (III. 6) and (III. 7):

(i) K. J. Kim (unpublished) derived a simple expression for $d\sigma/d\Omega dp$ using (II. 7) with a simple nuclear form factor of the form given by (B. 49). He

found that the terms with $G_2(\infty)$ are missing in this case if $m^2(1+l)^2$ is much larger than the inverse square of the nuclear radius, i. e., $m^2(1+l)^2/d \gg 1$ in the notation of (B.49). Therefore this term can appear only when the form factor does not become negligible for t greater than $m^2(1+l)^2$. From this derivation it is not obvious whether the terms with $G_2(\infty)$ should be kept for muon pair production because the expression $m_\mu^2/d \simeq (0.01/0.164)A^{2/3}$ is not much larger than unity when A is small. However comparisons with the exact calculation using (II.7) for a Be nucleus ($A=9$) shows that it is a better approximation to drop this term than keeping it when calculating the muon pair production.

(ii) The coefficient of X in (III.5) is proportional to the differential cross section of two real photon annihilation, $d\sigma(\gamma + \gamma \rightarrow \ell^+ + \ell^-)/d(p \cdot k)$ (see Eq. (C.1) of Kim and Tsai⁴³(1973)). In the Weizsacker-Williams approximation, one obtains exactly the term proportional to X . Therefore the terms proportional to $G_2(\infty)$ can be regarded as the correction to the W.W. approximation due to the fact that in the pair production, one of the photon in the reaction $\gamma + \gamma \rightarrow \ell^+ + \ell^-$ is off the mass shell. This also explains why terms with $G_2(\infty)$ in (II.7) will not show up if large t events are suppressed by the target form factors. As a consequence of this, the W.W. approximation actually works better for muon pair production than for electron pair production in the calculation of $d\sigma/d\Omega dp$. For the calculation of $d\sigma/dp$, the W.W. approximation yields a result identical to (III.7) regardless of the behavior of form factors except for the Coulomb correction term f . This observation is of great practical importance, because it takes less than one hour of work to obtain (III.7) from the W.W. method⁴³ whereas it takes about one month of hard work to obtain the same result from Eq. (II.7).

(iii) The fact that Eq. (III.1) is equivalent to Eq. (III.5), when conditions specified by (B.4) are satisfied, is probably the best justification for the upper

cut-off $t_{\text{up}} = m^2(1+l)^2$ of the integration in the definition of X used in the W.W. method proposed by Kim and Tsai (1973).⁴³ In the classical W.W. method, the uncertainty principle must be invoked to obtain a cut-off of this magnitude but one does not know exactly what expression should be used. The quantity X is proportional to the pseudo photon flux in the W.W. method. Our X^{el} is related to the quantity Γ of Olsen-Maximon⁴² by

$$X^{\text{el}} = Z^2 \left[2\Gamma + 3 + 2f((Z\alpha)^2) \right] . \quad (\text{III. 8})$$

Equation (III. 7) can also be written in terms of the functions φ_1 and φ_2 introduced by Bethe-Heitler¹³ for the elastic scattering part and functions ψ_1 and ψ_2 introduced by Wheeler-Lamb¹⁴ for the inelastic scattering part:

$$\begin{aligned} \frac{d\sigma}{dp} = \frac{\alpha r_0^2}{k} & \left[\left(\frac{4}{3} x^2 - \frac{4}{3} x + 1 \right) \left[Z^2(\varphi_1 - \frac{4}{3} \ln Z - 4f) + Z(\psi_1 - \frac{8}{3} \ln Z) \right] \right. \\ & \left. - \frac{2}{3} x(1-x) \left[Z^2(\varphi_1 - \varphi_2) + Z(\psi_1 - \psi_2) \right] \right] , \end{aligned} \quad (\text{III. 9})$$

where

$$Z^2(\varphi_1 - \frac{4}{3} \ln Z) \equiv 2 \int_0^\infty \frac{X^{\text{el}}}{(1+l)^2} dl \quad (\text{III. 10})$$

$$Z^2(\varphi_2 - \frac{4}{3} \ln Z) \equiv 12 \int_0^\infty \frac{l X^{\text{el}}}{(1+l)^4} dl \quad (\text{III. 11})$$

$$Z(\psi_1 - \frac{8}{3} \ln Z) \equiv 2 \int_0^\infty \frac{X^{\text{inel}}}{(1+l)^2} dl \quad (\text{III. 12})$$

$$Z(\psi_2 - \frac{8}{3} \ln Z) \equiv 12 \int_0^\infty \frac{l X^{\text{inel}}}{(1+l)^4} dl \quad (\text{III. 13})$$

In order to obtain φ_1 , φ_2 , ψ_1 and ψ_2 , we have to perform integrations with respect to t and l . Both of these integrations can be done analytically for Hydrogen and Helium form factors, Eqs. (B.12, 13, 14, 16, 17 and 18), and the simple form factors, Eqs. (B.36 and 37), given in Appendix B. The form factors for other elements, Li, Be, B, etc. and Thomas-Fermi atoms can be integrated only numerically. Bethe⁴⁴ (1934) has derived approximate formulas in which the variable l in (III.10) through (III.13) is already integrated out, his results are ($Q^2 \equiv t$)

$$\varphi_1 - \frac{4}{3} \ln Z = 4 \left[1 + Z^{-2} \int_{\delta}^m (Q-\delta)^2 G_2^{el} Q^{-3} dQ \right], \quad (\text{III. 14})$$

$$\varphi_2 - \frac{4}{3} \ln Z = 4 \left[5/6 + Z^{-2} \int_{\delta}^m (Q^3 - 6\delta^3 Q \ln(Q/\delta) + 3\delta^2 Q - 4\delta^3) G_2^{el} Q^{-4} dQ \right] \quad (\text{III. 15})$$

$$\psi_1 - \frac{8}{3} \ln Z = 4 \left[1 + Z^{-1} \int_{\delta}^m (Q-\delta)^2 G_2^{\text{inel}} Q^{-3} dQ \right], \quad (\text{III. 16})$$

$$\psi_2 - \frac{8}{3} \ln Z = 4 \left[5/6 + Z^{-1} \int_{\delta}^m (Q^3 - 6\delta^2 Q \ln(Q/\delta) + 3\delta^2 Q - 4\delta^3) G_2^{el} Q^{-4} dQ \right] \quad (\text{III. 17})$$

where $\delta = m^2 k / (2EE')$ and $E' = k - E$. Bethe's formula are only approximately true. Since the integration with respect to l in (III.9) through (III.13) can be carried out analytically for the form factors of hydrogen without using the Bethe's approximation we shall be able to check the accuracy of the latter in Section III.3 after we derive the analytical expressions for φ_1 , φ_2 , ψ_1 and ψ_2 for hydrogen and helium atoms in the next subsection.

2. Hydrogen and Helium Atoms

The atomic form factors for hydrogen are known exactly and they are given by (B.13) and (B.14). It happens that the analytical expressions for

X_{el} , X_{inel} , ϕ_1 , ϕ_2 , ψ_1 and ψ_2 can be obtained from (III.6, 9, 10, 11, 12 and 13) when the atomic form factors have these particular forms. As discussed in Appendix B, the elastic and inelastic helium atomic form factors can also be written in the above form if the correlation between the two atomic electrons is ignored. The uncorrelated wave function of the ground state of He atom was investigated by Hylleraas⁴⁵ (1929) using the variational method. The correlated wave function was investigated by Schull and Löwdin⁴⁶ (1956). Knasel⁴⁷ (1968) calculated the cross section for the pair production using both the correlated and uncorrelated wave functions. He found that two versions differ at most by .2%, hence we shall use the uncorrelated wave function for simplicity. The expression of X for H and He atoms can be written as

$$X = X_{el} + X_{inel},$$

$$X_{el}/Z^2 = 2 \ln(m/\delta) - \ln(1+B^2) + 1/6 - (4/3)/(1+B^2) + (1/6)/(1+B^2)^2 \quad (\text{III. 18})$$

$$X_{inel}/Z = 2 \ln(m/\delta) - \ln(1+B^2) + 11/6 - 4B^{-2} \ln(1+B^2) + (4/3)/(1+B^2) - (1/6)/(1+B^2)^2, \quad (\text{III. 19})$$

where

$$\delta = (t'_{min})^{1/2}/(1+l) = m^2/[2kx(1-x)], \quad (\text{III. 20})$$

$$B = 2\alpha m_e \eta / (t'_{min})^{1/2}, \quad (\text{III. 21})$$

$Z = 1$, $\eta = 1$ for hydrogen and $Z = 2$, $\eta = 1.6875$ for He. We note that X is not very sensitive to the change in production angle and atomic radius. Thus the angular distributions in pair production and bremsstrahlung are mostly determined by the coefficient of X in (III.5) and (III.80). When the energy is high

and the production angle is small we have $B \gg 1$ except when x is very close to 1 or 0. When $B \gg 1$, the screening is complete, in which case we have

Complete Screening Case ($B \gg 1$),

$$X_{el}/Z^2 = 2 \ln(m/B\delta) + 1/6, \quad (\text{III. 22})$$

$$X_{inel}/Z = 2 \ln(m/B\delta) + 11/6. \quad (\text{III. 23})$$

On the other hand when the screening is nonexistent, we have

No Screening Case ($B \ll 1$),

$$X_{el}/Z^2 = X_{inel}/Z = 2 \ln(m/\delta) - 1. \quad (\text{III. 24})$$

The integrations with respect to ℓ can be carried out analytically, we obtain from (III. 10) through (III. 13), using the expression of X given by (III. 18) and (III. 19):

$$\begin{aligned} \Phi_1 - \frac{4}{3} \ln Z &= 4 \ln [1/(2\eta\alpha)] + 13/3 \\ &\quad - 2\ln(1+C^2) - (13/2) C \arctan (1/C) + (1/6)/(1+C^{-2}), \end{aligned} \quad (\text{III. 25})$$

$$\begin{aligned} \Phi_2 - \frac{4}{3} \ln Z &= 4 \ln [1/(2\eta\alpha)] + 11/3 \\ &\quad - 2\ln(1+C^2) + 25C^2(1-C \arctan C^{-1}) - 14C^2 \ln(1+C^{-2}), \end{aligned} \quad (\text{III. 26})$$

$$\begin{aligned} \psi_1 - \frac{8}{3} \ln Z &= 4 \ln [1/(2\eta\alpha)] + 23/3 \\ &\quad - 2\ln(1+C^2) - 17.5 C \arctan C^{-1} + 8C^2 \ln(1+C^{-2}) - (1/6)/(1+C^{-2}), \end{aligned} \quad (\text{III. 27})$$

$$\begin{aligned}
\psi_2 - \frac{8}{3} \ln Z &= 4 \ln [1/(2\eta\alpha)] + 21/3 \\
&- 2 \ln (1+C^2) - 105 C^2 (1-C \arctan C^{-1}) + 50 C^2 \ln(1+C^{-2}) \\
&- 24C^2 \{ - \ln C^2 \ln(1+C^{-2}) + \Phi(1+C^{-2}) - \Phi(1) \} , \quad (\text{III. 28})
\end{aligned}$$

where $C = \delta/(2\alpha m_e \eta)$ and $\Phi(x)$ is the Spence function (or Euler's dilogarithm) defined by

$$\Phi(x) = - \int_0^x \frac{\ln |1-y|}{y} dy , \quad (\text{III. 29})$$

whose numerical values can be obtained by a computer using the following formulas:

$$\text{If } |x| \leq 1, \quad \Phi(x) = x + \frac{1}{4} x^2 + \frac{1}{9} x^3 + \dots + (x^n/n^2) + \dots$$

$$\Phi(1) = \pi^2/6 \quad \text{and} \quad \Phi(-1) = -\pi^2/12.$$

$$\text{If } x > 1, \quad \Phi(x) = - \frac{1}{2} \ln^2 |x| + \pi^2/3 - \Phi(1/x).$$

$$\text{If } x < -1, \quad \Phi(x) = - \frac{1}{2} \ln^2 |x| - \pi^2/6 - \Phi(1/x).$$

Following Wheeler-Lamb,¹⁴ we give φ_1 and φ_2 as functions of a variable γ defined by

$$\gamma = \frac{100 m k}{EE'Z^{1/3}} = 200 \delta/(m_e Z^{1/3}) \quad (\text{III. 30})$$

and ψ_1 and ψ_2 as functions of ϵ defined by

$$\epsilon = \frac{100 m k}{EE'Z^{2/3}} = 200 \delta/(m_e Z^{2/3}), \quad (\text{III. 31})$$

where

$$E' = k - E.$$

The quantity C in (III.25) through (III.28) can be written in terms of γ or ϵ as

$$C = \gamma Z^{1/3} / (400 \alpha \eta) = \epsilon Z^{2/3} / (400 \alpha \eta). \quad (\text{III.32})$$

The reason for using the variables γ and ϵ is that for Thomas-Fermi model $\Phi_1(\gamma)$, $\Phi_2(\gamma)$, $\psi_1(\epsilon)$ and $\psi_2(\epsilon)$ are universal functions independent of Z. Since we are going to use Thomas Fermi model for all elements with $Z \geq 5$, it is convenient to use these variables also for light elements for the purpose of making comparisons later.

When the screening is complete, we have $\gamma = \epsilon = C = 0$, hence

$$\Phi_1(0) = 4 \ln \left[Z^{1/3} / (2\eta \alpha) \right] + 13/3 = \begin{cases} 21.2417 \text{ for H} \\ 20.0729 \text{ for He} \end{cases}, \quad (\text{III.33})$$

$$\Phi_2(0) = \Phi_1(0) - 2/3, \quad (\text{III.34})$$

$$\psi_1(0) = 4 \ln \left[Z^{2/3} / (2\eta \alpha) \right] + 23/3 = \begin{cases} 24.5750 \text{ for H} \\ 24.3304 \text{ for He} \end{cases}, \quad (\text{III.35})$$

$$\psi_2(0) = \psi_1(0) - 2/3. \quad (\text{III.36})$$

When the screening is nonexistent, we have $C \gg 1$, hence

$$\begin{aligned} \Phi_1(\gamma) &= \Phi_2(\gamma) = 4 \ln(200/\gamma) - 2, \\ \psi_1(\epsilon) &= \psi_2(\epsilon) = 4 \ln(200/\epsilon) - 2. \end{aligned} \quad (\text{III.37})$$

The numerical values of $\Phi_1(\gamma)$, $\Phi_2(\gamma)$, $\psi_1(\epsilon)$ and $\psi_2(\epsilon)$ for a hydrogen atom are shown in Table III.1 and those for a helium atom are shown in Table III.2. The values of $\Phi_1(0)$ and $\psi_1(0)$ given by (III.33) and (III.35) are related to the radiation logarithms L_{rad} and L'_{rad} respectively and they come in the definition of radiation lengths of materials as will be shown in Section III.B. In the no screening limit, the

expressions for X_{el}/Z^2 and X_{inel}/Z given by (III. 24) and the expressions for φ_1 , φ_2 , ψ_1 and ψ_2 given by (III. 37) are universal functions independent of materials. The numerical values of (III. 37) are tabulated in the last column of Table III. 4. We note that when $\gamma > 2$, $\varphi_1(\gamma)$ and $\varphi_2(\gamma)$ are given approximately by the no screening expression, whereas $\psi_1(\epsilon)$ and $\psi_2(\epsilon)$ approach the no screening limit much earlier, roughly at $\epsilon \sim 1$.

3. Checking the Accuracy of Bethe Approximation

In the previous subsection we have derived the analytical expressions for φ_1 , φ_2 , ψ_1 and ψ_2 without using the Bethe approximation⁴⁴ (III. 14 to 17). In Table III. 3 the values of φ_1 , φ_2 , ψ_1 and ψ_2 for a hydrogen atom using the Bethe approximation are tabulated, which are to be compared with the results given in Table III. 1. We note that the Bethe approximation is in general very good, especially when the screening is effective. We shall assume that the Bethe approximation yield results with the same degree of accuracy when applies to other atoms for which the analytical expressions for φ_1 , φ_2 , ψ_1 and ψ_2 are not obtainable.

4. Thomas-Fermi Atoms

When Z is large, Thomas-Fermi model of atoms can be used. We shall use the Moliere representation of Thomas-Fermi atom discussed in Appendix B. Using these form factors and the Bethe's approximation, (III. 14) through (III. 17), we obtain the numerical values for $\varphi_1(\gamma)$, $\varphi_2(\gamma)$, $\psi_1(\epsilon)$ and $\psi_2(\epsilon)$; the results are shown in the columns labeled "TFM" in Table III. 4. Since numerical tables are hard to use in the practical application, we have constructed approximate analytical expressions which reproduce the numerical values obtained above to within $\frac{1}{2}\%$.

These expressions are:

$$\begin{aligned} \Phi_1(\gamma) &= 20.863 - 2 \ln [1 + (0.55846\gamma)^2] \\ &\quad - 4 [1 - 0.6 \exp(-0.9\gamma) - 0.4 \exp(-1.5\gamma)] , \end{aligned} \quad (\text{III. 38})$$

$$\Phi_2(\gamma) = \Phi_1(\gamma) - \frac{2}{3} \frac{1}{1 + 6.5\gamma + 6\gamma^2} , \quad (\text{III. 39})$$

$$\begin{aligned} \psi_1(\epsilon) &= 28.340 - 2 \ln [1 + (3.621\epsilon)^2] \\ &\quad - 4 [1 - 0.7 \exp(-8\epsilon) - 0.3 \exp(-29.2\epsilon)] , \end{aligned} \quad (\text{III. 40})$$

$$\psi_2(\epsilon) = \psi_1(\epsilon) - \frac{2}{3} \frac{1}{1 + 40\epsilon + 400\epsilon^2} . \quad (\text{III. 41})$$

In Table III.4, the columns labeled "Analytical Simulation" refer to the results using the above equations. These equations are not entirely obtained by curve fitting. They possess the following general properties which all these functions must have:

1. $\Phi_1(\gamma)$, $\Phi_2(\gamma)$, $\psi_1(\epsilon)$ and $\psi_2(\epsilon)$ are all monotonically decreasing functions, and in the no screening limit all of them must reduce to the common analytical expression given by (III.37).

2. The relations (III.34) and (III.36) must be satisfied in the complete screening limit, i.e.,

$$\Phi_1(0) - \Phi_2(0) = \psi_1(0) - \psi_2(0) = 2/3 . \quad (\text{III. 42})$$

Also in general, we have

$$\Phi_1(\gamma) \geq \Phi_2(\gamma) \quad \text{and} \quad \psi_1(\epsilon) \geq \psi_2(\epsilon) ,$$

where the equality signs hold only when γ and ϵ are large.

3. $\varphi_1(0)$ and $\psi_1(0)$ determine the radiation length of materials [see (III. 65)], therefore these two numbers must be fitted first, namely

$$\varphi_1(0) = 20,863 \quad \text{and} \quad \psi_1(0) = 28.352. \quad (\text{III. 43})$$

The particular analytical forms chosen in the above will become obvious after the next discussion.

In order to calculate energy-angle distribution, $d\sigma/d\Omega dp$ and $d\sigma/d\Omega_k dk$, we have to know X_{el} and X_{inel} . However, the angular distribution of bremsstrahlung and pair production are mostly determined by the multiple scatterings in the target, rather than the production mechanism. Therefore X_{el} and X_{inel} obtained from using the simple form factors discussed in Appendix B, see Eq. (B.38) and Eq. (B.39), should be adequate. The numerical values are only slightly greater, at most 4%, than those of Thomas-Fermi model in the intermediate screening region. In both the complete screening and no screening limits, the results must agree with that of Thomas-Fermi because of the way in which the simple form factors are constructed. In the following we give the expressions for X_{el} , X_{inel} , φ_1 , φ_2 , ψ_1 and ψ_2 corresponding to the simple atomic form factors given by (B.38) and (B.39):

$$X_{el} = Z^2 \left[\ln \frac{a^2 m^2 (1+\ell)^2}{a'^2 t'_{\min} + 1} - 1 \right], \quad (\text{III. 44})$$

$$X_{inel} = Z \left[\ln \frac{a'^2 m^2 (1+\ell)^2}{a'^2 t'_{\min} + 1} - 1 \right], \quad (\text{III. 45})$$

$$\varphi_1 = 2(1 + \ln a^2 Z^{2/3} m_e^2) - 2\ln(1 + b^2) - 4b \arctan(b^{-1}), \quad (\text{III. 46})$$

$$\begin{aligned} \varphi_2 &= 2(2/3 + \ln a^2 Z^{2/3} m_e^2) - 2\ln(1+b^2) \\ &+ 8b^2 \{1 - b \arctan(b^{-1}) - 0.75 \ln(1+b^{-2})\}, \end{aligned} \quad (\text{III.47})$$

$$\psi_1 = 2(1 + \ln a'^2 Z^{4/3} m_e^2) - 2\ln(1+b'^2) - 4b' \arctan(b'^{-1}), \quad (\text{III.48})$$

$$\begin{aligned} \psi_2 &= 2(2/3 + \ln a'^2 Z^{4/3} m_e^2) - 2\ln(1+b'^2) \\ &+ 8b'^2 \{1 - b' \arctan(b'^{-1}) - 0.75 \ln(1+b'^{-2})\}, \end{aligned} \quad (\text{III.49})$$

where a and a' are the atomic parameters which appear in the simple form factors (B.38) and (B.39) respectively. They are tabulated in Table B.4. b and b' are $b = a\delta$ and $b' = a'\delta$, where

$$\delta = \sqrt{t'_{\min}} / (1+l) = \frac{m_k^2}{2E(k-E)}. \quad (\text{III.50})$$

For Thomas-Fermi-Moliere atoms, we have

$$\varphi_1(0) = 2(1 + \ln a^2 Z^{2/3} m_e^2) = 20.863, \quad (\text{III.51})$$

$$\psi_1(0) = 2(1 + \ln a'^2 Z^{4/3} m_e^2) = 28.340, \quad (\text{III.52})$$

$$b = 0.55846\gamma, \quad (\text{III.53})$$

$$b' = 3.6201\epsilon. \quad (\text{III.54})$$

Substituting these relations into (III.46 through 49) and compare the results with (III.38 through 41), the reader will see how we have obtained the latter. We have obtained them by slightly changing the former to fit the numerical results given by "TFM" in Table III.4. The column labeled "Monopole Simulation" refers to the numerical results of using (III.46 through 49) with parameters given by (III.51 through 54). The name monopole comes from the fact that the atomic form

factor F defined in (B. 7) has a monopole structure for the simple form factor defined in (B. 38).

Another way to simulate the Thomas-Fermi-Moliere model is to use the hydrogen like form factors, regarding η in (III. 25) and (III. 27) as two different parameters determined by the values of ϕ_1 and ψ_1 in the complete screening limit given by (III. 43). The desired ϕ_1 and ϕ_2 can be obtained from Eqs. (III. 25) and (III. 26) by setting

$$\eta = \frac{Z^{1/3} \exp(13/12)}{2\alpha \ 184.15} , \quad (\text{III. 55})$$

and the desired ψ_1 and ψ_2 can be obtained from Eqs (III. 27) and (III. 28) by setting

$$\eta = \frac{Z^{2/3} \exp(23/3)}{2\alpha \ 1194} . \quad (\text{III. 56})$$

The results of this simulation are given in the column labeled "Dipole Simulation" in Table III.4. The name "dipole" comes from the fact that the atomic form factor F for a hydrogen atom has a dipole structure.

Let us discuss the numerical results shown in Table III.4:

1. As mentioned previously, in the limit of large γ and ϵ , all the functions $\phi_1(\gamma)$, $\phi_2(\gamma)$, $\psi_1(\epsilon)$ and $\psi_2(\epsilon)$ reduce to the common expression given by Eq. (III. 37), whose numerical values are also tabulated in the column labeled "Unscreened Target" in Table III.4. We notice that the inelastic screening functions $\psi_1(\epsilon)$ and $\psi_2(\epsilon)$ approach the asymptotic form much sooner than the elastic screening functions $\phi_1(\gamma)$ and $\phi_2(\gamma)$ do. Also the approach to the asymptotic form is the earliest for the "Dipole Simulation" and the next is the "Monopole Simulation" and the last is the "TFM". Since "Dipole Simulation" uses the hydrogen form factor and "TFM" is supposed to be good when Z is large, we expect that for

small Z elements the true values of the screening functions must lie somewhere between "Dipole Simulation" and "TFM". "Monopole Simulation" has such a property.

2. In Section 1 C of Appendix B, we show that the Thomas-Fermi-Moliere model of atom is applicable for elements with $Z \geq 5$ as far as the calculation of $\Phi_1(0)$ is concerned. Our investigation here shows that functions $\Phi_1(\gamma)$, $\Phi_2(\gamma)$, $\psi_1(\epsilon)$ and $\psi_2(\epsilon)$ are relatively insensitive to the detail of the atomic form factors as long as they are normalized correctly at $\gamma = 0$ and $\epsilon = 0$. "Monopole Simulation" differs from "TFM" by 2% at most and "Dipole Simulation" differs from "TFM" by 4% at most.

3. At high energies where the screening is almost complete in large part of the spectrum, the places these differences show up occupy but a small fraction of the total spectrum. The difference is appreciable only when

$$0.2 < \gamma < 3.0 \quad (\text{III. 57})$$

and

$$0.02 < \epsilon < 0.6 . \quad (\text{III. 58})$$

Using the definition of γ and ϵ given in (III. 30) and (III. 31), we see that there are two small regions in the pair production spectrum, at high energy and low energy tips, which are relatively sensitive to the detail of the form factors. Since the elastic contribution is more important than the inelastic unless Z is very small, let us consider the elastic case for example. From (III. 57) and (III. 30) we obtain

$$\frac{100 m_e}{3.0 k Z^{1/3}} < (1-x \text{ or } x) < \frac{100 m_e}{0.2 k Z^{1/3}} \quad (\text{III. 59})$$

where $x = E/k$. For $k = 10$ GeV, the right hand side is $1/(40 Z^{1/3})$.

On the other hand for the bremsstrahlung spectrum only the high energy tip is sensitive to the detail of the form factors, the corresponding inequality is

$$\frac{100 m_e}{3.0 E Z^{1/3}} < 1 - y < \frac{100 m_e}{0.2 E Z^{1/3}} \quad (\text{III. 60})$$

where $y = k/E$.

Let us summarize the result of this subsection by the following prescription:

1. For hydrogen and He atoms, $d\sigma/d\Omega dp$ can be obtained from Eq. (III. 5) with X given by (III. 18) and (III. 19). $d\sigma/dp$ can be obtained from Eq. (III. 9) with φ_1 , φ_2 , ψ_1 and ψ_2 given by Eqs. (III. 25, 26, 27 and 28).

2. For $Z \geq 3$, $d\sigma/d\Omega dp$ can be obtained from Eq. (III. 5) with X given by (III. 44) and (III. 45) and the parameters a and a' given in Table B. 4.

3. For $d\sigma/dp$, we use Eq. (III. 9) with φ_1 , φ_2 , ψ_1 and ψ_2 given by Eqs. (III. 46 through 49) for $Z = 3$ and $Z = 4$, and Eqs. (III. 38 through 41) for $Z \geq 5$.

The angular distribution of an electron for the pair production at small angles is mostly determined by the multiple scattering in the target rather than by the angular distribution of the production. Hence in general one needs to know only very qualitative features of $d\sigma/d\Omega dp$. This is the reason why we did not try to give a better prescription than 2. above, which is accurate only to within 4% as discussed before.

$d\sigma_b/d\Omega_k dk$ and $d\sigma_b/dk$ of the bremsstrahlung can be obtained from Eq. (III. 80) and (III. 82) with X, φ_1 , φ_2 , ψ_1 and ψ_2 given for various atoms prescribed above.

5. Total Pair Production Cross Sections

Equation (III. 9) can be integrated with respect to p to obtain the total cross section. The total pair production cross section is an important quantity because it

determines the attenuation constants for the photon in materials. In general, the integration can be carried out only numerically. However, when the energy is high ($k > 10$ GeV), the functions $\varphi_1(\gamma)$, $\varphi_2(\gamma)$, $\psi_1(\epsilon)$ and $\psi_2(\epsilon)$ can be approximated by their values at $\gamma = 0$ and $\epsilon = 0$, and the result can be integrated easily to yield

$$\sigma(\infty) = \frac{7}{9} \alpha r_0^2 \left[Z^2 \left\{ \varphi_1(0) - \frac{4}{3} \ln Z - 4f \right\} + Z \left\{ \psi_1(0) - \frac{8}{3} \ln Z \right\} - \frac{2}{21} \left\{ Z^2 + Z \right\} \right], \quad (\text{III. 62})$$

where we have used the relations

$$\varphi_1(0) - \varphi_2(0) = \psi_1(0) - \psi_2(0) = 2/3. \quad (\text{III. 63})$$

This is the cross section at an infinite energy. The numerical values of $\sigma(\infty)$ for various elements together with the quantity

$$\xi = \frac{\sigma(\infty) - \sigma(k)}{\sigma(\infty)} \quad (\text{III. 64})$$

as a function of photon energy are given in Table III.5. The values of $\sigma(\infty)$ are obtained from the values of radiation logarithms given in Table B.2 and Eq. (II. 62).

In the calculation of the energy dependence of the cross section, ξ , we have included the correction due to the recoil of the target electron which was ignored in Eq. (III. 9). The exact calculation of the lowest order cross section for pair production off an electron target was first performed by Votruba (1948). This calculation involves eight Feynman diagrams. Earlier, Borsellino (1947) and Ghizzetti (1947) considered an approximation in which only two diagrams shown in Fig. 1 are retained. Mork (1967) made detailed numerical comparisons

between Votruba's and Borsellino's formulas. He found that when the incident photon is above 8 MeV, the difference between the two is less than 0.1%. The cross section considered by Borsellino is a special case of the formula given in Section II. Letting $m = m_i = m_f = m_e$ and using the form factors corresponding to a pure Dirac particle, we obtained numerical results which are in complete agreement with the Borsellino cross section which was evaluated by Mork (1967). When $k > 50$ MeV, the Borsellino cross section can be written analytically as

$$\sigma_B = \alpha r_0^2 \left\{ \frac{28}{9} G - 8.074 - \left[\frac{4}{3} G^3 - 3G^2 + 6.84 G - 21.51 \right] m_e/k \right\} ,$$

where $G = \ln(2k/m_e)$. The first two terms can also be obtained by integrating Eq. (III.9) using Eq. (III.37), therefore the square bracket term represents the correction due to the recoil. The fractional decrease in cross section due to recoil is thus given by

$$\Delta(k) = \frac{m_e}{k} \left(\frac{4}{3} G^3 - 3G^2 + 6.84 G - 21.51 \right) / \left(\frac{28}{9} G - 8.074 \right) .$$

This correction factor is derived without taking the screening into account. However the screening is important only when the momentum transfer is much less than m_e , whereas the recoil is important only when the momentum transfer is not negligible compared with m_e . Therefore we are allowed to consider two effects separately. Let us denote the total cross section without the recoil correction by $\sigma(k)$ and the inelastic part of this cross section by $\sigma_{in}(k)$, then the expression for ξ with recoil correction can be written as

$$\xi = \frac{\sigma(\infty) - \sigma(k)}{\sigma(\infty)} + \frac{\sigma_{in}(k)}{\sigma(\infty)} \Delta .$$

The numerical values of Δ are given at the bottom of Table III.5. Because of G^3 term, Δ is not negligible even at $k = 1$ GeV. $\sigma_{in}(k)/\sigma(\infty)$ is proportional to

$1/(Z+1)$, hence the recoil correction is more important for light elements. In the calculation for ξ , we have used Eqs. (III. 25) through (III. 28) for H and He, whereas for all other atoms we used the Thomas-Fermi-Moliere model, Eqs. (III. 38) through (III. 41) and Eq. (III. 9). We note that ξ is not negligible even at photon energy of a few GeV especially for light elements. The importance of the recoil correction to the incoherent part of the cross section was first emphasized by Knasel (1970) who did a very detailed study of $\sigma(k)$ from H and He. It is comforting to know that our numerical results agree with his even though the intermediate steps involved in the two calculations are somewhat different. The effect of radiative corrections is not included in Table III. 5. This effect can be accounted for by multiplying $\sigma(\infty)$ given in column 3 by a factor 1.0093 according to Mork and Olsen (1965).

B. Radiation Lengths of Materials

When one is dealing with electrons and photons at high energies, it is convenient to measure the thickness of the material in units of radiation length.

Let us define the unit radiation length, denoted by X_0 , of a material by

$$X_0^{-1} = \alpha r_0^2 N A^{-1} \left[Z^2 \left\{ \varphi_1(0) - \frac{4}{3} \ln Z - 4f \right\} + Z \left\{ \psi_1(0) - \frac{8}{3} \ln Z \right\} \right], \quad (\text{III. 65})$$

or equivalently,

$$X_0 = 716.405 A / \left[Z^2 (L_{\text{rad}} - f) + Z L'_{\text{rad}} \right]. \quad (\text{III. 66})$$

In Table III.6, we give the numerical values of X_0 from $Z = 1$ to $Z = 92$. In this Table, we have used the values of L_{rad} and L'_{rad} from Table B.2 for elements $Z \leq 4$, and for $Z \geq 5$ we have used the Thomas-Fermi-Moliere expressions derived in Appendix B:

$$L_{\text{rad}} = \ln (184.15 Z^{-1/3}) \quad (\text{III. 67})$$

and

$$L'_{\text{rad}} = \ln (1194 Z^{-2/3}). \quad (\text{III. 68})$$

There are many Tables of radiation lengths available in the literature which involve different degrees of sophistication in the calculation. Let us comment on some of the well known ones. The Table I in Bethe and Ashkin²² (1952) can be obtained from Eq. (III.66) without the Coulomb correction f and with the radiation logarithms given by

$$L_{\text{rad}} = \ln (183 Z^{-1/3}) \quad (\text{III. 69})$$

and

$$L'_{\text{rad}} = \ln (1440 Z^{-2/3}) \quad (\text{III. 70})$$

for all elements including Hydrogen. As a consequence they obtained for example, X_0 for H 58 gm/cm² instead of our value of 63.05 gm/cm² and for Pb (Z=82) 5.8 gm/cm² instead of our value of 6.37 gm/cm². It is clear that (III. 69) and (III. 70) cannot be used for hydrogen and the Coulomb correction f is not negligible for lead. Therefore, the table given by Bethe and Askin cannot be trusted to within 10%.

Table 5.24.1 of Rossi²¹ (1952) can be obtained by assuming that both L_{rad} and L'_{rad} are given by $\ln(183 Z^{-1/3})$ and the Coulomb correction is taken care of by multiplying (III. 66) by a factor

$$[1 + 0.12 (Z/82)^2] , \quad (\text{III. 71})$$

and setting f in (III. 66) equal to zero. Since the inelastic contribution is relatively unimportant for high Z materials, Rossi's method gives fairly correct values for high Z materials but for light Z elements it is as bad as Bethe and Ashkins.²²

Table I of Dovzhenko and Pomanski⁴⁸ (1963), which is also reproduced in 1972 version of the Rosenfeld Tables,⁴⁹ is closest to our Table III.6. The slight difference in numerical values is due to the following reasons:

1. For H and He, we have used the analytical expressions for L_{rad} and L'_{rad} given by (III.33) and (III.35), whereas Dovzhenko and Pomanski⁴⁸ obtained L_{rad} and L'_{rad} from numerical integrations, which is probably not accurate enough. Their radiation lengths for H and He are 62.6 and 93.1 gm /cm² respectively.

2. For light elements, we used the same procedure to obtain L_{rad} , but a different procedure was used for L'_{rad} . Dovzhenko and Pomanski interpolated L'_{rad} between H and N assuming that for N the ratio $L'_{\text{rad}}/L_{\text{rad}}$ is

given by

$$L'_{\text{rad}}/L_{\text{rad}} = \ln(1400 Z^{-2/3})/\ln(191 Z^{-1/3}) . \quad (\text{III.72})$$

Our interpolation is between He and B, assuming that for B the ratio of radiation logarithm is given by

$$L'_{\text{rad}}/L_{\text{rad}} = \ln(1194 Z^{-2/3})/\ln(184.15 Z^{-1/3}) .$$

We do not know why they used the expression $L_{\text{rad}} = \ln(191 Z^{-1/3})$ because their Fig. 1 clearly show that this is an overestimate and our expression $\ln(184.15 Z^{-1/3})$ will fit the dots in their Fig. 1 much better. Their use of the expression $L'_{\text{rad}} = \ln(1440 Z^{-2/3})$ comes from the mislabeling of the graph in the original paper of Wheeler and Lamb¹⁴ (1939) which was later corrected in Errata in Wheeler and Lamb¹⁴ (1959). According to our calculation in Appendix B this number should be $\ln(1194 Z^{-2/3})$.

Let us discuss some facts concerning the use of Table III.6.

(a). If we ignore the term $(2/21)(Z^2 + Z)$ in Eq. (III.62), the total pair production cross section at infinite energy can be written as

$$\sigma(\infty) = \frac{7}{9} \frac{A}{X_0 N} . \quad (\text{III.73})$$

At a finite photon energy, we have

$$\sigma(k) = \sigma(\infty)(1 - \xi) . \quad (\text{III.74})$$

The values of parameter ξ for various elements are tabulated in Table IV.5.

Thus the attenuation of a photon beam in a target can be written as

$$\exp\left[-\frac{7}{9} t(1 - \xi)\right], \quad (\text{III.75})$$

if the thickness of the target t is measured in units of X_0 . At high energy, ξ is much less than one, but even at several GeV ξ can be a few percents as can be seen from Table III.5.

(b). The term ignored, $(2/21)(Z^2 + Z)$, comes from $\phi_1(0) - \phi_2(0) = \psi_1(0) - \psi_2(0) = 2/3$. The relative importance of this term increases with Z as can be seen from (III.62), but even for Pb ($Z = 82$) the error involved is less than 0.7%. If one is unwilling to tolerate this kind of error, one should use the total cross sections in calculating the attenuation factor instead of Eq. (III.75). The reason why this term is ignored in the definition of the radiation length is that one would like to use the radiation length in dealing with both the bremsstrahlung and the pair production, and the terms $\phi_1(0) - \phi_2(0)$ and $\psi_1(0) - \psi_2(0)$ appear with different sign and relative magnitude in two problems [compare (III.62) with (III.83)].

(c). Our definition of radiation length refers strictly to a free atom. We have ignored the effects due to molecular bindings, crystal structures, polarization of medium, etc. We have also ignored the radiative corrections. Using Heitler-London model of H_2 molecule, Bernstein and Panofsky⁵⁰ (1956) showed that in the complete screening limit the effect of the molecular binding is to increase the pair production cross section by 2.8 %, hence the radiation length for H_2 is 61.283 gm/cm² instead of 63.047 gm/cm² shown in Table III.6 for H. There seems to be no follow up calculations on this subject despite Bernstein and Panofsky's calculation indicates that the effect could be significant also for other molecules. The effects due to the crystal structure are investigated theoretically by Überall⁵¹ (1956, 1957). The bremsstrahlung produced by a thin crystal has many spikes and it is linearly polarized. Hence it is a source of linearly polarized semimonochromatic photon beam at high energy photon laboratories. This subject was extensively reviewed by Diambrini⁵² (1968). The attenuation constant

of a photon beam in a thick crystal is dependent on the polarization of the photon. Cabibbo, et al⁵³ (1962) proposed that this fact can be used to obtain a polarized photon beam and also that it can be used as an analyser for the photon polarization. The most up to date discussion on this subject can be found in a paper by Eisele et al⁵⁴ (1973). The effects of polarization of medium become important only when the energy is above 1000 GeV. The references on this subject can be traced back from the paper of Vartoloev and Svetlobov⁵⁵ (1959).

(d). Assuming that the molecular binding can be ignored, we can calculate from Table III.6 the radiation lengths of isotopes such as D₂, chemical compounds such as H₂O and CH₂, and mixtures of molecules such as air. Let us calculate the radiation lengths of D₂, H₂O, CH₂ and air as examples:

$$\begin{aligned} \underline{\text{Deuterium}} \quad X_0(\text{D}_2) &= X_0(\text{D}) = X_0(\text{H}_2) \frac{M(\text{D})}{M(\text{H})} \\ &\approx 63.047 \times 2 = 126.1 \text{ gm/cm}^2 \end{aligned}$$

H₂O Using the atomic weights and the radiation lengths of H(Z = 1) and O(Z = 8) given in Table III.6, we may calculate the radiation length of water denoted by X₀(H₂O) from the equation

$$\frac{2A(\text{H}) + A(\text{O})}{X_0(\text{H}_2\text{O})} = \frac{2A(\text{H})}{X_0(\text{H})} + \frac{A(\text{O})}{X_0(\text{O})} ,$$

which yields

$$X_0(\text{H}_2\text{O}) = 36.0823 \text{ gm/cm}^2 .$$

CH₂ Similarly, from the A and X₀ of Carbon (Z = 6) and H(Z = 1) in Table III.6, we obtain

$$X_0(\text{CH}_2) = 44.775 \text{ gm/cm}^2 .$$

Air Assuming that air consists of 76.9% Nitrogen ($Z = 7$), 21.8% Oxygen ($Z = 8$) and 1.3% Argon ($Z = 18$) by weight, we have

$$\frac{1}{X_0(\text{Air})} = \frac{.769}{X_0(\text{N})} + \frac{.218}{X_0(\text{O})} + \frac{.013}{X_0(\text{A})},$$

which yields

$$X_0(\text{Air}) = 36.664 \text{ gm/cm}^2.$$

C. Muon Pair Production

The existence of atomic electrons can be ignored in the muon pair production because t_{\min} involved is much larger than the inverse square of the atomic radius and also because the threshold energy required is too high for production in the electron field. Instead of atomic form factors, we need to consider the nuclear form factors. Most of the cross section occurs within a few units of the characteristic angle, $\theta_c \approx m_\mu/E$, and in this small angular range, only the elastic form factor is important. Equation (III.5) can be used for calculating the energy-angle distribution, except now $G_2(t)$ is a nuclear form factor. Since $G_2(\infty) = 0$ for nuclear form factor, the result of (III.5) is identical to that obtained by using the Weizsacker Williams approximation⁴³ except for the Coulomb correction f . Detailed derivation of Weizsacker-Williams approximation and numerical comparison with the result obtained from the Born approximation, Eq. (II.7), can be found in Kim and Tsai⁴³ (1973). For simple form factors given by (B.49), the integration with respect to t in (III.6) can be carried out analytically. We obtain

$$\begin{aligned} X &= Z^2 \int_{t'_{\min}}^{m^2(1+l)^2} \frac{(t-t'_{\min})}{(1+t/d)^2} \frac{dt}{t^2} \\ &= Z^2 \left[(1+2b) \ln \frac{1+b^{-1}}{1+c^{-1}} - \left(1 + \frac{b}{c}\right) \frac{1+2c}{1+c} \right], \end{aligned} \quad (\text{III.76})$$

where $d = 0.164 A^{-2/3} \text{ GeV}^2$, $b = t'_{\min}/d$ and $c = m^2(1 + \ell)^2/d$. At high energies and small angles, b is much less than unity, whereas c is of order unity for light nuclei. Hence X is relatively insensitive to small variations in angle, energy as well as nuclear radius. The energy-angle distribution are determined mostly by the coefficient of X in (III.5). We have also used the experimental nuclear form factors of Be nucleus shown in (B.50) and (B.51). We found that for small angles, the numerical values of X is quite insensitive to the detailed behavior of the form factor at large t .

When the production angle gets large, $(t'_{\min})^{1/2}$ becomes comparable to or greater than the internucleon distance, in which case the inelastic nuclear form factors [see Eqs. (B.52) and (B.53)] as well as the meson production form factors [see Eqs. (B.56) and (B.57)] must be taken into account. The contributions due to these form factors can be handled by inserting the appropriate form factors in Eq. (II.7). However if one wants to obtain a less accurate but a simple expression, we may use (III.5) with X calculated according to the Weizsacker Williams method given by Kim and Tsai⁴³

$$X = \frac{1}{2m_i} \int_{t_{\min}}^{t_{\text{up}}} \frac{dt}{t} \int_{\frac{m_i^2}{2}}^{(U-m)^2} dm_f^2 \left[(t - t_{\min}) W_2 + 2t'_{\min} W_1 \right],$$

where $t_{\text{up}} = m^2(1 + \ell)^2$. X 's for various form factors are considered in Kim and Tsai⁴³ (1973). The reader should refer to that paper for details.

D. Energy Angle Distribution of Bremsstrahlung

The matrix elements of the bremsstrahlung is related to those of pair production by the substitutions $k \leftrightarrow -k$ and $p \leftrightarrow -p$, where p is the four momentum of either the incident particle in the bremsstrahlung emission or the four momentum of the one of the pair of particles in the pair production. In the energy-angle

distribution of the bremsstrahlung, all the final particles except the photon is integrated out. In our calculation of the energy-angle distribution of the lepton, all the final particles except one lepton is integrated out. We show first that these two partially integrated cross sections are also related by the substitution rules. To the lowest order in α , the energy-angle distribution of the bremsstrahlung for an electron is the same as that for a positron. Similarly to the lowest order in α , the electron and the positron have the same energy-angle distribution in the pair production. For convenience let us call the incident particle in the bremsstrahlung a positron and the detected particle in the pair production an electron. With this convention, the final state integrations in both cases are with respect to a positron and the hadronic final states. Let k , p_i , p_f , p_+ be the four momenta of the photon, the initial hadron, the final hadron and the final positron respectively and p the momentum of either the initial positron in the bremsstrahlung or the final detected electron in the pair production process. In the laboratory system the energy-angle distribution of the bremsstrahlung can be written as

$$d\sigma_b = \frac{1}{m_i |\vec{p}|} \frac{d^3 k}{2k} \int \frac{d^3 p_+}{2E_+} \int \frac{d^3 p_f}{2E_f} \delta^4(k + p_+ + p_f - p - p_i) A(k, p_+, p_f, p, p_i), \quad (\text{III. 77})$$

where A is the matrix element squared averaged over the initial polarizations and summed over the final polarizations of all the particles. The substitution rule says that for the pair production the matrix element squared averaged over the initial polarizations and summed over the final polarizations of all the particles is given by $-A(-k, p_+, p_f, -p, p_i)$, where the minus sign in front of A comes

from the fact that in the pair production there is only one antiparticle and $\bar{v}v = -1$.

Hence the pair production cross section can be written as

$$d\sigma_{\text{pair}} = \frac{1}{m_i k} \frac{d^3 p}{2E} \int \frac{d^3 p_+}{2E_+} \int \frac{d^3 p_f}{2E_f} \delta^4(p + p_+ + p_f - k - p_i) \\ (-1) A(-k, p_+, p_f, -p, p_i) . \quad (\text{III. 78})$$

Comparing Eqs. (III. 77) and (III. 78), it is obvious that the two energy-angle distributions are related by

$$\frac{d\sigma_b}{d\Omega_k dk} = - \left(\frac{d\sigma_{\text{pair}}}{d\Omega dp} \right)_{\substack{k_\mu \rightarrow -k_\mu \\ p_\mu \rightarrow -p_\mu}} \frac{k^2 E}{p^3} . \quad (\text{III. 79})$$

It was shown by Olsen¹⁷ (1955) that Eq. (III. 79) is still correct even when the Coulomb correction is included. In the earlier paper of Bethe and Maximon¹⁵ (1954), it was erroneously stated that the Coulomb correction does not affect the bremsstrahlung cross section whereas it does affect the pair production cross section. Using the substitution rule (III. 79), we obtain the energy angle distribution of electron or positron bremsstrahlung from (III. 5):

$$\frac{d\sigma_b}{d\Omega_k dk} = \frac{2\alpha^3}{\pi k} \frac{E^2}{m^4} \left\{ \left[\frac{2y-2}{(1+l)^2} + \frac{12l(1-y)}{(1+l)^4} \right] G_2(\infty) \right. \\ \left. + \left[\frac{2-2y+y^2}{(1+l)^2} - \frac{4l(1-y)}{(1+l)^4} \right] \left[X - 2Z^2 f((\alpha Z)^2) \right] \right\} , \quad (\text{III. 80})$$

where $G_2(\infty) = G_2^{\text{el}}(\infty) + G_2^{\text{inel}}(\infty) = Z^2 + Z$, $y = k/E$ and $l = \theta_k^2 E^2/m^2$. The Coulomb correction f is given by (III. 3) and the function X is given by (III. 6).

The minimum momentum transfer t'_{\min} used for calculating X is

$$t'_{\min} = \left[\frac{km^2(1+l)^2}{2E(E-k)} \right]^2, \quad (\text{III.81})$$

which is identical analytically to that for the pair production. However numerically t'_{\min} can be quite different in two problems because in the pair production we have $E/k < 1$, whereas in the bremsstrahlung we have $k/E < 1$. This has a consequence that the complete screening formula has a wider range of applicability in the bremsstrahlung problem than the pair production.

After integrating with respect to the photon angle θ_k , the term proportional to $G_2(\infty)$ in (III.80) vanishes and we obtain

$$\begin{aligned} \frac{d\sigma_b}{dk} = & \frac{\alpha^3}{m^2} \frac{1}{k} \left[\left(\frac{4}{3} - \frac{4}{3}y + y^2 \right) \left[Z^2(\phi_1 - \frac{4}{3} \ln Z - 4f) + Z(\psi_1 - \frac{8}{3} \ln Z) \right] \right. \\ & \left. + \frac{2}{3} (1-y) \left[Z^2(\phi_1 - \phi_2) + Z(\psi_1 - \psi_2) \right] \right]. \end{aligned} \quad (\text{III.82})$$

The function ϕ_1 , ϕ_2 , ψ_1 and ψ_2 are identical to those for the pair production problem. When the energy is high and if one is not particularly concerned with the detailed shape at the high energy tip of the bremsstrahlung spectrum, the functions ϕ_1 , ϕ_2 , ψ_1 and ψ_2 can be approximated by their values at $\gamma = 0$ and $\epsilon = 0$. Under this approximation, usually referred to as the complete screening case, we may write (III.82) as

$$\begin{aligned} \frac{d\sigma_b}{dk} = & 4\alpha r_0^2 \frac{1}{k} \left[\left(\frac{4}{3} - \frac{4}{3}y + y^2 \right) \left[Z^2(L_{\text{rad}} - f) + Z L'_{\text{rad}} \right] \right. \\ & \left. + \frac{1}{9} (1-y) (Z^2 + Z) \right], \end{aligned} \quad (\text{III.83})$$

(Complete Screening Formula)

where L_{rad} and L'_{rad} are tabulated in Table B.2. If we ignore the term $(1-y)(Z^2+Z)/9$, then Eq. (III.83) becomes proportional to $1/X_0$ defined in (III.66). In the infrared limit ($y \rightarrow 0$) the term is roughly 2.5% of the terms retained. Hence for any accurate work these terms should be retained. However if we are willing to ignore 2.5 % error, then (III.83) without $(1-y)(Z^2+Z)$ can be written as

$$\rho(k) dk dT = \frac{dk}{k} \left(\frac{4}{3} - \frac{4}{3} y + y^2 \right) dT, \quad (y = k/E) \quad (\text{III.84})$$

where $\rho(k)dk$ is the number of photons in the energy range dk after an electron passed through a target of thickness dT radiation length. The advantage of (II.84) is that it is independent of target material. In Section IV we shall consider the effect of finite target thickness.

E. Bremsstrahlung in Colliding Beam Experiment

Let us consider the emission of a single photon in the electron-electron or electron-positron colliding beam experiment. In each case there are eight Feynman diagrams. The exact calculation was first done by Votruba⁵⁶ (1948), whose results are extremely complicated. Fortunately with the recent advance in computer, the derivation of Votruba's formula can easily be done using various algebraic routines, e.g., "Reduce" by A.C. Hearn⁵⁷ or "Shooship" by T. Veltman (1965).⁵⁸ The important thing is that the result of the computer derivation is usually already in a form usable for the computer to do further numerical calculations. Hence when one is dealing with a formula as complicated as that of Votruba, it is easier to start from scratch than starting from the expression given by Votruba. S. Swenson⁵⁹ (1967) investigated the process $e^+e^- \rightarrow e^+e^- + \gamma$ using his own version of algebraic computer routine. He concluded that near the forward direction only two Feynman diagrams similar to those shown in

Fig. II. 1 need be considered. Hence, the result is given by (III. 80) with $f = 0$, $G_2 = 1$ and X given by the right hand side of (III. 24):

$$\frac{d\sigma_b}{d\Omega_k dk} = \frac{2\alpha^3}{\pi k} \frac{E^2}{m^4} \left\{ \frac{2y-2}{(1+l)^2} + \frac{12l(1-y)}{(1+l)^4} + \left[\frac{2-2y+y^2}{(1+l)^2} - \frac{4l(1-y)}{(1+l)^4} \right] \left[2\ln(m/\delta) - 1 \right] \right\} . \quad (\text{III. 85})$$

where $y = k/E$, $l = \theta_k^2 E^2/m^2$ and $\delta = \frac{1}{2} m^2 y/E(1-y)$.

This expression is identical to the one obtained by Sommerfeld⁴¹ (1939). This formula can be written in such a way that it becomes usable both in the center of mass system and also in the laboratory system. The easiest way to do this is to realize that at high energies and small angles, both $y = k/E$ and $l = \theta_k^2 E^2/m^2$ are relativistically invariant and Eq. (III. 85) can be written covariantly as

$$\frac{d\sigma_b}{d\ell dy} = \frac{4\alpha^3}{y m^2} \left\{ \quad \right\} , \quad (\text{III. 86})$$

where $\left\{ \quad \right\}$ is the expression in the curly bracket of (III. 85). In the colliding beam experiment, the bremsstrahlung angular distribution is symmetric with respect to 90° . The backward peak disappears into the infrared after the Lorentz transformation from the center of mass system to the laboratory system. Equation (III. 85) can be integrated with respect to angle easily, we obtain

$$\frac{d\sigma_b}{dy} = \frac{4\alpha^3}{y m^2} \left\{ \frac{4}{3} - \frac{4}{3} y + y^2 \right\} \left[2\ln(m/\delta) - 1 \right] . \quad (\text{III. 87})$$

F. $e^+ + e^- \rightarrow 2\gamma, 3\gamma$

When a positron is incident on an atomic target, it can annihilate with an atomic electron and produce photons. The cross section for $e^+e^- \rightarrow 2\gamma$ is of

order α^2 compared to the cross section for $e^+ + e^- \rightarrow e^+ + e^- + \gamma$ which is of order α^3 . However at high energies the former is negligible compared with the latter except when the angle θ_k is near $(2m/E)^{1/2}$ which corresponds to 90° in the center of mass system of initial e^+ and e^- . Since $e^+ + e^- \rightarrow 2\gamma$ has a two body final state, the energy of the photon is fixed at a fixed angle:

$$k = \frac{m^2 + Em}{m + (E - pc \cos \theta_k)} \xrightarrow[\substack{\gamma \gg 1 \\ \theta_k \ll 1}]{} E / (1 + \frac{1}{2} \gamma \theta_k^2), \quad (\text{III. 88})$$

which is equal to the value of k_{max} in the reaction $e^+ + e^- \rightarrow e^+ + e^- + \gamma$. For θ_k near $(2/\gamma)^{1/2}$, the photon spectrum $d\sigma/d\Omega_k dk$ from $e^+ + H_2$ has a sharp spike. The spike, instead of being a δ function, has a finite width because of radiative corrections (Tsai, 1965⁶⁰). This spike is a very useful source of semimonochromatic photon beam. The detailed theoretical discussions of the properties of this spike and the background were given by Dufner, Swanson and Tsai (1966).⁶¹ The cross section for $e^+ + e^- \rightarrow 2\gamma$ can be written as

$$\frac{d\sigma_a}{d\Omega_k} \xrightarrow[\substack{\theta_k \ll 1 \\ \gamma \gg 1}]{} \frac{\alpha^2}{2m^2(1+z)^2} \left[\frac{2\gamma}{1+\ell} + \frac{1+\ell}{2\gamma} + \frac{4\ell(1+z)^2}{(1+\ell)^2} \right], \quad (\text{III. 89})$$

where $\gamma = E/m$ of the incident positron, $z = \gamma \theta_k^2/2$ and $\ell = \gamma^2 \theta_k^2$. If one is interested in obtaining the semimonochromatic photon beam, then the angle θ_k must be chosen so that z is of order unity, in which case the spike is very pronounced compared with the ordinary bremsstrahlung background given by (III. 80). On the other hand if one is not interested in obtaining a semimonochromatic beam but wants to know how the angle-integrated photon spectrum is affected by the

annihilation photons, it is more convenient to write (III.89) in terms of $d\sigma_a/dk$ using the relation (III.88). We obtain

$$\frac{d\sigma_a}{dk} \approx \frac{\alpha^2 \pi}{E_m^2} \left[\frac{y}{(y/2\gamma) + (1-y)} + \frac{(y/2\gamma) + (1-y)}{y} \right], \quad (\text{III.90})$$

where $y = k/E$. We have ignored the last term in (III.89). This equation must be multiplied by Z before we can make the comparison with (III.82). The effect is largest for hydrogen, therefore let us consider this as an example. When k is small we have

$$(d\sigma_a/dk)/(d\sigma_b/dk) \xrightarrow[k \rightarrow 0]{} \frac{\pi}{\alpha \gamma 50} \approx 7/\gamma \quad (\text{III.91})$$

which shows that effect in the soft photon region is not noticeable unless the incident positron energy is below 300 MeV. Near the high energy end of the spectrum ($y \rightarrow 1$), we have

$$(d\sigma_a/dk)/(d\sigma_b/dk) \xrightarrow[k \rightarrow E]{} \frac{10}{\gamma} \frac{1}{1/(2\gamma) + (1-y)}, \quad (\text{III.92})$$

which is clearly peaked at $y = 1$ with a small width ($\Delta y \sim (1/2\gamma)$). If the effect of the radiative correction is included, the width of this spike gets widened. Hence when $E > 1$ GeV it is probably unnoticeable.

G. Muon Bremsstrahlung

As noted previously, even though t'_{\min} for the bremsstrahlung has an identical analytical expression to that for the pair production, numerically the former can be much smaller than the latter. In the muon pair production, the atomic screening as well as the production in the electron field can be ignored, but for

the muon bremsstrahlung neither of these effects can be ignored when the photon emitted is very soft. The atomic radius is roughly given by $a \sim Z^{-1/3} 137/m_e$, hence the atomic screening becomes important when

$$1 \lesssim t_{\min}^{1/2} a = \frac{m_{\mu}^2 k(1+\ell)}{2E(E-k)} \frac{Z^{-1/3} 137}{m_e} \quad (\text{III. 93})$$

In the forward angle, this gives

$$\frac{y}{1-y} \lesssim \frac{Z^{1/3} E}{1370 \text{ GeV}} \quad (\text{III. 94})$$

which shows that when E is above one hundred GeV, the atomic screening is not negligible. On the other hand, when E is much below one hundred GeV, the atomic screening becomes non-negligible only when very soft photons are emitted.

The energy loss of a muon due to bremsstrahlung is negligible compared with that due to ionization when the energy is so low that its range is considerably less than $(m_{\mu}/m_e)^2 X_0$, where X_0 is the unit radiation length defined previously. However when the muon energy is one hundred GeV or higher, its range becomes comparable to or greater than $40,000 X_0$. After a muon passes through a material of thickness comparable to $40,000 X_0$, its energy is greatly affected by the bremsstrahlung. When the muon energy is higher than one hundred GeV, the nuclear form factor is negligible except at the bremsstrahlung tip, whereas the atomic form factor affects the low energy photon emission. This means that Eq. (III.82) can also be used for the muon bremsstrahlung except near the high energy tip of the bremsstrahlung. The parameters γ and ϵ defined in (III.30) and (III.31) should now read respectively

$$\gamma = \frac{100 m_{\mu}^2 k}{E(E-k) Z^{1/3} m_e} \quad (\text{III. 95})$$

and

$$\epsilon = \frac{100 m_{\mu}^2 k}{E(E-k) Z^{2/3} m_e} \quad (\text{III. 96})$$

As noted previously, the function ϕ_1 and ϕ_2 become approximately equal to the value given by the unscreened target at around $\gamma = 2$. Substituting $\gamma = 2$ in (III. 95), we obtain a relation similar to (III. 94).

It should be emphasized that the problem we are discussing here is usually called the "outer bremsstrahlung" or "external bremsstrahlung", in contrast to the "inner bremsstrahlung" or "internal bremsstrahlung" which one deals with when discussing the bremsstrahlung emission during the large angle (angle much larger than one characteristic angle) scattering. There are two major distinctions between the two kinds of phenomena (Mo and Tsai⁶², 1969). For inner-bremsstrahlung the scattered electron or muon is detected at an angle much greater than one characteristic angle. In this case the bremsstrahlung emission is roughly proportional to $\ln(-q^2/m^2) - 1$, hence the radiative corrections to muon scattering is about 0.25 to 0.5 of the radiative corrections to the electron scattering in the q^2 range of 1 to 10 GeV². This is to be contrasted with the corresponding ratio $(m_e/m_{\mu})^2 \approx 40,000^{-1}$ for the outer-bremsstrahlung. For the inner-bremsstrahlung, the angular distribution of photons are concentrated in the two directions, namely, along the incident electron (or muon) and the outgoing electron (or muon). The root mean square angle between the photon and the electron (or muon) is $\langle \theta_k^2 \rangle^{1/2} \approx (m/E)^{1/2}$, where E is the energy of the incident or outgoing lepton. For the outer-bremsstrahlung the characteristic angle is m/E with respect to the incident lepton.

In the electron scattering experiment, both the external and the internal bremsstrahlung have to be considered (see Mo-Tsai, 1969⁶² and Tsai, 1971⁶⁵), whereas in

the muon scattering experiments we need to consider only the corrections due to the internal bremsstrahlung. The external bremsstrahlung of muons is important when one is dealing with shielding of muons which have energies of more than one hundred GeV.

IV. EFFECTS DUE TO FINITE TARGET THICKNESS

When one is dealing with photons or electrons in any experiment at high energies, it is important to take into account the attenuation of the photon beam and the straggling of the electron in the medium. At high energies the attenuation in the intensity of a photon beam is mainly due to the electron pair production given by (III.75). The effects such as ionization, Compton scattering, nuclear excitation, meson production etc. are negligible even though these effects have one or two less powers of α in their expressions for the cross section than the pair production. The straggling of the electron at high energies is mainly due to bremsstrahlung. The Landau straggling (Landau⁶³ 1944), i.e., the energy straggling of the electron due to the e-e scattering, can be ignored compared with that due to the bremsstrahlung emission if the energy loss ΔE satisfies the inequality⁶⁵

$$\frac{2\alpha}{\pi} (Z L_{\text{rad}} + L'_{\text{rad}}) \Delta E/m \gg 1, \quad (\text{IV.1})$$

where L_{rad} and L'_{rad} are radiation logarithms tabulated in Table B.2. For hydrogen, this condition is equivalent to $\Delta E \gg 10$ MeV. The combined effects of Landau and bremsstrahlung straggling can be found in the works of Bergstrom⁶⁴ (1967) and Tsai⁶⁵ (1971). This consideration is important when one is interested in obtaining the shape of a resonance using electrons with energy less than several hundred MeV.

In this section we shall follow the notation of Tsai and Whitis (1966).⁶⁶ Let the number of photons produced by an incident electron with energy E_0 from a target of infinitesimal thickness dt radiation length in the energy interval dk be

$$\rho(E_0, k) dt dk \equiv \frac{d\sigma_b}{dk} \frac{N}{A} X_0 dt dk, \quad (\text{IV.2})$$

where N is the Avogadro's number, A is atomic weight, X_0 is the unit radiation length given in Table III.6, $d\sigma_b/dk$ is calculated according to (III.82). The attenuation factor for a photon after passing through a medium of t radiation length is $e^{-\mu t}$, where $\mu = -\frac{7}{9}(1 - \xi)$, with ξ given in Table III.5. The energy distribution of the first generation electron is denoted by $I_e^{(1)}(E_0, E, t)$. An electron initially with energy E_0 , after passing through a target of thickness t will have a probability $I_e^{(1)}(E_0, E, t) dE$ of being in the energy interval between E and $E + dE$. The number of photons in the energy between k and $k + dk$ after an electron, initially with an energy E_0 , passed through a target of thickness t is denoted by $I_\gamma^{(1)}(E_0, k, t) dk$. It was shown in Tsai and Whitis⁶⁶ that the second generation electrons as well as the second generation photons are negligible compared with the first generation ones as long as the target thickness is less than two radiation lengths. Hence we shall omit the superscript "(1)" from $I_e^{(1)}(E_0, E, t)$ and $I_\gamma^{(1)}(E_0, k, t)$. Another important quantity denoted by b is defined as

$$b \equiv \lim_{k \rightarrow 0} k\rho(E, k) = \frac{4}{3} \left(1 + \frac{1}{12} \frac{Z^2 + Z}{Z^2 L_{\text{rad}} + Z L'_{\text{rad}}} \right), \quad (\text{IV.3})$$

where the radiation logarithms L_{rad} and L'_{rad} are tabulated in Table B.2.

A. Straggling of an Electron due to Bremsstrahlung

The straggling function of an electron $I_e(E_0, E, t)$ was first considered by Bethe and Heitler¹³ (1934), which was later rederived and extended by Eyges⁶⁷ (1949). Eyges showed that if the bremsstrahlung distribution function $\rho(E, k)$ were given by

$$\rho(E, k) = \frac{1}{E} b(1-y)^a [\ln(1-y)]^{-1}, \quad (\text{IV.4})$$

where $y = k/E$, a and b are arbitrary positive numbers, then the straggling function for an electron would be given by

$$I_e(E_0, E, t) = \frac{(1+a)^{bt}}{\Gamma(1+bt)} \left[\ln\left(\frac{E_0}{E}\right) \right]^{bt} \rho(E_0, k)t, \quad (\text{IV.5})$$

where $k = E_0 - E$ and Γ is the Gamma function which for small bt is given by

$$\Gamma(1+bt) \xrightarrow{bt \ll 1} 1 - 0.5772bt.$$

The original treatment of Bethe-Heitler is a special case where $a = 0$. Now the trouble is that the actual bremsstrahlung spectrum (IV.2) has a very different shape from (IV.4). At high energies, the complete screening formula given by Eq. (III.84) is adequate except near the bremsstrahlung tip. If we normalize the parameter b in (IV.4) at the infrared limit, namely (IV.3), we see that (IV.4) is way too low at the high energy side of the bremsstrahlung spectrum. The factor $(1-y)^a$ tends to suppress the high energy end of the spectrum, hence $a = 0$ is the most reasonable choice for this parameter. If t is so small that an electron suffers only a single collision, then by definition we must have

$$\lim_{t \rightarrow 0} I_e(E_0, E, t) = \rho(E_0, E_0 - E) t. \quad (\text{IV.6})$$

This shows that the factor $[\ln(E_0/E)]^{bt}/\Gamma(1+bt)$ in (IV.5) represents the correction due to multiple collisions. If we assume that this correction factor is independent of the expression of $\rho(k)$, from which it was derived, then we can simply use a correct expression for $\rho(k)$ in (IV.5) instead of using (IV.4). This procedure was first proposed by Mo and Tsai⁶² (1969). Subsequently R. A. Early⁶⁷ (1972) made a detailed study of numerical solution of the electron diffusion equation using the complete screening formula for $\rho(k)$ as given by Eq. (III.84). He found that the maximum disagreement between his numerical result for $I_e(E_0, E, t)$ and that given by Eq. (IV.5) with $\rho(k)$ given by (III.84) instead of (IV.4) is less than one percent if t is less than 0.01 r.l. However, when $t = 0.1$ r.l. Eq. (IV.5) in general overestimates $I_e(E_0, E, t)$ at low energy end of the electron spectrum; for example, the overestimate is about 9% at $E/E_0 = 0.1$. Based on Early's numerical work, a better straggling function (Tsai⁶⁵ 1971) was proposed:

$$I_e(E_0, E, t) = \left(\frac{E_0 - E}{E_0}\right)^{bt} \rho(E_0, E_0 - E) t / \Gamma(1 + bt) . \quad (IV.7)$$

This function is within 1% of Early's numerical work when $t < 0.05$ r.l. and $E/E_0 > 0.2$. The best fit to Early's numerical work was obtained by G. Miller⁶⁹ (1971) whose result is

$$I_e(E_0, E, t) = \frac{1}{\Gamma(1+bt)} \left(\ln \frac{E_0}{E}\right)^{bt} \rho(k) t \times [1 + bty \{ .53875 + y (-2.1938 + .9634y) \}] , \quad (IV.8)$$

where

$$y = (E_0 - E)/E_0 .$$

This formula agrees with Early's numerical results to within 0.6% for $E/E_0 > 0.1$ and $t < 0.1$ r.l. The precise form of $I_e(E_0, E, t)$ is very important in the radiative corrections to the electron scattering experiment. ^{62, 65, 69}

B. Thin Target Bremsstrahlung

The photon spectrum from a target with thickness t can be calculated from the following formula (Tsai and Whitis ⁶⁶)

$$I_\gamma(E_0, k, t) = \int_0^t e^{-\mu(t-t')} dt' \int_k^{E_0} I_e(E_0, E, t') \rho(E, k) dE, \quad (IV.9)$$

where $\mu = \frac{7}{9} (1 - \xi)$ and ξ is tabulated in Table III.5. The integration with respect to t' can be carried out analytically if the target is so thin ($t \leq 0.1$) that the inverse of the gamma function in (IV.7) can be approximated by $\Gamma^{-1}(1 + bt') \sim 1 + 0.5772 bt'$. We notice that when $t \ll 1$ r.l., $I_e(E_0, E, t)$ is very large near $E = E_0$, hence we need to know very accurately its value only near $E = E_0$, in which case (IV.9) can be approximated by

$$I_\gamma(E_0, k, t) \xrightarrow{t \ll 1} \int_0^t dt' e^{-\mu(t-t')} (1 + 0.5772 bt') \int_k^{E_0} \left(\frac{E_0 - E}{E_0}\right)^{bt'-1} \rho(E, k) \frac{dE}{E_0} \quad (IV.10)$$

$$= \int_k^{E_0} e^{-\mu t} \left[\frac{T e^{BT}}{B} + \left(\frac{1}{B^2} - \frac{2\gamma}{B^3} \right) (1 - e^{BT}) + \gamma e^{BT} \left(\frac{T^2}{B} - \frac{2T}{B^2} \right) \right]$$

$$\rho(E, k) dE/E_0, \quad (IV.11)$$

where

$$T = bt, \quad B = -7/(9b) + \ln(1 - E/E_0),$$

$\gamma = 0.5772$, $\rho(E, k)$ and b are given by Eqs. (IV.2) and (IV.3) respectively. It should be emphasized that even for t as small as 0.01 r.l. the result of (IV.11)

differs by several percents from that of using (IV.2) near the bremsstrahlung tip ($0.98 < k/E_0 < 1$), therefore for any accurate work using the bremsstrahlung tip, one should use (IV.11) instead of (IV.2).

C. Approximate Expression for Thick Target Bremsstrahlung

It is sometimes desirable to have a simple formula for $I_\gamma(E_0, E, t)$ valid also for target of thickness up to 2 radiation lengths, for example, in the estimation of the secondary particle yields from an electron machine. Let us first consider some qualitative features. From Eq. (IV.5) or (IV.7), we see that the electron spectrum $I_e(E_0, E, t)$ changes its shape abruptly at $t = b^{-1} \approx .75$ r.l. For $t < 0.75$ we have $I_e(E_0, E_0, t) = \infty$, whereas for $t > 0.75$ we have $I_e(E_0, E_0, t) = 0$. This tells us that practically all high energy γ 's are produced from $t = 0$ to $t = 0.75$, and after $t = 0.75$, the intensity of γ 's is just attenuated by the absorption factor $e^{-7/9(t-0.75)}$. At $t = .75$, the electron spectrum is essentially flat. It was shown by Tsai and Whitis (1966) that because of the nuclear absorption of the photoproduced hadrons, the optimum thickness for the production of high energy hadrons is roughly 2 r.l. for Be and slightly larger for heavier elements. For production of muons (or heavy leptons) the nuclear absorption is negligible, but even in this case one reaches more than 90% of the possible maximum yield when $t = 4$ r.l. In order to obtain a simple formula for $I_\gamma(E_0, k, t)$ which is approximately true when $E_0 > k > \frac{1}{2} E_0$, we note that the integrand in (IV.9) is dominated by the region $E_0 \rightarrow E$ and $t' \ll 1$. Hence we need to know very accurately about the integrand only in this region. The gamma function has values $\Gamma(1) = \Gamma(2) = 1$ and $\Gamma(x) \leq 1$ for x between 1 and 2, the minimum occurs at $\Gamma(1.46) = .8856$. Hence we shall approximate $\Gamma(1+bt')$ by one, which will result in underestimating I_γ by less than 10%. We shall also ignore the energy dependence of μ and approximate it by $\mu = 7/9$. Since we are interested in the high energy component of the

the photons, we may approximate $\rho(E, k)$ by $1/k$, which gives at most 10% over-estimate at high energy half of the spectrum. The result is

$$[I_{\gamma}(E_0, E, t)]_{\text{approx}} = \frac{1}{k} \frac{(1 - k/E_0)^{bt} - e^{-(7/9)t}}{k[7/9 + \frac{4}{3} \ln(1-k/E_0)]} \quad (\text{IV.12})$$

The numerical values of this expression from $t = 0.01$ to $t = 2.0$ and $0.1 < k/E_0 < 0.999$ are tabulated in Tsai and Whitis paper⁶⁶ (1966) together with the results of using (IV.9). The difference between the two values is about 0 to 15%.

D. Production of Particles Using a Photon Beam

The photon source may be a bremsstrahlung beam obtained by placing a radiator up stream in the case of electron accelerator or it may be the photon beam produced by π^0 decay as usually the case for the proton accelerator. In the former case the photon flux is given by $I_{\gamma}(E_0, k, t)dk$ per incident electron or positron. In the latter case π^0 flux is usually estimated by assuming that it is the average of π^+ and π^- fluxes. In either case the photon spectrum can be determined by a pair spectrometer. Let us assume that the photon flux impinges upon a target of thickness T r.l. and the photoproduction cross section is given by $d\sigma/d\Omega dp$. The number of events induced by a single photon in this target is then

$$\int_0^T \exp(-\mu t) \frac{d\sigma}{d\Omega dp} \frac{NX_0}{A} dt = \frac{1 - \exp(-\mu T)}{\mu} \frac{NX_0}{A} \frac{d\sigma}{dp d\Omega} \quad (\text{IV.13})$$

where μ is the absorption coefficient for photon $\mu = (7/9)(1 - \xi)$ as given previously. This simple formula tells us two things: 1) There is no use making the target thickness more than two radiation lengths. When $T = 2$, we have

$\exp(-7T/9) = 0.22$, hence only 22% of the photon beam is wasted. As the target gets thicker, the effects due to the straggling, multiple scatterings and the absorption of the produced particles become complicated. 2) The factor NX_0/A is roughly proportional to $(Z^2 + Z)^{-1}$. For production of particles other than electrons or muons the cross sections are usually proportional to A or $A^{2/3}$. Hence as far as maximizing the yield is concerned, small Z material is preferable. This is the reason why we have chosen H and Be in our calculation of the production of heavy leptons. If the produced particle is a muon it will come out of the target essentially unaffected except some loss of energy due to ionization. If the produced particle (or the decay product of the produced particle) is an electron, its energy will straggle due to the emission of bremsstrahlung. This bremsstrahlung has two parts: inner and outer bremsstrahlung. The effect due to outer bremsstrahlung can be calculated by using $I_e(E_0, E, T-t)$. The effect due to the inner bremsstrahlung is part of the usual radiative corrections, which is independent of target thickness. If the produced particles are hadrons, then the effect due to nuclear absorption must be taken into account.

E. Production of Particles Using an Electron Beam

For particle production in an electron machine the maximum yield is obtained if the electron beam is used directly on the target. We shall show in the next subsection, that the production by the virtual photon is negligible compared with the production by the real photon if the target thickness is much more than $1/25$ of a radiation length. Consider "a" monochromatic electron with an energy E_0 incident on a target of T radiation lengths. Let $\sigma(k)$ represent some photoproduction cross section. $\sigma(k)$ can be either $d\sigma/d\Omega dp$, $d\sigma/dp$ or σ , etc. The total number of events per incident electron induced by the real photon in the target material

is given by

$$Y = \frac{NX_0}{A} \int_0^T dt \int_{k_{\min}}^{E_0} I_\gamma(t, k) \sigma(k) dk \quad (IV.14)$$

Using the approximate expression of I_γ given in (IV.12), Eq. (IV.14) can be integrated with respect to dt . We obtain

$$Y = \frac{NX_0}{A} \int_{k_{\min}}^{E_0} \sigma(k) \left\{ (1 - e^{-fT})/f - \frac{9}{7} (1 - e^{-(7/9)T}) \right\} \left/ \left(\frac{7}{9} - f \right) \frac{dk}{k} \right. \quad (IV.15)$$

where

$$f = -\frac{4}{3} \ln(1 - k/E_0).$$

In the limits $T \rightarrow 0$ and $T \rightarrow \infty$ we have respectively

$$Y \xrightarrow{T \rightarrow 0} \frac{NX_0}{A} \frac{T^2}{2} \int_{k_{\min}}^{E_0} \sigma(k) \frac{dk}{k} \quad (IV.16)$$

and

$$Y \xrightarrow{T \rightarrow \infty} \frac{NX_0}{A} \int_{k_{\min}}^{E_0} \sigma(k) \frac{9}{7f} \frac{dk}{k} \quad (IV.17)$$

From Eqs. (IV.15 through IV.17), we see that the yield of secondary particles by an electron is proportional to T^2 when T is small and becomes independent of T as T becomes infinity. How fast this maximum is reached depends upon whether the process requires soft or hard component of the bremsstrahlung. High energy component of the photon diminishes more rapidly than the low energy component as the target thickness is increased. When $k/E_0 = 0.442$ (which corresponds to $f = 7/9$), the ratio of the integrand of Eq. (IV.15) to that of Eq. (IV.17) is equal

to $[1 - (1 - 7T/9) \exp(-7T/9)]$, hence when $T = 3$ one already gets 68% of the maximum value. If the target thickness is increased beyond $T = 3$, we gain somewhat in the yield but the increased absorption and straggling of the outgoing particles in the target may render this small gain in yield not worthwhile. For hadron production, $T = 2$ is the optimal thickness if one takes into account the nuclear absorption of the hadrons (Tsai and Whitis, 1966).

F. Production by Virtual Photons. (Equivalent Radiator for Electroproduction)

When an electron is used for production of particles, the contribution due to the direct electroproduction is approximately equal to the contribution from a real bremsstrahlung beam produced by letting the electron pass through a radiator of thickness $\sim 1/50$ radiation lengths (called the equivalent radiator whose thickness is denoted by t_{eq}). This implies that the production due to the virtual photon is negligible compared with that due to the real photons if the target is much thicker than $2 t_{eq}$. This fact is well known among experts but sounds strange to many people because the electroproduction cross section has two powers of α less than the combined α dependence of the bremsstrahlung emission cross section and the production cross section by a real photon. In the following we derive the expression for t_{eq} using the Weizsacker-Williams method. Let E and E' be the energies of the incident and outgoing electrons respectively and θ be the scattering angle of the electrons. The cross section can be written as

$$\frac{d\sigma}{d\nu dt} = \frac{2\pi\alpha^2}{t^2} \frac{1}{E^2 - m_e^2} \left[\left\{ 2E(E-\nu) - \frac{t}{2} \right\} W_2 + (t - 2m_e^2) W_1 \right] \quad (IV.18)$$

where $\nu = E - E'$ and $t = -(p-p')^2$. We have retained the mass of the electron because t_{min} is proportional to m_e^2 as given by Eq. (A.11). From the definition

of the tensor $W_{\mu\nu}$ given in Section II, we obtain

$$W_1 = W_{xx}$$

$$W_2 = \frac{t^2}{\nu^2(t + \nu^2)} \left[W_{zz} + (\nu^2/t) W_{xx} \right], \quad (IV.19)$$

where the direction of the momentum transfer in the laboratory system is chosen as the z axis. The transverse tensor W_{xx} is related to the photoproduction cross section

$$\sigma_\gamma(\nu) = \frac{4\pi^2\alpha}{\nu} W_{xx}(t=0, \nu). \quad (IV.20)$$

Since W_{zz} and W_{xx} are not singular at $t=0$, we can ignore W_{zz} in (IV.19) when $\nu^2 \gg t$. Ignoring the t dependence of W_{xx} and assuming $\nu^2 \gg t$, we have

$$\frac{d\sigma}{d\nu} \approx \frac{\alpha}{2\pi} \frac{\sigma_\gamma(\nu)}{\nu} \int_{t_{\min}}^{t_{\max}} \left[(2 - 2y + y^2) \frac{1}{t} - \frac{2m_e^2 y^2}{t^2} \right] dt$$

$$\approx \frac{\sigma_\gamma(\nu)}{\nu} \frac{\alpha}{\pi} \left[(1 - y + \frac{1}{2}y^2) \ln(t_{\max}/t_{\min}) - (1 - y) \right], \quad (IV.21)$$

where $y = \nu/E$ and $t_{\min} = m_e^2 y^2 / (1 - y)$. The true t_{\max} is $4E(E - \nu)$ which can be very large. Rather than using this value of t_{\max} , it is better to regard it as a cut-off parameter which approximately takes care of the t dependence of W_{xx} . Now this t dependence is different for different processes and different targets. Fortunately (IV.21) is not very sensitive to t_{\max} . A convenient choice is $t_{\max} \sim m_\rho^2 \approx 0.5 \text{ GeV}^2$ which is roughly the cut off required for production of hadrons.

Now the bremsstrahlung spectrum of an electron after passing through a target of t radiation lengths ($t \ll 1$) is roughly tdk/k . Hence Eq. (IV.21) says

that the desired expression for t_{eq} is given by

$$t_{eq} = \frac{\alpha}{\pi} \left[(1 - y + \frac{1}{2}y^2) \ln \frac{m_\rho^2(1-y)}{m_e^2 y^2} - (1 - y) \right] \quad (IV.22)$$

$$\sim \frac{\alpha}{\pi} \ln (m_\rho / m_e) = 0.017 \quad (IV.23)$$

The last expression is given there for the purpose of indicating the order of magnitude of t_{eq} .

The equivalent radiator introduced here represents the pseudophoton flux of the incident electron. The equivalent radiator representing the pseudophoton flux of the target nucleus has been considered in great detail by Kim and Tsai (1973). The concept of a pseudophoton flux of a charged particle has a meaning only in the frame where the particle is moving with extreme relativistic speed. (See e. g. , Appendix C of Kim and Tsai, 1973). Since the incident electron is already relativistic in the laboratory system, the concept of pseudophoton flux is directly usable in the laboratory system without making a Lorentz transformation which is required when one is dealing with the pseudophoton flux of a target particle. The interesting characteristics of t_{eq} given by (IV.22) is that it is a function of scaling variable y only.

Let us consider the number of events induced by a single incident electron in a target of T radiation lengths. We denote the part due to the virtual photon by $Y_{virtual}$ and the part due to the real photon by Y_{real} . When the target

is thin we may ignore the straggling of the electron in the target, hence the yield due to the virtual photon is

$$Y_{\text{virtual}} \xrightarrow{T \rightarrow 0} \frac{NX_0}{A} T \int_{k_{\text{min}}}^{E_0} t_{\text{eq}} \frac{\sigma(k)}{k} dk \quad (\text{IV.25})$$

Comparing Eq. (IV.25) with Eq. (IV.16) we see that when $T = 2 t_{\text{eq}}$, the virtual photon contribution is approximately equal to the real photon contribution. When the target is thick, Y_{virtual} will not increase linearly with T because of straggling. We expect it to level out at around three or four radiation lengths. The yield by virtual photons of an electron in a target of thickness T can be written as

$$Y_{\text{virtual}} = \frac{NX_0}{A} \int_0^T dt \int_{k_{\text{min}}}^{E_0} I_e(E_0, E, t) dE \int_{k_{\text{min}}}^E dk t_{\text{eq}} \frac{\sigma(k)}{k} \quad (\text{IV.26})$$

where I_e is the straggling function of the electron given by Eq. (IV.5). Since we are interested in the high energy component of the photon, we may approximate the factor $(2-2k/E+k^2/E^2)$ by 1 and the $\rho(E,k)$ in Eq. (IV.5) by b/k . $\Gamma(1+bt)$ can also be approximated by unity because most of the contribution comes from the region $bt < 1$. With these approximations and the identity

$$\int_{k_{\min}}^{E_0} dE \int_{k_{\min}}^E dk = \int_{k_{\min}}^{E_0} dk \int_k^{E_0} dE$$

the integration with respect to dt and dE can be carried out when $T = \infty$. We obtain

$$Y_{\text{virtual}} \xrightarrow{T \rightarrow \infty} \frac{NX_0}{Ab} \int_{k_{\min}}^{E_0} \sigma(k) t_{\text{eq}} / \ln [E_0/(E_0-k)] \frac{dk}{k} . \quad (\text{IV.27})$$

From Eqs. (IV.17) and (IV.27), we obtain

$$(Y_{\text{virtual}}/Y_{\text{real}}) \xrightarrow{T \rightarrow \infty} \frac{7}{9} t_{\text{eq}} . \quad (\text{IV.28})$$

V. PRODUCTION OF MUONS AND HEAVY LEPTONS (NUMERICAL EXAMPLES)

In this section we present numerical examples of calculations using (II.7), which is an exact result in the lowest order Born approximation. The target particles are assumed to be either hydrogen or beryllium. The elastic and inelastic nuclear form factors necessary for the calculations are discussed in Appendix B. The numerical examples given in this section are intended to help experimentalists in designing experiments to discover heavy leptons. The calculations for muons are also included because they can be used in estimating the

yield of muons from an electron machine and also in estimating the background for the heavy lepton experiment. The various numerical tables given can also be used for checking the accuracy of various approximation schemes such as the Weizsacher Williams method. Since different experiments involve different kinematical conditions, the experimenters have to recompute many quantities. Our numerical tables can serve as convenient reference for such calculations. Let us begin by discussing some kinematics which defines the physical region of the problem.

A. Kinematics

The minimum energy of the photon required to produce a pair of leptons, each of mass m , and one of the leptons having a momentum p and an angle θ can be obtained by setting the expression for $U^2 = (p_f + p_+)^2$ given by Eq. (II.4) equal to $(m_f + m)^2$:

$$k_{\min} = (m_f^2 - m_i^2 + 2m m_f + 2m_i E) / (2m_i - 2E + 2p \cos \theta) . \quad (V.1)$$

For the coherent scattering from a nucleus we set $m_f = m_i = Am_p$, for the elastic scattering from a proton we set $m_f = m_i = m_p$, and for the meson production from a proton we set $m_i = m_p$ and $m_f = m_p + m_\pi$. The computer has to be instructed to skip the calculation unless the conditions

$$k > k_{\min} \quad \text{and} \quad k_{\min} > 0 \quad (V.2)$$

are satisfied.

For the calculation of

$$\frac{d\sigma}{dp} = 2\pi \int_{\cos \theta_{\max}}^1 \frac{d\sigma}{d\Omega dp} d\cos \theta , \quad (V.3)$$

we need to know $\cos \theta_{\max}$ and the allowed range of p . In order to obtain $\cos \theta_{\max}$, we notice from Eq. (II.4) that for given k and p , U^2 increases with $\cos \theta$. Hence $\cos \theta_{\max}$ can be obtained by setting U^2 to its minimum value, $(m_f + m)^2$. Of course $\cos \theta_{\max}$ can not be smaller than -1 , therefore we first define

$$\cos \theta'_{\max} = \left[(m_f^2 - m_i^2)/2 + m m_f - m_i(k-E) + kE \right] / (kp), \quad (\text{V.4})$$

which is obtained by setting $U^2 = (m_f + m)^2$. Then the desired expression for $\cos \theta_{\max}$ is

$$\cos \theta_{\max} = \cos \theta'_{\max}, \quad \text{if} \quad \cos \theta'_{\max} > -1; \quad (\text{V.5})$$

and

$$\cos \theta_{\max} = -1, \quad \text{if} \quad \cos \theta'_{\max} \leq -1. \quad (\text{V.6})$$

The allowed range of momentum p in Eq. (V.3) can be obtained by setting $U^2 = (m_f + m)^2$ and $\cos \theta = 1$. We obtain:

$$p_{\max}^{\min} = \left[kX \pm (k + m_i) (X^2 - m^2 S)^{1/2} \right] / S, \quad (\text{V.7})$$

where

$$X = m_i k - m_f m - (m_f^2 - m_i^2)/2$$

and

$$S = m_i^2 + 2k m_i.$$

If p_{\min} calculated according to the above formula is less than zero, then $p_{\min} = 0$.

The total cross section σ is calculated from

$$\sigma = \int_{p_{\min}}^{p_{\max}} \frac{d\sigma}{dp} dp, \quad (\text{V.8})$$

where p_{\max} and p_{\min} are calculated according to the prescription given above. In the calculation of both $d\sigma/dp$ and σ , the computer has to be instructed to skip the calculation unless the threshold condition,

$$k > [(2m + m_f)^2 - m_i^2] / 2m_i, \quad (\text{V.9})$$

is satisfied.

B. Energy-Angle Distributions

$d\sigma/d\Omega dp$ for photoproduction of muons are given in Table V.1. Because of the limitation of space, only two incident energies $k = 20$ GeV and $k = 200$ GeV are shown. The cross sections at large angles are also given because they are important background for the heavy lepton experiment. Tables V.1 A, B, C and D are sufficient to illustrate most of the interesting features of the energy-angle distributions of muons. We make the following comments on Table V.1:

i) From Eq. (III.5) with X given by (III.76) we see that the width at half height is roughly at $\theta = m/p$, when the form factor is equal to unity. As t_{\min} increases, the nuclear form factors make this width smaller and the cross section falls off much faster than θ^{-4} at large angles. From the approximate expression of t_{\min} given in Eqs. (B.2) and (B.3), we see that the forward peak as a function of ℓ gets narrower as $m^2/[kx(1-x)]$ is increased.

ii) The total $d\sigma/d\Omega dp$ from a Be target can be obtained approximately from "Be Coherent" + "Be Quasielastic" + $9 \times$ "Proton Inelastic". The "Proton Inelastic" is the contribution from the meson production parts of W_1 and W_2 given by Eqs. (B.58) and (B.59). There are four protons and five neutrons in Be.

The meson production parts of neutron form factors are slightly smaller (Kendall, 1972)⁸¹ than those of proton, therefore $9 \times$ "Proton Inelastic" would give a slight over-estimate of the cross section. For "Be Coherent" we have used the simple form factor given by Eq. (B.49) instead of the more accurate ones given by Eqs. (B.45), (B.46), (B.50) and (B.51). For small angles the two kinds of form factors give almost identical results but at large angles the cross section given by the latter is much smaller because of the exponential factors in the form factors. However, at large angles the coherent cross section is negligible compared with quasi-elastic and the meson production parts of the form factors.

iii) At large angles "Proton Elastic" is comparable to "Proton Inelastic", even though at smaller angles the latter is negligible compared with the former.

iv) The effect of the Pauli exclusion principle can be obtained by

$$\text{Pauli Suppression} = \frac{\text{"Be Quasielastic"}}{4 \times \text{"Proton Elastic"} + 5 \times \text{"Neutron Elastic"}}$$

This ratio is almost zero at small angles and unity at large angles.

v) At large angles the magnetic form factor of the proton dominates the cross section because the ratio of the cross sections from "Proton Elastic" to "Neutron Elastic" is roughly given by the ratio $(\mu_p/\mu_n)^2 = (2.79/1.91)^2 = 2.13$.

vi) Tables VI.C and VI.D give the momentum distributions of muons at angles $\theta = 0, 0.1$ and 0.2 radians. We see that at $\theta = 0$, there are more high energy particles than low energy ones whereas at $\theta = 0.1$ and 0.2 , the opposite is true. The entries "0.0" in the cross sections mean that they are not kinematically allowed. Since we have ignored the Fermi motion in evaluating "Be Quasielastic", the nonphysical regions of "Be Quasielastic" is identical to those of proton elastic. If Fermi motion is properly taken into account these zeroes will be replaced by some finite numbers.

In Table V.2, the energy angle distribution of heavy leptons are given. We note that the width at half height is roughly at $p\theta/m \approx 0.4$ for $m = 4$ and 6 compared with $p\theta/m \approx 0.8 \sim 0.9$ for the muon production at $k = 200$. For production of very heavy particles, the coherent production is small compared with the incoherent production and the Pauli suppression is negligible.

C. Energy Distribution

In Table V.3, the numerical values of $d\sigma/dp$ are given. The values of p chosen are

$$p = p_{\min} + N(p_{\max} - p_{\min})^{0.1}$$

where $N = 0.1, 0.3, 0.5, 0.7$ and 0.9 , and p_{\max} and p_{\min} are obtained from Eq. (V.7) using $m_i = m_f = Am_p$. The important thing to notice is that for muons, these distributions are almost flat with a slight dip in the middle and both ends. For heavy leptons, the distributions are still quite monotonous except a slight bulge near the middle.

D. Total Cross Sections

The total cross sections are given in Table V.4 and Table V.5. "Be Total" in Table V.4 is calculated by the approximate formula:

$$\text{"Be Total"} = \text{"Be Coherent"} + \text{"Be Quasielastic"} + 9 \times \text{"Proton Inelastic"}.$$

It was a surprise to us to find out the the "Proton Inelastic" is so unimportant compared with "Proton Elastic" even for production of very heavy leptons ($m = 20$ GeV) at very high energy ($k = 2000$ GeV). The ratio of the two contributions is roughly 1/3 according to Table V.5. Table V.4 covers the energy range of "Positron-Electron-Proton" colliding beam machine (PEP) being proposed by SLAC and LBL.

VI. ACKNOWLEDGMENTS

Dr. K. J. Kim participated in the early stage of this work, and his contributions are acknowledged in many places in the text. Van S. Whitis did much of the programming for the muon and heavy lepton productions for me in 1965 and 1966. Part of his work was incorporated in the present work. Hills Lee helped greatly in debugging many of our computer programs. Dr. D. Tompkins read the earlier version of the manuscript and suggested numerous improvements. The earlier manuscript of this paper dealt mostly with pair production of muons and heavy leptons, and only very crude treatments were given for electron pair production and bremsstrahlung. The fairly comprehensive treatment of the latter two subjects given in this paper was prompted by an anonymous referee who insisted that they should be treated more thoroughly. I am pleased in the end because these seemingly well known subjects have indeed many uncertainties in practical application. I hope this paper clarified many of them. The author wishes to thank Dr. William T. Toner of Rutherford Laboratory and Dr. Hartwig Spitzer of DESY for pointing out errors in the manuscript.

APPENDIX A

Minimum Momentum Transfer

Let us consider a general interaction shown in Fig. A.1 and define a momentum transfer squared t as:

$$t = -(p_1 - p_3)^2 = -(p_4 - p_2)^2. \quad (\text{A.1})$$

Let us further define

$$p_1^2 = M_1^2, \quad p_2^2 = M_2^2, \quad p_3^2 = (h_1 + h_2 + \dots)^2 = M_3^2$$

$$p_4^2 = (g_1 + g_2 + \dots)^2 = M_4^2 \quad \text{and} \quad s = (p_1 + p_2)^2 = (p_3 + p_4)^2.$$

t is minimum when \vec{p}_3 is parallel to \vec{p}_1 , hence in the laboratory system we have

$$t_{\min} = 2E_1E_3 - 2p_1p_3 - M_1^2 - M_3^2 = 2M_2E_4 - M_2^2 - M_4^2$$

$$= 2M_2(E_1 - E_3) - (M_4^2 - M_2^2). \quad (\text{A.2})$$

Solving Eq. (A.2) for E_3 and substituting its value back into Eq. (A.2), we obtain

$$t_{\min} = s^{-1} \left[s(p_1 \cdot p_2 - M_4^2) + (p_1 \cdot p_2 + M_2^2) (M_4^2 - M_3^2) \right. \\ \left. - \left\{ (p_1 \cdot p_2)^2 - M_1^2 M_2^2 \right\}^{1/2} \left\{ (s + M_3^2 - M_4^2)^2 - 4s M_3^2 \right\}^{1/2} \right]. \quad (\text{A.3})$$

This expression is exact, but it expresses a small number by a difference of two big numbers. Let us obtain various approximate expressions for t_{\min} in the following:

Case 1: $s \gg M_1^2, M_2^2, M_3^2, M_4^2.$ (A.4)

Expanding by Taylor series the square root terms in Eq. (A.3) up to $(M_i^2/s)^3$, we obtain

$$t_{\min} \approx s^{-1} \left[(M_4^2 - M_2^2)(M_3^2 - M_1^2) + s^{-1} (M_3^2 + M_4^2 - M_1^2 - M_2^2)(M_3^2 M_4^2 - M_1^2 M_2^2) \right]. \quad (\text{A.5})$$

This equation shows that:

$$\text{a. } t_{\min} = 0 \text{ if } M_1^2 = M_3^2 \text{ and } M_2^2 = M_4^2. \quad (\text{A.6})$$

$$\text{b. } t_{\min} \approx s^{-2} M_2^2 (M_3^2 - M_1^2)^2 \text{ if } M_2^2 = M_4^2 \text{ and } M_3^2 \neq M_1^2. \quad (\text{A.6})$$

$$\text{c. } t_{\min} \approx s^{-1} (M_4^2 - M_2^2)(M_3^2 - M_1^2) \text{ if } M_2^2 \neq M_4^2 \text{ and } M_3^2 \neq M_1^2. \quad (\text{A.7})$$

Comparing (A.6) with (A.7) we can understand why the deep inelastic nucleon form factors contribute so little to the total production cross section of the heavy lepton pair. In other words, from the kinematical consideration alone we can understand why nature does not like to have the target fragmentation and the projectile fragmentation simultaneously.

Case 2: Photopair production from a heavy nuclei.

$$M_1^2 = 0, \quad M_3^2 \geq 4m^2,$$

$$E_1 = k \gg M_3, \quad k \gg M_4 - M_2, \quad \text{and} \quad M_2 \gg M_4 - M_2.$$

When the target is a proton and the laboratory incident energy is more than a few GeV, Eq. (A.4) can easily be satisfied. However when the target is a heavy nuclei, s is often comparable to M_2^2 and M_4^2 in magnitude and the result of case 1 may not be used. However under the condition specified above, we can show that

$$t_{\min} \approx \frac{M_3^4}{4k^2} + \frac{M_3^2(M_4 - M_2)}{k}. \quad (\text{A.8})$$

This relation can be derived in the following way: In the center-of-mass system, we have

$$t_{\min} = -(k - p_3)_{\min}^2 = -M_3^2 + 2k(\tilde{E}_3 - \tilde{p}_3). \quad (\text{A.9})$$

Expanding p_3 by Taylor series we have

$$\tilde{p}_3 \approx \tilde{E}_3 \left(1 - \frac{M_3^2}{2\tilde{E}_3^2} + \frac{M_3^4}{8\tilde{E}_3^4} \right).$$

Hence

$$t_{\min} \approx M_3^2(k - \tilde{E}_3)/\tilde{E}_3 + M_3^4\tilde{k}/(4\tilde{E}_3^3). \quad (\text{A.10})$$

Substituting $\tilde{k} = k \cdot (p_2 + k)/\sqrt{s} = M_2 k/\sqrt{s}$ and $\tilde{E}_3 = p_3 \cdot (p_4 + p_3)/\sqrt{s} = M_2 \tilde{k}/\sqrt{s} + \frac{1}{2}(M_2^2 - M_4^2 + M_3^2)/\sqrt{s}$ into (A.10), we obtain Eq. (A.8).

Case 3: Electroproduction. In this case p_1 and p_3 denote the initial and final electrons respectively, hence $M_1 = M_3 = m_e$ and

$$t_{\min} = (|\vec{p}_1| - |\vec{p}_3|)^2 - (E_1 - E_3)^2 = 2(E_1 E_3 - |\vec{p}_1| |\vec{p}_3| - m_e^2).$$

Assuming $E_1 \gg m_e$ and $E_3 \gg m_e$, we have

$$t_{\min} \approx m_e^2(E_1 - E_3)^2/(E_1 E_3). \quad (\text{A.11})$$

We have obtained t_{\min} in the above assuming M_3 is fixed and \vec{p}_3 comes out in the forward direction. In the pair production experiment where only one of the pair of particles is detected at a finite angle, t_{\min} is given by Eq. (II.9). The approximate expression for this t_{\min} is derived in Appendix A of Kim and Tsai (1973) and the result is given in Eqs. (B.2) and (B.3) of Appendix B.

APPENDIX B

Atomic and Nuclear Form Factors

W_1 and W_2 are normalized such that the cross section for the electron scattering from the target is given by (mass of electron ignored):

$$\frac{d\sigma(e + Z \rightarrow e' + \text{anything})}{d\Omega' dE'} = \frac{\alpha^2 \cos^2 \theta/2}{4 E^2 \sin \theta/2} \left[W_2 + 2 \tan^2 \frac{\theta}{2} W_1 \right]. \quad (\text{B.1})$$

Since the integration with respect to t in Eqs. (II.7) and (II.8) is dominated by t very close to t_{\min} , the value of t_{\min} tells us what form factors need to be considered. Roughly speaking, if t_{\min}^{-1} is comparable to the atomic radius squared, then we have to consider the atomic form factor; if t_{\min}^{-1} is comparable to the nuclear radius squared then we have to consider the elastic nuclear form factors; if t_{\min}^{-1} is comparable to the internucleon distance within a nucleus, then we have to deal with the quasielastic form factors; if $t_{\min}^{1/2}$ is larger than twice the Fermi momentum of the nucleons within the nucleus, then we can ignore the Pauli suppression; if t_{\min} is so large that the elastic nucleon form factors are much less than unity, then the meson production form factors should be considered. There are tremendous cancellations among different terms in Eq. (II.9) for the expression of t_{\min} . An approximate expression for t_{\min} is (see Appendix A of Kim and Tsai⁴³, 1973):

$$t_{\min} \approx t'_{\min} + 2\Delta (t'_{\min})^{1/2}, \quad (\text{B.2})$$

where

$$t'_{\min} = \left(\frac{k \cdot p}{k - E} \right)^2 \approx \frac{m^4 (1+l)^2}{4k^2 x^2 (1-x)^2}, \quad (\text{B.3})$$

with $\gamma = E/m$, $\ell = \gamma^2 \theta^2$, $x = E/k$, and $\Delta = (m_f^2 - m_i^2)/(2m_i)$. This approximate expression for t_{\min} can be derived under the conditions:

$$(E \text{ and } k - E) \gg [(k \cdot p)^{1/2}, k \cdot p/m_i, m \text{ and } \Delta]. \quad (\text{B.4})$$

From Eqs. (B.2) and (B.3), we observe the following:

(i) Pair-production cross section accompanied by the target excitation is greatly suppressed due to the second term in Eq. (B.2).

(ii) t_{\min} is smallest when $\Delta = 0$, $\theta = 0$ and $x = 1/2$. Hence the true minimum value of t is

$$t_{\min}(\Delta = 0, \theta = 0, x = 1/2) = 4m^4/k^2.$$

(iii) t_{\min} is independent of m^2 if the transverse momentum of the detected lepton is much larger than its mass (i.e., $\ell \gg 1$).

(iv) For electron pair production, the exact expression for t_{\min} given by Eq. (II.9) can not be used in the energy and angular range we are interested because of the round off errors of the computer. In all of our numerical calculations, except when dealing with electrons, we use exact expressions for t_{\min} . The approximate expression for t_{\min} given by Eqs. (B.2) and (B.3) is very accurate when we are dealing with electrons.

We give in the following expressions for W_1 and W_2 used in our calculation.

1. Atomic Form Factors

The existence of atomic electrons outside a nucleus has two effects: 1.) The nuclear Coulomb field is screened by these electrons so that its effective strength is reduced; 2.) Atomic electrons also serve as the targets from which the scattering takes place. For pair production of muons or heavier particles, the existence of atomic electrons can be ignored completely because 1.) t_{\min}^{-1} is much smaller than the square of the atomic radius hence the screening effect is

negligible and 2.) the threshold energy required to produce a pair of heavy particles from an atomic electron is too high. For example from Eq. (V.9) we see that the minimum photon energy required to produce a muon pair from an atomic electron is 40 GeV. The existence of atomic electrons can also be ignored in the electron pair production at large angles where t_{\min} is such that the screening becomes negligible and kinematics, see Eq. (V.4), is such that the production in electron field is impossible. Thus only for electron pair production near forward angle need we consider the atomic form factors.

When momentum transfer is small compared with the electron mass, we can ignore W_1 compared with W_2 . W_2 for an atom consists of two parts: elastic and inelastic. Let $\psi_0(r_1 \dots r_z)$ be the ground state wave function of the atom and $\psi_n(r_1 \dots r_z)$ be the wave function for the nth excited state. Let us decompose W_2 into elastic and inelastic parts:

$$W_2(t, m_f^2) = 2m_i \delta(m_f^2 - m_i^2) G_2^{\text{el}}(t) + W_2^{\text{inel}}(t, m_f^2). \quad (\text{B.5})$$

The elastic part is

$$G_2^{\text{el}}(t) = (Z - F(t))^2, \quad (\text{B.6})$$

where

$$F(t) = \int |\psi_0(r_1 \dots r_z)|^2 \prod_{i=1}^z \exp(i\vec{q} \cdot \vec{r}_i) d^3r_1 \dots d^3r_z. \quad (\text{B.7})$$

The inelastic part is

$$W_2^{\text{inel}}(t, m_f^2) = \left| \sum_{n \neq 0} \int \psi_{(n)}^*(r_1 \dots r_z) \sum_{j=1}^z \exp(i\vec{q} \cdot \vec{r}_j) \psi_0(r_1 \dots r_z) d^3r_1 \dots d^3r_z \right|^2 \delta(E_n - E_0 - q_0), \quad (\text{B.8})$$

where $t = \vec{q}^2$ and $m_f^2 = m_i^2 + 2q_0 m_i$.

Equations (B.5 through B.8) can be obtained by comparing the expressions for the cross section given by (B.1) with the expression for the cross sections of fast electron-atomic scattering given for example in Mott and Massay's book.⁷¹

Two things should be mentioned about (B.8): 1.) If we include the ground state ψ_0 , then ψ_n 's form a complete set of states, hence from the closure theorem we have

$$\int W_2^{\text{inel}}(t, m_f^2) dq_0 \equiv G_2^{\text{inel}}(t)$$

$$= Z - |F|^2 + \int |\psi_0(r_1 \dots r_z)|^2 \sum_{j \neq i}^z \exp i \vec{q} \cdot (\vec{r}_i - \vec{r}_j) d^3 r_1 \dots d^3 r_z. \quad (\text{B.9})$$

2.) Since we are treating the atomic system nonrelativistically, we can identify q_0 with Δ defined previously. If electrons were free, then t and q_0 would be related by $q_0 = t/(2m_e)$. For bound electrons, we expect $W_2^{\text{inel}}(t, m_f^2)$ to have a quasielastic peak at $q_0 = t/(2m_e)$. Now we are interested in $t'_{\text{min}} \ll m_e^2$, hence the second term in Eq. (B.2) can be ignored compared with the first term even though we are dealing with the inelastic processes. If we approximate $W_2^{\text{inel}}(t, m_f^2)$ by a δ function at the quasielastic peak, we may write

$$W_2^{\text{inel}}(t, m_f^2) = 2 m_e \delta(m_f^2 - m_e^2) G_2^{\text{inel}}(t), \quad (\text{B.10})$$

where $G_2^{\text{inel}}(t)$ is given by (B.9).

$G_2^{\text{el}}(t)$ can be regarded as the form factor associated with the scattering from a screened Coulomb field of nucleus, whereas $G_2^{\text{inel}}(t)$ can be regarded as the form factor associated with the scattering from electron field screened by the nucleus. From (B.6), (B.7) and (B.9), we see immediately the following

properties:

$$\begin{aligned}
 F(\infty) = 0, \quad G_2^{\text{el}}(\infty) = Z^2, \quad G_2^{\text{inel}}(\infty) = Z, \\
 F(0) = Z, \quad G_2^{\text{el}}(0) = 0, \quad G_2^{\text{inel}}(0) = 0.
 \end{aligned}
 \tag{B.11}$$

$G_2^{\text{el}}(t)$ and $G_2^{\text{inel}}(t)$ can be calculated from the ground state wave function ψ_0 of an atom. For hydrogen atom ψ_0 is well known, hence these form factors can be calculated readily. For heavy atoms ψ_0 obtained from Thomas-Fermi method is used. When Z is small, the atomic form factors are calculated by Hartree-Fock method. A good reference to these calculations can be found in International Tables for X-Ray Crystallography, Vol.III.⁷² In these Tables the values of $F(q)$ for various elements are given numerically up to $q = 1.3 \times 4 \pi \text{\AA}^{-1} = 1.3 \times 24.797$ KeV, whereas we need to know the values of $F(q)$ up to $q = m_e = 511$ KeV in most of our calculations. Fortunately, $F(q)$ is small compared with Z above the maximum value of q given in the Tables and we are interested in $|Z - F(q)|^2$ in our calculations. Hence our calculation is not very sensitive to the values of $F(q)$ not tabulated in the Tables. When q is large, we expect $F(q)$ is determined by the K shell electrons, which can be represented by hydrogen-like wave function in the 1s state. We have used hydrogen like $F(q)$ in the region where it is not tabulated. In the following we give details of various atomic form factors used in our calculation.

A. Hydrogen Atom ($Z = 1$)

Since there is only one electron in the hydrogen atom, the last term in Eq. (B.9) is absent. Using the ground state wave function of a hydrogen atom

$$\psi_0 = (\pi a_0^3)^{-1/2} e^{-r/a_0},$$

where $a_0 = 137/m_e$ is the Bohr radius, we obtain from (B.7), (B.6) and (B.9),

$$F(t) = (a_0^2 t/4 + 1)^{-2}, \quad (\text{B.12})$$

$$G_2^{\text{el}}(t) = (1 - F(t))^2, \quad (\text{B.13})$$

and

$$G_2^{\text{inel}}(t) = 1 - |F(t)|^2. \quad (\text{B.14})$$

B. He Atom ($Z = 2$)

Knasel⁴⁷ investigated the total pair production cross section from He atom in detail. He used two kinds of He wave functions, the radially correlated and the uncorrelated models of Shull and Löwdin.⁴⁶ The numerical difference in the total cross sections between the two models is at most .2%, thus we shall use the simpler version, the uncorrelated model to calculate various quantities. The wave function for the uncorrelated model is

$$\psi_0 = N' \exp[-\eta (r_1 + r_2)/a_0], \quad (\text{B.15})$$

where N' is the normalization factor, $\eta = 1.6875$ and a_0 is the Bohr radius, $a_0 = (\alpha m_e)^{-1}$.

Substituting (B.15) into (B.7) and (B.9) we obtain the elastic and inelastic atomic factors respectively:

$$G_2^{\text{el}} = (Z - F(t))^2 \quad (\text{B.16})$$

and

$$G_2^{\text{inel}} = Z - (F(t))^2/Z, \quad (\text{B.17})$$

where

$$F(t) = Z/[1 + t a_0^2/(4\eta^2)]^2. \quad (\text{B.18})$$

Letting $Z = 1$ and $\eta = 1$, we obtain the hydrogen form factors. Hence the formulas obtained for pair production and bremsstrahlung for He can be used to calculate the corresponding quantities for hydrogen by changing these parameters.

C. Light Z Elements ($Z = 3$ to $Z = 7$)

The elastic atomic form factors for all elements are given in the international table⁷² up to the value $q = 1.3 \times (24.8 \text{ KeV})$. In Table B.1 the values of $F(q)$ for elements $Z = 3$ to 7 are shown. The values of $F(q)$ beyond $q = 1.3 \times (24.8 \text{ KeV})$ can be obtained by using an analytic form:

$$F(q) = F(1.3) (1 + 1.3^2 c)^2 / (1 + tc)^2, \quad (\text{B.19})$$

where

$$c = a_0^2 / (4Z^2) = 11.05518 / Z^2 \text{ in units of } (24.8 \text{ KeV})^{-2}.$$

This form factor corresponds to the atomic form factor of 1s state.

There is no convenient table for the inelastic form factors. Also it is rather inconvenient to use numerical tables for the elastic form factors to compute various quantities of interest. Therefore we determine first what is the element with the smallest Z for which the Thomas-Fermi method still yields a reasonably accurate result. To this end, we compute the radiation logarithm defined by

$$L_{\text{rad}} \equiv \left[\phi_1(0) - \frac{4}{3} \ln Z \right] \quad (\text{B.20})$$

$$= 1 + \int_0^m e [1 - F(q)/Z]^2 q^{-1} dq, \quad (\text{B.20}')$$

where the function $\phi_1(0)$ is defined in (III.14). The Thomas-Fermi-Moliere

(TFM) model, which will be treated in the next section, gives

$$L_{\text{rad}}(\text{TFM}) = \ln(184.15 Z^{-1/3}) . \quad (\text{B.21})$$

In Table B.2, the numerical values of $L_{\text{rad}}(\text{TFM})$ and L_{rad} calculated using Table B.1 and Eq. (B.19) are given for elements with $Z = 3$ to $Z = 7$. The entries labeled $L_{\text{rad}}(c \rightarrow 2c)$ are calculated similarly to L_{rad} except that the parameter c in Eq. (B.19) is replaced by $2c$. This is done to check how sensitively L_{rad} is dependent upon the values of $F(q)$ for large values of q . By comparing the values of $L_{\text{rad}}(\text{TFM})$, L_{rad} and $L_{\text{rad}}(c \rightarrow 2c)$ in Table B.2, we conclude that L_{rad} is quite insensitive to the values of $F(q)$ for $q > 1.3 \times (24.8 \text{ KeV})$ and also that the Thomas-Fermi-Moliere method can be safely used even for $B(Z = 5)$. Since L_{rad} is used for the definition of radiation length, Eq. (III.66), we also give L_{rad} (Best estimate) which represents the best estimate of this quantity to be used in all the rest of the calculations.

Next let us consider the inelastic atomic form factors. Since we have concluded in the above that TFM model is applicable for elements with $Z \geq 5$ for elastic form factors we shall assume that we can also use it to calculate the inelastic form factors when $Z \geq 5$. The radiation logarithm for the inelastic form factor is defined by

$$L'_{\text{rad}} \equiv \frac{1}{4} \left[\psi_1(0) - \frac{8}{3} \ln Z \right] \quad (\text{B.22})$$

$$= 1 + \frac{1}{2} \int_0^{m_e^2} Z^{-1} G_2^{\text{inel}}(t) t^{-1} dt , \quad (\text{B.22}')$$

where the function $\psi_1(0)$ is defined in (III.16). The Thomas-Fermi-Moliere (TFM) model, which will be treated in the next section, gives

$$L'_{\text{rad}}(\text{TFM}) = \ln(1194 A^{-2/3}) . \quad (\text{B.23})$$

L'_{rad} for H and He can be calculated using Eqs. (III.35) and (B.22). L'_{rad} for Li ($Z = 3$) and Be ($Z = 4$) can be obtained from the interpolation between its values for He ($Z = 2$) and B ($Z = 5$), the results are given in Table B.2.

The elastic and inelastic radiation logarithms, L_{rad} and L'_{rad} , determine completely the behavior of radiation problems in the complete screening limit. Since all atomic models give identical results for the no screening limit, we do not have any problem in this limit. In the intermediate screening limit, the behavior of the functions X_{el} , X_{inel} , $\varphi_1(\gamma)$, $\varphi_2(\gamma)$, $\psi_1(\epsilon)$ and $\psi_2(\epsilon)$ for Li and Be must lie somewhere between those for He and B. This problem is discussed in Section III.4.

D. Thomas Fermi Model

Let $V(r)$ be the electrostatic potential at a point \vec{r} from an atomic nucleus, then

$$V(r) = -\alpha \int \left(\frac{Z}{r} - \sum_{n=1}^Z \frac{1}{|\vec{r} - \vec{r}_n|} \right) |\psi_0(\vec{r}_1 \dots \vec{r}_Z)|^2 dV_1 \dots dV_Z$$

$$\equiv -\frac{\alpha Z}{r} \phi(x), \quad (\text{B.24})$$

where $x = r/a$ with $a = 121Z^{-1/3}/m_e$. $\phi(x)$ is the screening function, which plays a central role in Thomas-Fermi method.⁷¹ $\phi(x)$ is tabulated by Fermi⁷¹ (Mott, 1965). An approximate analytical expression representing $\phi(x)$ is given by Moliere⁷⁰ (1947):

$$\phi(x) = \sum_{i=1}^3 \alpha_i e^{-b_i x}, \quad (\text{B.25})$$

where

$$\begin{aligned} \alpha_1 &= 0.1, & \alpha_2 &= 0.55, & \alpha_3 &= 0.35 \\ b_1 &= 6.0, & b_2 &= 1.20, & b_3 &= 0.30. \end{aligned}$$

Multiplying $e^{i\vec{q} \cdot \vec{r}}$ on both sides of (B.24) and integrating it with respect to d^3r , and squaring the whole thing, we obtain

$$G_2^{\text{el}}(t) = Z^2 t \left| \int_0^\infty \phi(x) \sin qr \, dr \right|^2 \quad (\text{B.26})$$

Using Moliere representation, (B.25), we have

$$G_2^{\text{el}}(t) = Z^2 t^2 \left| \sum_{i=1}^3 \alpha_i (t + (b_i/a)^2)^{-1} \right|^2, \quad (\text{B.27})$$

where

$$a = 121 Z^{-1/3} / m_e.$$

Heisenberg⁷⁴ (1931) showed that the inelastic form factor can also be expressed in terms of the screening function $\phi(x)$ as follows:

$$G_2^{\text{inel}}(t) = Z \left(1 - \int_0^{x_0} x^2 \left[\left(\frac{\phi(x)}{x} \right)^{1/2} - \nu \right]^2 \left[\left(\frac{\phi(x)}{x} \right)^{1/2} + \frac{\nu}{2} \right] dx \right), \quad (\text{B.28})$$

where $\nu = q 455 \text{ m}^{-1} Z^{-2/3}$ and x_0 is the solution of $(\phi(x_0)/x_0)^{1/2} = \nu$. Let us give a simple derivation which makes the physical meaning of (B.28) transparent.

If the electrons were completely free and there is no Pauli exclusion principle, then we expect $G_2^{\text{inel}}(t) = Z$. We now show that the factor multiplying Z in (B.28) represents the suppression due to Pauli exclusion principle. Let us use the symbol P to represent the momentum of an electron in the atom. For a neutral atom a bound electron must satisfy $P^2/2m_e + V(r) < 0$, hence the maximum momentum denoted by P_0 is

$$P_0 = \left[-2m_e V(r) \right]^{1/2}. \quad (\text{B.29})$$

Let the electrons be uniformly distributed in the phase space. The number of electrons between r and $r + dr$ is then

$$4 \pi r^2 dr \int_{p < p_0} \frac{d^3 p}{(2\pi)^3} \times 2, \quad (\text{B.30})$$

where the factor 2 comes from the spin. Pauli exclusion principle says that not all these electrons can be excited by a photon of momentum \vec{q} because some of the final states are already occupied. The portion of the phase space excluded can be calculated by drawing two spheres, each with a radius P_0 and the distance between the two centers being q . The intersection of these two spheres is the excluded region of the phase space, whose volume can be computed easily to be

$$\frac{4\pi}{3} (P_0 - \frac{q}{2})^2 (P_0 + \frac{q}{4}) \quad \text{if} \quad P_0 > \frac{q}{2}, \quad (\text{B.31})$$

and 0 if $P_0 < \frac{q}{2}$. The volume of the sphere is of course $4\pi P_0^3/3$. Now the maximum momentum P_0 is a function of r as given by (B.29). Hence the ratio of the available phase space to the total phase space is

$$S = 1 - \int_0^{r_0} r^2 (P_0 - \frac{1}{2} q)^2 (P_0 + q/4) dr / \int_0^\infty r^2 P_0^3 dr \quad (\text{B.32})$$

where r_0 is the solution of $P_0(r_0) = q/2$. G_2^{inel} is obtained by simply multiplying (B.32) by Z . Writing P_0 in terms of $\phi(r)$, and q in terms of ν , we obtain

$$G_2^{\text{inel}}(t) = Z \left\{ 1 - D^{-1} \int_0^{x_0} x^2 \left[\left(\frac{\phi(x)}{x} \right)^{1/2} - \nu \right]^2 \left[\left(\frac{\phi(x)}{x} \right)^{1/2} + \frac{\nu}{2} \right] dx \right\}, \quad (\text{B.33})$$

where

$$D = \int_0^\infty [\phi(x)]^{3/2} x^{1/2} dx. \quad (\text{B.34})$$

Equation (B.33) is identical to Eq. (B.28) except the factor D^{-1} . D is equal to unity in the true Thomas-Fermi model, where the screening function $\phi(x)$ satisfies

$$\frac{d^2\phi}{dx^2} = \phi^{3/2} x^{-1/2}, \quad (\text{B.35})$$

and the boundary conditions $\phi(\infty) = d\phi(\infty)/dx = 0$ and $\phi(0) = 0$. Thus

$$D = \int_0^\infty \frac{d^2\phi}{dx^2} x dx = \left[x \frac{d\phi}{dx} - \phi \right]_0^\infty = 1.$$

Moliere representation of $\phi(x)$, Eq. (B.25), does not satisfy the differential equation (B.35), hence it does not yield $D = 1$, but gives $D = 0.9360$. In our calculation, we shall use Moliere representation and Eq. (B.33) instead of (B.28). The function S , defined in (B.32) and (B.33), represents the suppression factor due to Pauli exclusion principle. In Table B.3 we give the numerical values of S calculated from the true Thomas-Fermi model by Bewilogua⁷⁵ (1931) and Wheeler-Labm,¹⁴ (1939) and our calculation using the Moliere representation. In the calculation of S by a computer, the upper limit of the integration x_0 in (B.33) can be handled in the following way:

1. The integrand is set equal to zero whenever $(\phi(x)/x)^{1/2} \leq \nu$.
2. x_0 is replaced by a function of ν :

$$UP = (5\nu - 4.5 \ln \nu - 2)/(1 - \nu + 3\nu^3), \quad (\text{B.36})$$

which is slightly greater than x_0 .

From Table B.3, we see that the suppression factor S (Moliere) is always less than S (Thomas-Fermi). The difference is quite significant when ν is small. However the quantities we are interested in are quite insensitive to this difference. For example the radiation logarithm for the production in the electron

field,

$$L'_{\text{rad}} = \int_0^{m_e} S q^{-1} dq + 1, \quad (\text{B.37})$$

is equal to $\ln(1194 Z^{-2/3})$ if we use S (Moliere) whereas it is equal to $\ln(1274 Z^{-2/3})$ if we use S (Thomas-Fermi) according to Wheeler-Lamb (1956). In the original paper of Wheeler-Lamb (1939) and all the subsequent papers in which their results were quoted, the value $\ln(1440 Z^{-2/3})$ was used. Now $\ln(1194 Z^{-2/3})$ differs from $\ln(1274 Z^{-2/3})$ only by less than one percent when $Z = 1$. The percentage difference increases with Z , but the contribution of the production in the electron field becomes less important compared with the production in the nuclear field as Z is increased, hence we shall use S (Moliere) for elements with $Z \geq 5$ because it is easier to handle by a computer than S (Thomas-Fermi).

E. Simple Atomic Form Factors

Since the elastic and inelastic atomic form factors are often very complicated and their values are often known only numerically, they are not convenient to use in both theoretical and practical calculations. L. I. Schiff (1952) demonstrated that the simple elastic form factor of the type

$$G_2^{\text{el}}(t) = Z^2 \frac{a^4 t^2}{(1 + a^2 t)^2} \quad (\text{B.38})$$

can yield numerical results for $d\sigma/d\Omega_{\mathbf{k}} dk$ which are very close to the values obtained from the Thomas Fermi elastic form factor, provided the parameter "a" is chosen so that in the complete screening limit the expression for the energy angle distribution of the bremsstrahlung $d\sigma/d\Omega_{\mathbf{k}} dk$ agrees with that obtained from a more respectable calculation. By its construction this form factor will yield results which agree completely with the correct result in both the complete

screening and no screening limits. In the intermediate screening region, Schiff found that there is at most 4% difference in $d\sigma/d\Omega_k dk$ from the result using Thomas-Fermi Form factor. We found that such a simple form can also be used for the inelastic atomic factor, namely

$$G_2^{\text{inel}}(t) = Z \frac{a'^4 t^2}{(1 + a'^2 t)^2}, \quad (\text{B.39})$$

where the parameter a' is again determined such that in the limit of complete screening one obtains the desired expression for $d\sigma/d\Omega_k dk$. Compared with the results obtained from using ZS (Moliere) given by (B.33), the resultant $d\sigma/dkd\Omega_k$ agrees completely in both the complete screening and no screening cases (by its construction) and differ at most by 4% in the intermediate screening region. We also found that these simple form factors yield numerical results for $d\sigma/dkd\Omega_k$ for H and He with similar accuracy provided the parameters a and a' are chosen according to the prescription given before.

An equivalent and yet more straightforward way of evaluating the parameters a and a' in (B.38) and (B.39) is to compare the expressions for the radiation logarithms, L_{rad} and L'_{rad} . Substituting (B.38) into (B.20') and (B.39) into (B.22') we obtain

$$L_{\text{rad}} = \ln [2.718^{1/2} a m_e] \quad (\text{B.40})$$

and

$$L'_{\text{rad}} = \ln [2.718^{1/2} a' m_e] \quad (\text{B.41})$$

Using the expressions for L_{rad} and L'_{rad} for various atoms in Table B.2, we obtain the values for a and a' . For example for Thomas Fermi atom, using

Moliere representation, we obtain

$$a = 184.15 (2.718)^{-1/2} Z^{-1/3}/m_e \quad (\text{B.42})$$

$$a' = 1194 (2.718)^{-1/2} Z^{-2/3}/m_e \quad (\text{B.43})$$

The values of a and a' for light Z elements are shown in Table V.4.

Because of their simple structure and also because they give almost correct answers, these simple form factors have many practical uses. This is very similar to the situation in the elementary quantum mechanics course where the square well potential is sometimes used to illustrate the properties of some complicated practical problems.

2. Elastic Form Factors of Nucleons

We use the dipole approximation for the elastic form factors of a proton and a neutron:

$$\begin{bmatrix} W_{2p}^{el} \\ W_{1p}^{el} \\ W_{2n}^{el} \\ W_{1n}^{el} \end{bmatrix} = \frac{2m_p \delta(m_f^2 - m_i^2)}{(1 + t/.71)^4} \begin{bmatrix} (1 + 2.79^2 \tau)/(1 + \tau) \\ 2.79^2 \tau \\ 1.91^2 \tau/(1 + \tau) \\ 1.91^2 \tau/(1 + \tau) \end{bmatrix} \quad (\text{B.44})$$

where $\tau = t/(4m_p^2)$. The discussion of the accuracy of these form factors can be found in the paper by R. Wilson (1972).⁷⁶

3. Elastic Form Factors of Nuclei

The elastic form factors of a nucleus can be written as

$$W_2(t, m_f^2) = 2m_i \frac{G_e^2(t) + \tau G_m^2(t)}{1 + \tau} \delta(m_f^2 - m_i^2) \quad (\text{B.45})$$

and

$$W_1(t, m_f^2) = 2m_i \tau G_m^2(t) \delta(m_f^2 - m_i^2), \quad (\text{B.46})$$

where $\tau = t/4m_i^2$ and the electric and the magnetic form factors, G_e and G_m , are normalized such that

$$G_e^2(0) = Z^2, \quad (\text{B.47})$$

and⁷⁷ (Pratt, 1965)

$$G_m^2(0) = \frac{j+1}{3j} \left(\frac{m_i}{m_p}\right)^2 \mu_n^2, \quad (\text{B.48})$$

where j is the spin of the target and μ_n is the nuclear dipole magnetic moment in units of $e\hbar(2m_p)^{-1} \equiv$ nuclear magneton.

The nuclear magnetic dipole moment μ_n for an arbitrary nucleus is roughly given by the Schmidt value, namely between 2.79 and -1.91. Now τ is a very small number near t_{\min} especially for heavy nuclei. In our calculation we ignore W_1 and τ when dealing with nuclear targets other than the proton. The expression for W_2 used in our numerical calculation is

$$W_2(\text{coherent}) = 2m_i \delta(m_f^2 - m_i^2) Z^2 / (1 + t/d)^2, \quad (\text{B.49})$$

where $d = 6/(1.2 \text{ fermi } A^{1/3})^2 \simeq 0.164 A^{-2/3} \text{ GeV}^2$. The advantage of this expression is that the integration with respect to t can be done analytically.

For the particular case of Be nucleus ($Z = 4$, $A = 9$, $j = 3/2$ and $\mu_n = -1.18$), both the electric and magnetic form factors are known experimentally:⁷⁸ (Rand, 1965)

$$G_{\text{E}}^2_{\text{Be}} = 16 \left(1 - \frac{16}{3} t\right)^2 e^{-32t} \quad (\text{B.50})$$

and

$$G_{\text{M}}^2_{\text{Be}} = 1.18^2 \times 45 \times (1 - 25.6t + 314t^2) e^{-32t} \quad (\text{B.51})$$

We have computed the lepton production cross sections from Be target using the simple expression Eq. (B.49) and the more precise expression Eqs. (B.50) and (B.51). Because of the exponential factor in the latter, the form factors decrease much more rapidly at large t for the later than the former. However when t is so large that two form factors are appreciably different, usually the incoherent processes become more important than the coherent ones. Hence the simple expression is adequate for estimating the total yield if we add together all the contributions. The same comment can be applied to the form factors of other nuclei.

4. Inelastic Nuclear Form Factors

A nucleus when excited by an electron has many excited levels and a broad bump called quasielastic peak. In the calculation such as what we are doing, it is impractical to consider the contribution from each excited level because there are too many of them. The most logical thing to do is to draw a smooth curve representing the local average of the low lying excited levels, the giant resonance and the quasielastic peak. As far as we know, nobody ever tried to construct some smooth functions to represent the local average of actual $W_1(q^2, m_f^2)$ and $W_2(q^2, m_f^2)$ for nuclei. Fortunately in nuclear physics, the inelastic excitation function is dominated by the quasielastic peak which can be reproduced very well by the Fermi Gas Model as shown by Moniz, et al.⁷⁹ Actually in the

experiment of Moniz, et al.,⁷⁹ (1971) they measured the inelastic electron scattering from various nuclei (Li to Pb) for an electron incident energy of 500 MeV and a scattering angle of 60° . In this kinematical region, hardly any discrete level or giant resonance is visible in the spectra. It would be interesting to see whether the Fermi gas model roughly reproduces local average of the inelastic spectra at smaller scattering angles where discrete levels and the giant resonance peak as well as the quasielastic peak show up. If we assume that this is what happens in nature, we can use the expressions of $W_1(q^2, m_f^2)$ and $W_2(q^2, m_f^2)$ given by Moniz⁸⁰ (1969) with the parameters given by Moniz, et al.,⁷⁰ (1971) in the calculation of the pair production. If one is interested only in a very crude estimate of the cross section, one can make one further approximation, namely, replacing the quasielastic peak obtained by the Fermi gas model by a δ function. This is done in order to avoid doing the numerical integration with respect to m_f^2 in Eq. (II.7). Under this approximation we have $m_f = m_i = m_p$ and

$$W_2^{\text{quasi-elastic}} = C(t) \left[Z W_{2p}^{\text{el}} + (A - Z) W_{2n}^{\text{el}} \right], \quad (\text{B.52})$$

and

$$W_1^{\text{quasi-elastic}} = C(t) \left[Z W_{1p}^{\text{el}} + (A - Z) W_{1n}^{\text{el}} \right], \quad (\text{B.53})$$

where $C(t)$ is the Pauli suppression factor given by $C(t) = 1$ if $Q > 2P_F = 0.5$ GeV,

and

$$C(t) = \frac{3}{4} \frac{Q}{P_F} \left[1 - \frac{1}{12} \left(\frac{Q}{P_F} \right)^2 \right] \quad (\text{B.54})$$

if $Q < 2P_F$, with Q defined by

$$Q = t^2 / (2m_p)^2 + t. \quad (\text{B.55})$$

The approximation of the quasielastic bump by a δ function is equivalent to ignoring the Fermi motion of the nucleons within the nucleus. Since nucleons can move parallel as well as antiparallel to the direction of the incident photon, the Fermi motion does not affect the gross features of the cross section except near the threshold of the production.

5. Meson Production Form Factors

In this case we assume the target to be completely incoherent, namely

$$m_i = m_p,$$

$$W_2(\text{meson production}) = Z W_{2p}(t, m_f^2) + (A - Z) W_{2n}(t, m_f^2) \quad (\text{B.56})$$

and

$$W_1(\text{meson production}) = Z W_{1p}(t, m_f^2) + (A - Z) W_{1n}(t, m_f^2), \quad (\text{B.57})$$

where W_{2p} and W_{1p} are the meson production form factors from the proton target, and W_{2n} and W_{1n} are those from the neutron target. The shadowing effect due to the vector dominance mechanism and Pauli suppression due to the exclusion principle are ignored because from the data⁸¹ (Kendall, 1972) on e-nucleus scatterings, these effects are not important in the meson production region. From the deuteron data,⁸¹ (Kendall, 1972) the neutron cross section is slightly less than the proton cross section. The contributions to our production cross section from these form factors are in general not very significant due to the expression for t_{\min} . Therefore only a very rough estimate of this contribution will be given. The neutron and the proton are assumed to have the same cross section. For W_{1p} and W_{2p} , we use the parameterization given by suri and Yennie⁸² (1972):

$$W_{1p} = C \left[\frac{m_\rho^4 (m_f^2 - m_p^2)}{(m_\rho^2 + t)^2} 97.5 + \frac{250.6 m_p^2 (1 - x)^4}{(1 - 1.26x + 0.96x^2)} \right] \quad (\text{B.58})$$

$$W_{2p} = \frac{1}{1 + \nu^2/t} \left[W_{1p} + C \frac{56.3(m_f^2 - m_p^2) t m_\rho^2}{(m_\rho^2 + t)^2} \left\{ 1 - t/(2 m_p \nu) \right\}^2 \right] \quad (\text{B.59})$$

where

$$C = 10^{-4} / [(0.197)^2 \alpha \pi^2 8 m_p] ,$$

$$\nu = (m_f^2 - m_p^2 + t)/(2m_p) ,$$

$$x = t/(2m_p \nu + m_p^2)$$

and

$$m_\rho^2 = 0.585 .$$

K. J. Kim compared this parameterization against all the available data from SLAC-MIT ep inelastic scattering⁸³ with the help of IBM 2250 scope. The fits are excellent in the smooth region, whereas in the resonance region, the curves go through roughly the local average of the resonance peaks. Since in our calculation these curves are integrated, we expect no gross error to occur by using this fit.

REFERENCES

- Alberigi-Quaranta, A., M. DePretis, G. Marini, A. Odian, G. Stoppini, and L. Tau, 1962, *Phys. Rev. Letters* 9, 226.
- Anderson, C. D., 1932, *Phys. Rev.* 41, 405; 1933, *Phys. Rev.* 43, 491, 1933, *Phys. Rev.* 44, 406.
- Asbury, J. G., W. K. Bertram, U. Becker, P. Joos, M. Rohde, A. J. S. Smith, S. Friedlander, C. L. Jordan, and C. C. Ting, 1967, *Phys. Rev. Letters* 18, 65.
- Bergstrom, J., 1967, in MIT 1967 Summer Study (Laboratory for Nuclear Science, MIT), p. 251.
- Bernstein, D. and W.K.H. Panofsky, 1956, *Phys. Rev.* 102, 522.
- Bethe, H. A., 1934, *Proc. Camb. Phil. Soc.* 30, 524.
- Bethe, H. and J. Ashkin, 1953, in Experimental Nuclear Physics, (John Wiley and Sons, Inc., New York), Vol. I, edited by E. Segre.
- Bethe, H. A., and W. Heitler, 1934, *Proc. Roy. Soc. (London)* A146, 83.
- Bethe, H. A., and L. C. Maximon, 1954, *Phys. Rev.* 93, 768.
- Bewilogua, L., 1931, *Physik. Zeitschr.* 32, 740.
- Bjorken, J. D., 1960, unpublished.
- Bjorken, J. D., and C. H. Llewellyn Smith, 1973, *Phys. Rev.* D7, 887.
- Borsellino, A., 1947, *Nuovo Cimento* 4, 112; *Rev. Univ. Nucl. Tucuman* A6, 7 (1947).
- Cabibbo, N., G. DaPrato, G. DeFranceschi, and U. Mosco, 1962, *Phys. Rev. Letters* 9, 270; and 1962, *Phys. Rev. Letters* 9, 435.
- Davies, H., H. A. Bethe, and L. C. Maximon, 1953, *Phys. Rev.* 93, 788.
- dePagter, J. K., J. I. Friedman, G. Glass, M. Gettner, E. VonGoeler, Roy Weinstein, and A. M. Boyarski, 1967, *Phys. Rev. Letters* 17, 767.
- Diambrini Palazzi, G., 1968, *Rev. Mod. Phys.* 40, 611.
- Dirac, P. A. M., 1928, *Proc. Roy. Soc. (London)* 117, 610.
- Dovzhenko, O. I., and A. A. Pomanskii, 1963, *J. Exptl. Theoret. Phys. (USSR)* 45, 268-278. Translation 1964, *Soviet Phys. JETP* 18, 187.
- Drell, S. D., and J. D. Walecka, 1964, *Ann. Phys. (NY)* 28, 18.

- Dufner, A., S. Swanson, and Y. S. Tsai, 1966, Stanford Linear Accelerator Report No. SLAC-67.
- Early, R. A., 1973, Nucl. Instr. and Methods 109, 93.
- Eisele, R. L., D. J. Sherden, R. H. Siemann, C. K. Sinclair, D. J. Quinn, J. P. Rutherford, M. A. Shupp, 1973, Nucl. Instr. and Methods (to be published), Stanford Linear Accelerator Report SLAC PUB-1231.
- Eyges, L., 1949, Phys. Rev. 76, 264.
- Georgi, H., and S. L. Glashow, 1972, Phys. Rev. Letters 28, 1494.
- Ghizzetti, A. G., 1947, Rev. Univ. Nacl. Tucuman A6, 37 (1947).
- Hayes, S., R. Imlay, P. M. Joseph, A. S. Keiser, J. Knowles, and P. C. Stein, 1970, Phys. Rev. Letters 24, 1369.
- Hearn, A. C., Reduce 2 User's Manual, Stanford Artificial Intelligence Project, Memo AIM-133 (unpublished).
- Heisenberg, W., 1931, Physik. Zeitschr. 32, 737.
- Heitler, W., and F. Sauter, 1933, Nature 132, 892.
- Hyllerass, E. A., 1929, Zeits. f. Physik. 54, 347.
- International Tables for X-Ray Crystallography, 1962, Vol. III, Amsterdam.
- Kendall, H. W., 1972, in Proc. of 1971 International Symposium on Electron and Photon Interactions at High Energies (Laboratory of Nuclear Studies, Cornell University).
- Kim, K. J., and Y. S. Tsai, 1973, Phys. Rev. D8, 3109.
- Knasel, T. M., 1968, Phys. Rev. 171, 1643.
- Knasel, T. M., 1970, DESY 70/2 and DESY 70/3 (unpublished).
- Kramers, H. A., 1923, Phil. Mag. 46, 836.
- Landau, L., 1944, J. Phys. (USSR) 8, 201.
- Lattes, C. M. G., G. P. S. Occhialini, and C. F. Powell, 1947, Nature 160, 453.
- Lieberman, A. D., C. M. Hoffman, E. Engles, Jr., D. C. Imrie, P. G. Innocenti, R. Wilson, C. Zajde, W. A. Blanpied, D. G. Stairs, D. J. Drickey, 1969, Phys. Rev. Letters 22, 663.
- Low, F. E., 1965, Phys. Rev. Letters 14, 238.
- Masek, G., and W. K. H. Panofsky, 1956, Phys. Rev. 101, 1094.
- Miller, G., 1971, Stanford Linear Accelerator Report No., SLAC-129.
- Mo, L. W., and Y. S. Tsai, 1969, Rev. Mod. Phys. 41, 205.

- Moliere, G., 1947, Z. Naturforsch. 2A, 133.
- Moniz, E. J., 1969, Phys. Rev. 184, 1154.
- Moniz, E. J., I. Sik, R. R. Whitney, J. R. Ficenece, R. D. Kephart, and W. P. Trower, 1971, Phys. Rev. Letters 26, 445.
- Mork, K. J., 1967, Phys. Rev. 160, 1065.
- Mork, K. J., and H. Olsen, 1965, Phys. Rev. B140, 1661.
- Mott, N. F., and H.S.W. Massey, 1965, The Theory of Atomic Collisions (Oxford).
- Motz, J. W., H. A. Olsen, and H. W. Koch, 1959, Rev. Mod. Phys. 36, 881 and 1969, Rev. Mod. Phys. 41, 581.
- Neddermeyer, S. H., and C. D. Anderson, 1937, Phys. Rev. 51, 884.
- Nishina, Y., and S. Tomonaga, 1933, Proc. Phys.-Math. Soc. Japan 15, 298.
- Olsen, H., 1955, Phys. Rev. 99, 1335.
- Olsen, H., and L. C. Maximon, 1959, Phys. Rev. 114, 887.
- Oppenheimer, J. R., and M. S. Plesset, 1933, Phys. Rev. 44 53.
- Panofsky, W.K.H., and M. Phillips, 1955, Classical Electricity and Magnetism, (Addison-Wesley, Cambridge, Massachusetts).
- Perl, M. L., 1972, Stanford Linear Accelerator Report No. SLAC-PUB-1062 (unpublished).
- Pratt, R. H., J. D. Walecka, and T. A. Griffy, 1965, Nucl. Phys. 64, 677.
- Rand, R. E., R. Frosch, and M. R. Yearian, 1965, Phys. Rev. Letters 14, 234.
- Rossi, B., 1932, Naturwiss. 20, 65.
- Rossi, B., 1952, High Energy Physics (Prentice-Hall, Englewood, Cliff, New Jersey).
- Schiff, L. I., 1957, Phys. Rev. 83, 252.
- Schulz, H. D., and G. Lutz, 1968, Phys. Rev. 167, 1280.
- Shull, H., and P. Löwdin, 1956, J. Chem. Phys. 25, 1035.
- Siemann, R. H., W. W. Ash, K. Berkelman, D. L. Hartill, C. A. Lichtenstein, and R. M. Littauer, 1969, Phys. Rev. Letters 22, 421.

SLAC Users Handbook, 1971, Section C, (Stanford Linear Accelerator Center, Stanford, California).

Söding, P., J. Bartels, A. Barbaro-Galtieri, J. E. Enstrom, T. A. Lasinski, A. Rittenberg, A. H. Rosenfeld, T. G. Trippe, N. Barash-Schmidt, C. Bricman, V. Chaloupka, and M. Roos, 1972, Lawrence Berkeley Laboratory Report LBL-100.

Sommerfeld, A., 1939, Wellenmechanik (Ungar, New York), p. 551.

Street, J. C., and E. C. Stevenson, 1937, *Phys. Rev.* 52, 1033.

suri, A., and D. R. Yennie, 1972, *Ann. Phys.* 72, 243.

Swanson, S. M., 1967, *Phys. Rev.* 154, 1601.

Tsai, Y. S., 1965, *Phys. Rev.* 137, B730.

Tsai, Y. S., and Van Whitis 1966, *Phys. Rev.* 149, 1248.

Tsai, Y. S., 1971, *Phys. Rev.* D4, 2821.

Tsai, Y. S., 1971, "Radiative Corrections to Electron Scattering," Stanford Linear Accelerator Report No. SLAC-PUB-848, to be published in Electron Scattering and Nuclear Structure, edited by B. Bosco (Gordon and Breach, Inc., New York).

Überall, H., 1956, *Phys. Rev.* 103, 1055 and 1957, *Phys. Rev.* 107, 223.

Varfolomeev, A. A., and I. A. Svetolobov, 1959, *JETP* 36, 1771. Translation 1959, *Soviet Phys. JETP* 9, 1263.

Veltman, M. 1965, An IBM Programme for Symbolic Manipulation of Algebraic Expressions, Especially Feynman Diagrams (CERN, unpublished).

Von Gehlen, R., 1960, *Phys. Rev.* 118, 1455.

Votruba, V., 1948, *Phys. Rev.* 73, 1468; 1948, *Acad. Tcheque Sci. Bull. Intern.* 49, 19.

Wheeler, J. A., and W. E. Lamb, Jr., 1939, *Phys. Rev.* 55, 858; 1956, *Phys. Rev.* 101E, 1834.

Williams, E. J., and G. E. Roberts, 1940, *Nature* 145, 102.

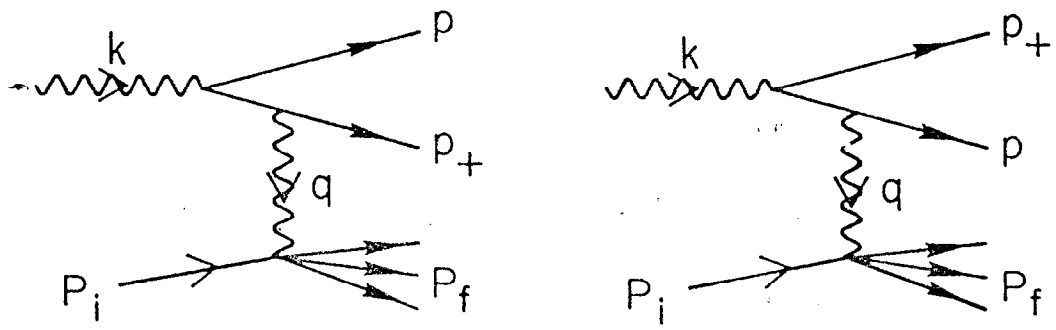
Wilson, R., 1972, in Proceedings of the 1971 International Symposium on Electron and Photon Interactions at High Energies (Laboratory of Nuclear Studies, Cornell University).

Yukawa, H. , 1935, Phys. Math. Soc. Japan 17, 48.

Zel'dovich, Ya. B. , 1962, Usp. Fiz. Nauk 78, 549. Translation 1963, Soviet
Phys. Usp. 5, 931.

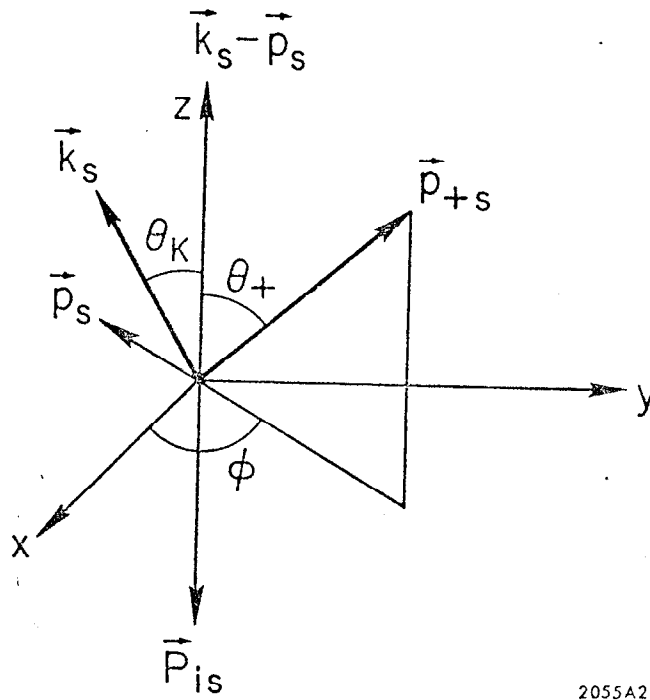
FIGURE CAPTIONS

- II.1 Feynman diagrams for the photoproduction of a lepton pair.
- II.2 The coordinate system used in the integration of the unobserved particle p_+ . The subscript s refers to the rest frame of $U = p_+ + p_f$.
- A.1 Notations used in Appendix A.



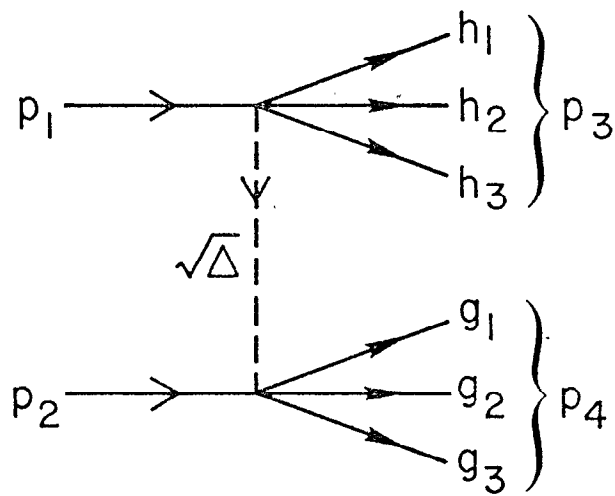
2055A1

FIG. II.1



2055A2

FIG. II-2



2130A1

FIG. A.1

TABLE III. 1

Functions $\phi_1(\gamma)$, $\phi_2(\gamma)$, $\psi_1(\epsilon)$ and $\psi_2(\epsilon)$
 for a hydrogen atom using the analytical expressions
 given by Eqs. (III. 25) through (III. 28)

γ or ϵ	$\phi_1(\gamma)$	$\phi_2(\gamma)$	$\psi_1(\epsilon)$	$\psi_2(\epsilon)$
0.00	21.2417	20.58	24.5750	23.91
0.02	21.17	20.57	24.39	23.87
0.1	20.90	20.49	23.71	23.50
0.2	20.56	20.32	22.96	22.91
0.4	19.93	19.87	21.69	21.74
0.6	19.34	19.36	20.65	20.71
0.8	18.79	18.84	19.71	19.82
1.0	18.27	18.34	19.01	19.05
1.2	17.80	17.86	18.36	18.38
1.4	17.36	17.41	17.78	17.80
1.8	16.94	16.99	17.27	17.29
1.8	16.56	16.60	16.82	16.83
2.0	16.20	16.24	16.41	16.41
4.0	13.62	13.63	13.65	13.65
6.0	12.02	12.02	12.03	12.03
8.0	10.87	10.87	10.88	10.88
10.0	9.98	9.98	9.98	9.98

TABLE III. 2

Function $\phi_1(\gamma)$, $\phi_2(\gamma)$, $\psi_1(\epsilon)$ and $\psi_2(\epsilon)$
 for a helium atom using the analytical expressions
 given by Eqs. (III. 25) through (III. 28)

γ or ϵ	$\phi_1(\gamma)$	$\phi_2(\gamma)$	$\psi_1(\epsilon)$	$\psi_2(\epsilon)$
0.00	20.0729	19.41	24.3304	23.66
0.02	20.02	19.40	24.16	23.63
0.1	19.81	19.35	23.52	23.29
0.2	19.56	19.24	22.80	22.74
0.4	19.08	18.94	21.59	21.63
0.6	18.62	18.58	20.58	20.64
0.8	18.18	18.19	19.72	19.77
1.0	17.76	17.81	18.98	19.02
1.2	17.37	17.43	18.34	18.37
1.4	16.99	17.06	17.77	17.79
1.6	16.64	16.70	17.26	17.28
1.8	16.31	16.37	16.81	16.82
2.0	15.99	16.05	16.40	16.41
4.0	13.58	13.59	13.65	13.65
6.0	12.01	12.01	12.03	12.03
8.0	10.87	10.87	10.88	10.88
10.0	9.98	9.98	9.98	9.98

TABLE III. 3

Functions $\phi_1(\gamma)$, $\phi_2(\gamma)$, $\psi_1(\epsilon)$ and $\psi_2(\epsilon)$
 for a hydrogen atom using the Bethe approximation
 given by Eqs. (III. 14) through (III. 17)

γ or ϵ	$\phi_1(\gamma)$	$\phi_2(\gamma)$	$\psi_1(\epsilon)$	$\psi_2(\epsilon)$
0.00	21.24	20.58	24.58	23.91
0.02	21.17	20.57	24.39	23.87
0.1	20.90	20.49	23.72	23.50
0.2	20.57	20.32	22.97	22.91
0.4	19.94	19.86	21.71	21.74
0.6	19.36	19.36	20.67	20.71
0.8	18.82	18.84	19.80	19.82
1.0	18.31	18.34	19.05	19.05
1.2	17.85	17.86	18.41	18.39
1.4	17.41	17.42	17.84	17.80
1.6	17.01	17.00	17.34	17.29
1.8	16.63	16.61	16.89	16.83
2.0	16.28	16.25	16.49	16.42
4.0	13.78	13.65	13.81	13.67
6.0	12.26	12.06	12.26	12.06
8.0	11.19	10.94	11.19	10.94
10.0	10.38	10.07	10.38	10.07

TABLE III.4

Screening Functions for Thomas-Fermi-Moliere Model.

$\Phi_1(\gamma)$					
γ	TFM	Analytic Simulation	Monopole Simulation	Dipole Simulation	Unscreened Target
0.0	20.863	20.863	20.863	20.863	∞
0.02	20.771	20.77	20.79	20.80	34.84
0.1	20.418	20.41	20.52	20.55	28.40
0.2	20.006	20.00	20.19	20.25	25.63
0.4	19.274	19.27	19.56	19.68	22.86
0.6	18.642	18.63	18.98	19.14	21.24
0.8	18.088	18.08	18.44	18.64	20.09
1.0	17.596	17.59	17.95	18.16	19.19
1.2	17.153	17.13	17.49	17.72	18.46
1.4	16.752	16.71	17.07	17.31	17.85
1.6	16.386	16.34	16.68	16.92	17.31
1.8	16.049	15.99	16.32	16.56	16.84
2.0	15.737	15.66	15.98	16.23	16.42

$\Phi_2(\gamma)$				
γ	TFM	Analytic Simulation	Monopole Simulation	Dipole Simulation
0.0	20.196	20.196	20.196	20.196
0.02	20.184	20.18	20.19	20.19
0.1	20.026	20.02	20.11	20.12
0.2	19.746	19.73	19.93	19.98
0.4	19.137	19.12	19.47	19.58
0.6	18.558	18.54	18.96	19.12
0.8	18.027	18.01	18.46	18.65
1.0	17.545	17.53	17.98	18.18
1.2	17.105	17.09	17.53	17.74
1.4	16.702	16.68	17.11	17.32
1.6	16.332	16.31	16.72	16.92
1.8	15.990	15.96	16.35	16.55
2.0	15.673	15.64	16.01	16.20

TABLE III.4 (cont'd)

 $\psi_1(\epsilon)$

ϵ	TFM	Analytic Simulation	Monopole Simulation	Dipole Simulation	Unscreened Target
0.0	28.34	28.34	28.34	28.34	∞
0.02	27.41	27.39	27.90	27.88	34.84
0.1	25.48	25.42	26.32	26.35	28.40
0.2	24.01	24.07	24.76	24.85	25.63
0.4	22.11	22.19	22.58	22.71	22.86
0.6	20.81	20.88	21.10	21.22	21.24
0.8	19.82	19.87	20.01	20.10	20.09
1.0	19.03	19.05	19.14	19.23	19.19
1.2	18.36	18.36	18.43	18.51	18.46
1.4	17.79	17.77	17.82	17.90	17.85
1.6	17.29	17.25	17.29	17.38	17.31
1.8	16.85	16.80	16.83	16.91	16.84
2.0	16.45	16.38	16.41	16.50	16.42

 $\psi_2(\epsilon)$

ϵ	TFM	Analytic Simulation	Monopole Simulation	Dipole Simulation
0.0	27.673	27.673	27.67	27.67
0.02	27.063	27.05	27.54	27.51
0.1	25.381	25.34	26.32	26.34
0.2	23.979	24.04	24.80	24.91
0.4	22.100	22.18	22.60	22.72
0.6	20.801	20.87	21.12	21.21
0.8	19.808	19.86	20.02	20.08
1.0	19.004	19.05	19.15	19.19
1.2	18.329	18.36	18.43	18.47
1.4	17.748	17.77	17.82	17.85
1.6	17.239	17.25	17.30	17.32
1.8	16.785	16.80	16.83	16.85
2.0	16.377	16.38	16.41	16.43

TABLE III.5

Total Electron Pair Production Cross Section

			[$\sigma(\infty) - \sigma(k)$]/ $\sigma(\infty)$ corrected for recoil already								
			k (GeV)								
Name	Z	$\sigma(\infty)$ mb*	100	10	6	2	1	0.6	0.4	0.2	0.1
H	1	20.73	.011	.028	.039	.079	.126	.174	.222	.323	.441
He	2	55.06	.012	.023	.030	.058	.091	.128	.166	.253	.367
Li	3	108.8	.004	.024	.034	.073	.113	.154	.195	.283	.391
Be	4	179.4	.003	.020	.029	.064	.101	.139	.178	.263	.370
C	6	361.5	.002	.016	.023	.053	.087	.122	.158	.238	.343
N	7	473.8	.002	.015	.022	.050	.082	.116	.151	.230	.334
Ne	10	896.1	.002	.012	.019	.044	.073	.105	.137	.213	.315
Al	13	1,443	.002	.011	.017	.040	.068	.098	.129	.202	.302
Fe	26	5,182	.001	.009	.014	.033	.057	.084	.112	.180	.275
Ca	29	6,343	.001	.009	.013	.032	.056	.082	.110	.177	.272
Sn	50	17,276	.001	.008	.012	.029	.051	.075	.102	.166	.259
W	74	34,869	.001	.007	.011	.028	.049	.073	.099	.162	.256
Pb	82	41,720	.001	.007	.011	.028	.049	.072	.098	.162	.257
U	92	50,870	.001	.007	.011	.028	.048	.072	.098	.162	.258

Recoil correction off a free electron target

$$\Delta = \frac{\sigma_{\text{no recoil}} - \sigma_{\text{recoil}}}{\sigma_{\text{no recoil}}} \quad .0004 \quad .0027 \quad .0040 \quad .0098 \quad .0169 \quad .0251 \quad .0343 \quad .0576 \quad .0954$$

* The effect of radiative corrections is not included. This can be accounted for by multiplying these numbers by a factor 1.0093 according to Mork and Olsen (1965).

TABLE III. 6

Unit Radiation Lengths of Atoms

Z = atomic number, A = atomic weight

f = Coulomb corrections Eq. (III.3), X_0 = unit radiation length

Z	A	f	$X_0(\text{gm/cm}^2)$	Z	A	f	$X_0(\text{gm/cm}^2)$
1	1.0080	6.4005 E-5	63.0470	47	107.8700	1.2850 E-1	8.9701
2	4.0026	2.5599 E-4	94.3221	48	112.4000	1.3351 E-1	8.9945
3	6.9390	5.7583 E-4	82.7559	49	114.8200	1.3859 E-1	8.8491
4	9.0122	1.0234 E-3	65.1899	50	118.6900	1.4373 E-1	8.8170
5	10.8110	1.5984 E-3	52.6868	51	121.7500	1.4893 E-1	8.7244
6	12.0111	2.3005 E-3	42.6983	52	127.6000	1.5419 E-1	8.8267
7	14.0067	3.1294 E-3	37.9879	53	126.9040	1.5951 E-1	8.4803
8	15.9994	4.0845 E-3	34.2381	54	131.3000	1.6489 E-1	8.4819
9	18.9984	5.1654 E-3	32.9303	55	132.9050	1.7032 E-1	8.3052
10	20.1830	6.3715 E-3	28.9367	56	137.3400	1.7581 E-1	8.3073
11	22.9898	7.7022 E-3	27.7362	57	138.9100	1.8134 E-1	8.1381
12	24.3120	9.1566 E-3	25.0387	58	140.1200	1.8693 E-1	7.9557
13	26.9815	1.0734 E-2	24.0111	59	140.9070	1.9256 E-1	7.7579
14	28.0860	1.2434 E-2	21.8234	60	144.2400	1.9824 E-1	7.7051
15	30.9738	1.4255 E-2	21.2053	61	145.0000	2.0396 E-1	7.5193
16	32.0640	1.6196 E-2	19.4953	62	150.3500	2.0972 E-1	7.5727
17	35.4530	1.8256 E-2	19.2783	63	151.9600	2.1553 E-1	7.4377
18	39.9480	2.0435 E-2	19.5489	64	157.2500	2.2137 E-1	7.4830
19	39.1020	2.2731 E-2	17.3167	65	158.9240	2.2725 E-1	7.3563
20	40.0800	2.5142 E-2	16.1442	66	162.5000	2.3317 E-1	7.3199
21	44.9560	2.7668 E-2	16.5455	67	164.9300	2.3911 E-1	7.2332
22	47.9000	3.0308 E-2	16.1745	68	167.2600	2.4509 E-1	7.1448
23	50.9420	3.3059 E-2	15.8425	69	168.9340	2.5110 E-1	7.0318
24	51.9960	3.5921 E-2	14.9444	70	173.0400	2.5714 E-1	7.0214
25	54.9380	3.8892 E-2	14.6393	71	174.9700	2.6321 E-1	6.9237
26	55.8470	4.1971 E-2	13.8389	72	178.4900	2.6930 E-1	6.8907
27	58.9332	4.5156 E-2	13.6174	73	180.9480	2.7541 E-1	6.8177
28	58.7100	4.8445 E-2	12.6820	74	183.8500	2.8155 E-1	6.7630
29	63.5400	5.1837 E-2	12.8616	75	186.2000	2.8771 E-1	6.6897
30	65.3700	5.5331 E-2	12.4269	76	190.2000	2.9389 E-1	6.6763
31	69.7200	5.8924 E-2	12.4734	77	192.2000	3.0008 E-1	6.5936
32	72.5900	6.2615 E-2	12.2459	78	195.0900	3.0629 E-1	6.5433
33	74.9216	6.6402 E-2	11.9401	79	196.9670	3.1252 E-1	6.4608
34	78.9600	7.0284 E-2	11.9082	80	200.5900	3.1876 E-1	6.4368
35	79.9090	7.4258 E-2	11.4230	81	204.3700	3.2502 E-1	6.4176
36	83.8000	7.8323 E-2	11.3722	82	207.1900	3.3128 E-1	6.3688
37	85.4700	8.2478 E-2	11.0272	83	208.9800	3.3756 E-1	6.2899
38	87.6200	8.6719 E-2	10.7623	84	210.0000	3.4384 E-1	6.1907
39	88.9050	9.1046 E-2	10.4101	85	210.0000	3.5013 E-1	6.0651
40	91.2200	9.5456 E-2	10.1949	86	222.0000	3.5643 E-1	6.2833
41	92.9060	9.9948 E-2	9.9225	87	223.0000	3.6273 E-1	6.1868
42	95.9400	1.0452 E-1	9.8029	88	226.0000	3.6904 E-1	6.1477
43	99.0000	1.0917 E-1	9.6881	89	227.0000	3.7535 E-1	6.0560
44	101.0700	1.1389 E-1	9.4825	90	232.0380	3.8166 E-1	6.0726
45	102.9050	1.1869 E-1	9.2654	91	231.0000	3.8797 E-1	5.9319
46	106.4000	1.2356 E-1	9.2025	92	238.0300	3.9429 E-1	5.9990

(A)

TABLE V. 1

 $d\sigma/d\Omega dp$ for Photoproduction of Muon ($\text{cm}^2/\text{GeV}/\text{sr}$)

$k = 20, m = 0.1056$	Be Coherent	Proton Elastic	Neutron Elastic	Be Quasi- Elastic	Proton Inelastic
	P = 4.0				
0	4.467D-29	3.136D-30	1.565D-32	1.556D-30	6.436D-32
0.5	3.062D-29	2.168D-30	1.165D-32	1.143D-30	4.722D-32
1.0	1.173D-29	8.719D-31	6.589D-33	5.926D-31	2.580D-32
2.0	1.373D-30	1.255D-31	2.301D-33	1.550D-31	8.537D-33
4.0	5.234D-32	7.965D-33	4.506D-34	1.946D-32	1.654D-33
7.0	1.520D-33	4.855D-34	6.173D-35	1.768D-33	2.401D-34
10.0	7.927D-35	5.454D-35	1.170D-35	2.507D-34	4.187D-35
15.0	1.368D-36	2.182D-36	8.356D-37	1.290D-35	1.927D-36
20.0	6.326D-38	2.301D-38	1.045D-38	1.443D-37	1.881D-38
	P = 8.0				
0	1.584D-28	1.116D-29	5.865D-32	5.529D-30	2.758D-31
0.5	1.189D-28	8.332D-30	4.199D-32	4.043D-30	1.952D-31
1.0	4.809D-29	3.486D-30	2.259D-32	2.083D-30	1.024D-31
2.0	5.619D-30	4.897D-31	7.751D-33	5.413D-31	3.474D-32
4.0	2.266D-31	3.060D-32	1.525D-33	6.830D-32	7.405D-33
7.0	8.609D-33	2.004D-33	2.073D-34	6.495D-33	1.180D-33
10.0	6.242D-34	2.592D-34	4.073D-35	1.029D-33	2.384D-34
15.0	1.484D-35	1.652D-35	4.746D-36	8.708D-35	2.023D-35
20.0	7.145D-37	1.087D-36	4.365D-37	6.532D-36	1.303D-36
	P = 12.0				
0	3.564D-28	2.510D-29	1.317D-31	1.243D-29	6.630D-31
0.5	2.675D-28	1.874D-29	9.433D-32	9.090D-30	4.707D-31
1.0	1.082D-28	7.842D-30	5.075D-32	4.682D-30	2.502D-31
2.0	1.264D-29	1.102D-30	1.743D-32	1.218D-30	8.731D-32
4.0	5.104D-31	6.901D-32	3.441D-33	1.541D-31	1.877D-32
7.0	1.949D-32	4.562D-33	4.729D-34	1.482D-32	2.960D-33
10.0	1.434D-33	5.997D-34	9.403D-35	2.383D-33	6.049D-34
15.0	3.561D-35	3.954D-35	1.102D-35	2.067D-34	5.360D-35
20.0	1.805D-36	2.720D-36	1.044D-36	1.610D-35	3.515D-36
	P = 16.0				
0	7.145D-28	5.014D-29	2.486D-31	2.480D-29	1.210D-30
0.5	4.897D-28	3.465D-29	1.852D-31	1.822D-29	8.979D-31
1.0	1.876D-28	1.394D-29	1.048D-31	9.447D-30	5.084D-31
2.0	2.198D-29	2.009D-30	3.668D-32	2.474D-30	1.800D-31
4.0	8.428D-31	1.287D-31	7.248D-33	3.141D-31	3.541D-32
7.0	2.538D-32	8.195D-33	1.029D-33	2.982D-32	4.993D-33
10.0	1.438D-33	9.955D-34	2.026D-34	4.523D-33	8.870D-34
15.0	2.977D-35	4.697D-35	1.570D-35	2.664D-34	4.466D-35
20.0	1.610D-36	9.891D-37	4.032D-37	5.972D-36	4.747D-37

TABLE V.1 (continued)

(B)

K = 200, m = 0.1056

\rightarrow Pe/m	Be Coherent	Proton Elastic	Neutron Elastic	Be Quasi- Elastic	Proton Inelastic
	P = 40.0				
0	5.797D-28	4.751D-29	1.570D-31	1.590D-29	4.746D-31
0.5	4.249D-28	3.441D-29	1.169D-31	1.174D-29	3.487D-31
1.0	1.843D-28	1.454D-29	6.608D-32	6.139D-30	1.908D-31
2.0	2.718D-29	2.156D-30	2.308D-32	1.632D-30	6.363D-32
4.0	1.606D-30	1.522D-31	4.550D-33	2.181D-31	1.303D-32
7.0	1.177D-31	1.295D-32	6.499D-34	2.460D-32	2.415D-33
10.0	1.934D-32	2.377D-33	1.374D-34	5.068D-33	7.080D-34
15.0	1.973D-33	3.110D-34	2.179D-35	7.939D-34	1.637D-34
20.0	3.006D-34	6.675D-35	6.249D-36	2.045D-34	5.266D-35
	P = 80.0				
0	1.889D-27	1.560D-28	5.889D-31	5.604D-29	2.031D-30
0.5	1.515D-27	1.237D-28	4.216D-31	4.118D-29	1.440D-30
1.0	6.902D-28	5.513D-29	2.267D-31	2.135D-29	7.558D-31
2.0	1.003D-28	7.988D-30	7.779D-32	5.605D-30	2.574D-31
4.0	5.802D-30	5.369D-31	1.538D-32	7.342D-31	5.891D-32
7.0	4.348D-31	4.529D-32	2.142D-33	8.025D-32	1.197D-32
10.0	7.551D-32	8.460D-33	4.406D-34	1.636D-32	3.616D-33
15.0	8.783D-33	1.168D-33	6.810D-35	2.622D-33	8.321D-34
20.0	1.587D-33	2.682D-34	1.941D-35	7.094D-34	2.657D-34
	P = 120.0				
0	4.439D-27	3.599D-28	1.325D-30	1.261D-28	4.983D-30
0.5	3.563D-27	2.845D-28	9.485D-31	9.267D-29	3.548D-30
1.0	1.615D-27	1.255D-28	5.100D-31	4.804D-29	1.885D-30
2.0	2.301D-28	1.798D-29	1.750D-31	1.261D-29	6.631D-31
4.0	1.306D-29	1.208D-30	3.462D-32	1.652D-30	1.609D-31
7.0	9.783D-31	1.019D-31	4.827D-33	1.808D-31	3.469D-32
10.0	1.699D-31	1.905D-32	9.942D-34	3.687D-32	1.073D-32
15.0	1.977D-32	2.630D-33	1.538D-34	5.911D-33	2.407D-33
20.0	3.573D-33	6.043D-34	4.383D-35	1.600D-33	7.270D-34
	P = 160.0				
0	1.069D-26	8.033D-28	2.509D-30	2.545D-28	1.038D-29
0.5	7.728D-27	5.728D-28	1.868D-30	1.879D-28	7.732D-30
1.0	3.276D-27	2.355D-28	1.056D-30	9.820D-29	4.399D-30
2.0	4.462D-28	3.451D-29	3.691D-31	2.610D-29	1.630D-30
4.0	2.570D-29	2.436D-30	7.284D-32	3.492D-30	4.043D-31
7.0	1.883D-30	2.076D-31	1.045D-32	3.951D-31	8.922D-32
10.0	3.095D-31	3.814D-32	2.221D-33	8.160D-32	2.713D-32
15.0	3.160D-32	4.999D-33	3.532D-34	1.280D-32	5.462D-33
20.0	4.825D-33	1.075D-33	1.011D-34	3.299D-33	1.455D-33

TABLE V.1 (continued)

(C)

 $k = 20, m = 0.1056$

P	Be Coherent	Proton Elastic	Neutron Elastic	Be Quasi- Elastic	Proton Inelastic
	$\Theta = 0.0$				
2	1.086D-29	7.710D-31	4.126D-33	4.204D-31	1.496D-32
4	4.467D-29	3.136D-30	1.565D-32	1.556D-30	6.436D-32
6	9.452D-29	6.640D-30	3.382D-32	3.260D-30	1.503D-31
8	1.584D-28	1.116D-29	5.865D-32	5.529D-30	2.758D-31
10	2.418D-28	1.705D-29	9.082D-32	8.496D-30	4.452D-31
12	3.564D-28	2.510D-29	1.316D-31	1.243D-29	6.630D-31
14	5.146D-28	3.614D-29	1.835D-31	1.772D-29	9.286D-31
16	7.145D-28	5.014D-29	2.486D-31	2.480D-29	1.210D-30
18	8.787D-28	6.225D-29	3.301D-31	3.373D-29	1.303D-30
	$\Theta = 0.1$				
2	3.569D-31	3.461D-32	7.272D-34	4.770D-32	2.233D-33
4	7.050D-32	1.017D-32	5.277D-34	2.367D-32	1.932D-33
6	1.732D-32	3.392D-33	2.870D-34	1.005D-32	1.345D-33
8	5.064D-33	1.308D-33	1.479D-34	4.428D-33	8.589D-34
10	1.593D-33	5.706D-34	8.150D-35	2.164D-33	5.263D-34
12	4.892D-34	2.708D-34	5.032D-35	1.166D-33	3.098D-34
14	1.311D-34	1.275D-34	3.230D-35	6.390D-34	1.560D-34
16	2.706D-35	4.290D-35	1.446D-35	2.439D-34	4.054D-35
18	4.013D-36	0.0	0.0	0.0	0.0
	$\Theta = 0.2$				
2	1.223D-32	2.258D-33	1.506D-34	6.156D-33	4.031D-34
4	8.391D-34	3.100D-34	4.398D-35	1.186D-33	1.712D-34
6	9.414D-35	6.169D-35	1.290D-35	2.797D-34	5.849D-35
8	1.348D-35	1.535D-35	4.474D-36	8.148D-35	1.884D-35
10	2.318D-36	3.659D-36	1.348D-36	2.138D-35	4.879D-36
12	4.651D-37	4.168D-37	1.726D-37	2.530D-36	4.861D-37
14	1.050D-37	0.0	0.0	0.0	0.0
16	2.606D-38	0.0	0.0	0.0	0.0
18	6.805D-39	0.0	0.0	0.0	0.0

TABLE V.1 (continued)

(D)

k = 200, m = 0.1056

P	Be Coherent	Proton Elastic	Neutron Elastic	Be Quasi- Elastic	Proton Inelastic
	$\Theta = 0.0$				
20	1.679D-28	1.326D-29	4.137D-32	4.383D-30	1.109D-31
40	5.797D-28	4.751D-29	1.570D-31	1.590D-29	4.746D-31
60	1.150D-27	9.502D-29	3.395D-31	3.312D-29	1.106D-30
80	1.889D-27	1.560D-28	5.889D-31	5.604D-29	2.031D-30
100	2.909D-27	2.389D-28	9.125D-31	8.609D-29	3.295D-30
120	4.439D-27	3.599D-28	1.325D-30	1.261D-30	4.983D-30
140	6.854D-27	5.421D-28	1.847D-30	1.804D-28	7.241D-30
160	1.069D-26	8.033D-28	2.509D-30	2.545D-28	1.038D-29
180	1.605D-26	1.099D-27	3.344D-30	3.549D-28	1.526D-29
	$\Theta = 0.1$				
20	4.868D-35	1.697D-35	2.306D-36	6.262D-35	1.177D-35
40	1.127D-36	1.192D-36	3.394D-37	6.204D-36	1.397D-36
60	6.332D-38	1.161D-37	4.753D-38	7.021D-37	1.521D-37
80	5.688D-39	3.093D-39	1.417D-39	1.946D-38	4.466D-39
100	6.688D-40	0.0	0.0	0.0	0.0
120	8.885D-41	0.0	0.0	0.0	0.0
140	1.152D-41	0.0	0.0	0.0	0.0
160	1.325D-42	0.0	0.0	0.0	0.0
	$\Theta = 0.2$				
20	4.528D-38	8.198D-38	3.412D-38	4.985D-37	7.213D-38
40	3.510D-40	0.0	0.0	0.0	0.0
60	1.257D-41	0.0	0.0	0.0	0.0
80	8.243D-43	0.0	0.0	0.0	0.0
100	7.386D-44	0.0	0.0	0.0	0.0
120	8.687D-45	0.0	0.0	0.0	0.0

TABLE V. 2

(A)

$d\sigma/d\Omega dp$ for Photoproduction of Heavy Leptons ($\text{cm}^2/\text{GeV}/\text{sr}$)

$k = 200, m = 4.0$

$P\theta/m$	Be Coherent	Proton Elastic	Neutron Elastic	Be Quasi Elastic	Proton Inelastic
$P = 40$					
0	1.093D-36	1.153D-36	3.286D-37	5.997D-36	3.993D-37
0.2	9.178D-37	1.028D-36	3.033D-37	5.437D-36	3.564D-37
0.4	5.471D-37	7.200D-37	2.326D-37	3.976D-36	2.528D-37
0.6	2.418D-37	3.897D-37	1.412D-37	2.261D-36	1.405D-37
0.8	8.650D-38	1.598D-37	6.430D-38	9.608D-37	5.915D-38
1.0	2.754D-38	4.635D-38	2.011D-38	2.860D-37	1.745D-38
$P = 80$					
0	1.136D-35	6.485D-36	1.251D-36	2.809D-35	2.509D-36
0.2	1.006D-35	6.070D-36	1.217D-36	2.676D-35	2.315D-36
0.4	6.743D-35	4.786D-36	1.069D-36	2.217D-35	1.814D-36
0.6	3.373D-36	3.62D-36	7.972D-37	1.525D-35	1.202D-36
0.8	1.337D-36	1.615D-36	4.969D-37	8.721D-36	6.693D-37
1.0	4.592D-37	7.219D-37	2.577D-37	4.166D-36	3.109D-37
$P = 120$					
0	2.553D-35	1.459D-35	2.818D-36	6.322D-35	6.322D-36
0.2	2.259D-35	1.365D-35	2.740D-36	6.019D-35	5.834D-36
0.4	1.514D-35	1.076D-35	2.405D-36	4.985D-35	4.564D-36
0.6	7.576D-36	6.880D-36	1.793D-36	3.429D-35	3.000D-36
0.8	3.006D-36	3.633D-36	1.118D-36	1.961D-35	1.649D-36
1.0	1.035D-36	1.625D-36	5.798D-37	9.3750-36	7.544D-37
$P = 160$					
0	1.720D-35	1.825D-35	5.247D-36	9.525D-35	8.233D-36
0.2	1.444D-35	1.626D-35	4.837D-36	8.627D-35	7.297D-36
0.4	8.615D-36	1.138D-35	3.700D-36	6.298D-35	5.044D-36
0.6	3.825D-36	6.158D-36	2.239D-36	3.578D-35	2.665D-36
0.8	1.380D-36	2.526D-36	1.016D-36	1.518D-35	1.034D-36
1.0	4.452D-37	7.299D-37	3.155D-37	4.497D-36	2.661D-37

TABLE V.2 (continued)

(B)

k = 200, m = 6.0

P Θ /m	Be Coherent	Proton Elastic	Neutron Elastic	Be Quasi Elastic	Proton Inelastic
P = 40					
0	1.081D-38	1.432D-38	6.412D-39	8.932D-38	5.069D-39
0.2	8.824D-39	1.021D-38	4.608D-39	6.387D-38	3.606D-39
0.4	4.885D-39	3.207D-39	1.472D-39	2.019D-38	1.131D-39
0.6	1.966D-39	2.370D-40	1.103D-40	1.500D-39	8.184D-41
P = 80					
0	1.590D-37	2.805D-37	1.081D-37	1.662D-36	1.141D-37
0.2	1.354D-37	2.451D-37	9.648D-38	1.463D-36	9.798D-38
0.4	8.199D-38	1.526D-37	6.315D-38	9.260D-37	5.920D-38
0.6	3.595D-38	5.868D-38	2.564D-38	3.629D-37	2.224D-38
0.8	1.249D-38	1.121D-38	5.095D-39	7.030D-38	4.097D-39
1.0	3.825D-39	5.809D-40	2.698D-40	3.673D-39	1.823D-40
P = 120					
0	3.560D-37	6.282D-37	2.426D-37	3.726D-36	2.702D-37
0.2	3.029D-37	5.484D-37	2.162D-37	3.275D-36	2.309D-37
0.4	1.834D-37	3.405D-37	1.411D-37	2.068D-36	1.369D-37
0.6	8.052D-38	1.305D-37	5.706D-38	8.074D-37	4.923D-38
0.8	2.808D-38	2.469D-38	1.122D-38	1.549D-37	8.167D-39
1.0	8.643D-39	1.219D-39	5.655D-40	7.702D-39	2.671D-40
P = 160					
0	1.650D-37	1.990D-37	8.970D-38	1.244D-36	4.445D-38
0.2	1.346D-37	1.387D-37	6.297D-38	8.697D-37	2.806D-38
0.4	7.480D-38	3.937D-38	1.814D-38	2.482D-37	5.333D-39
0.6	3.049D-38	1.476D-39	6.882D-40	9.345D-39	6.353D-42

TABLE V.3
 $d\sigma/dp$ (cm^2/GeV)

$m = 0.1056 \text{ GeV}$ $k = 20 \text{ GeV}$ P (GeV)	Be Coherent 10^{-32}	Proton Elastic 10^{-33}	Neutron Elastic 10^{-35}	Be Quasi- Elastic 10^{-33}	Proton Inelastic 10^{-34}
1.99	7.78	6.35	8.90	6.16	2.77
5.97	8.92	6.85	7.20	5.32	3.06
9.95	8.77	6.66	6.63	4.94	3.24
13.93	8.92	6.84	7.17	5.29	3.68
17.90	7.90	6.42	8.79	6.12	3.41
$m = 0.10566 \text{ GeV}$ $k = 200 \text{ GeV}$ P (GeV)	10^{-32}	10^{-33}	10^{-36}	10^{-34}	10^{-35}
2.00	1.49	1.16	8.92	6.72	2.10
6.00	1.34	1.09	7.23	5.51	2.29
10.00	1.29	1.04	6.66	5.10	2.46
14.00	1.43	1.11	7.22	5.51	3.04
18.00	1.61	1.17	8.90	6.72	4.54
$m = 4.0 \text{ GeV}$ $k = 200 \text{ GeV}$ P (GeV)	10^{-38}	10^{-38}	10^{-39}	10^{-37}	10^{-38}
19.5	0.10	0.14	0.60	0.08	0.04
58.5	1.85	1.91	5.63	1.00	0.72
97.5	3.03	2.50	6.48	1.23	1.04
136.5	2.09	2.05	5.87	1.06	0.93
175.5	0.21	0.33	1.36	0.20	0.10
$m = 6.0 \text{ GeV}$ $k = 200 \text{ GeV}$ P (GeV)	10^{-40}	10^{-39}	10^{-40}	10^{-39}	10^{-40}
19.2	0.14	0.00	0.00	0.00	0.00
57.5	4.11	0.56	2.43	3.45	2.06
95.8	8.06	1.30	5.31	7.84	5.18
134.2	5.30	0.78	3.34	4.80	2.94
172.5	0.47	0.00	0.00	0.00	0.00

TABLE V. 4

Total Heavy Lepton Production Cross Section (cm^2)

GeV k	Be Coherent	Proton Elastic	Neutron Elastic	Be-Quasi- Elastic	Proton Inelastic	Be Total
m = 0.105	10^{-30}	10^{-31}	10^{-33}	10^{-31}	10^{-33}	10^{-30}
20	1.611	1.267	1.546	1.081	6.114	1.774
40	2.047	1.551	1.557	1.134	6.336	2.238
100	2.579	1.926	1.563	1.171	6.044	2.750
200	2.787	2.177	1.565	1.184	5.683	2.956
m = 0.5	10^{-32}	10^{-33}	10^{-34}	10^{-33}	10^{-34}	10^{-32}
20	0.902	1.607	1.342	4.443	3.559	1.666
40	1.913	2.604	1.536	5.895	5.355	2.984
100	3.784	4.122	1.672	7.324	6.846	5.133
200	5.487	5.352	1.717	8.034	7.161	6.934
m = 1.0	10^{-33}	10^{-34}	10^{-35}	10^{-33}	10^{-34}	10^{-33}
20	0.170	0.923	1.958	0.410	0.288	0.839
40	0.797	2.293	3.070	0.814	0.728	2.266
100	3.014	5.063	4.014	1.358	1.343	5.578
200	5.857	7.698	4.442	1.703	1.664	9.057
m = 2.0	10^{-34}	10^{-35}	10^{-36}	10^{-34}	10^{-35}	10^{-34}
40	0.053	0.634	2.085	0.350	0.234	0.614
100	0.764	3.404	6.293	1.420	1.290	3.345
200	2.963	7.396	8.781	2.472	2.353	7.553
m = 4.0	10^{-36}	10^{-36}	10^{-37}	10^{-35}	10^{-36}	10^{-35}
100	0.243	0.371	1.498	0.223	0.140	0.374
200	2.856	2.758	7.990	1.432	1.131	2.735
m = 6.0	10^{-38}	10^{-38}	10^{-38}	10^{-37}	10^{-38}	10^{-36}
100	0.376	0.006	0.003	0.004	0	0
200	6.932	9.975	4.178	6.079	3.826	1.021

2130A5

TABLE V.5
Total Heavy Lepton Production Cross Section (cm^2)
from Proton at PEP Energies

Photon Energy GeV	Proton Energy	Proton Inelastic	Proton Total
m = 5			
500	4.043×10^{-36}	1.488×10^{-36}	5.531×10^{-36}
1,000	9.592×10^{-36}	2.896×10^{-36}	1.249×10^{-35}
1,500	1.404×10^{-35}	3.693×10^{-36}	1.773×10^{-35}
2,000	1.767×10^{-35}	4.189×10^{-36}	2.186×10^{-35}
m = 10			
500	2.111×10^{-38}	7.821×10^{-39}	2.893×10^{-38}
1,000	2.702×10^{-37}	1.018×10^{-37}	3.720×10^{-37}
1,500	6.325×10^{-37}	2.289×10^{-37}	8.612×10^{-37}
2,000	1.014×10^{-36}	3.480×10^{-37}	1.362×10^{-36}
m = 15			
1,000	4.563×10^{-39}	1.603×10^{-39}	6.166×10^{-39}
1,500	3.528×10^{-38}	1.267×10^{-38}	4.795×10^{-38}
2,000	8.860×10^{-38}	3.227×10^{-38}	1.209×10^{-37}
m = 20			
1,000	4.860×10^{-43}	1.619×10^{-43}	6.050×10^{-43}
1,500	6.616×10^{-40}	2.249×10^{-40}	8.865×10^{-40}
2,000	5.328×10^{-39}	1.811×10^{-39}	7.139×10^{-39}

TABLE B.1

Elastic Form Factors of Atoms $F(q)$ q in unit of $4\pi\text{\AA}^{-1} = 24.797\text{ KeV}$

q	Z=3 Li	Z=4 Be	Z=5 B	Z=6 C	Z=7 N
0.00	3.000	4.000	5.000	6.000	7.000
0.05	2.710	3.706	4.726	5.760	6.781
0.10	2.215	3.067	4.066	5.126	6.203
0.15	1.904	2.469	3.325	4.358	5.420
0.20	1.741	2.067	2.711	3.581	4.600
0.25	0.627	1.838	2.276	2.976	3.856
0.30	1.512	1.705	1.993	2.502	3.241
0.35	1.394	1.613	1.813	2.165	2.760
0.40	1.269	1.531	1.692	1.950	2.397
0.50	1.032	1.367	1.534	1.685	1.944
0.60	0.823	1.201	1.406	1.536	1.698
0.70	0.650	1.031	1.276	1.426	1.550
0.80	0.513	0.878	1.147	1.322	1.444
0.90	0.404	0.738	1.016	1.218	1.350
1.0	0.320	0.620	0.895	1.114	1.263
1.1	0.255	0.519	0.783	1.012	1.175
1.2	0.205	0.432	0.682	0.916	1.083
1.3	0.164	0.365	0.596	0.821	1.005

TABLE B.2

Radiation Logarithm

$$L_{\text{rad}} \equiv \frac{1}{2} \int_0^{m_e^2} Z^{-2} G_2^{\text{el}}(t) \frac{dt}{t} + 1 \equiv \frac{1}{4} \left[\varphi_1(0) - \frac{4}{3} \ln Z \right]$$

$$L'_{\text{rad}} \equiv \frac{1}{2} \int_0^{m_e^2} Z^{-1} G_2^{\text{inel}}(t) \frac{dt}{t} + 1 = \frac{1}{4} \left[\psi_1(0) - \frac{8}{3} \ln Z \right]$$

Z	1	2	3	4	5	6	7
	H	He	Li	Be	B	C	N
L_{rad}	5.310*	4.787*	4.738 ^a	4.705 ^a	4.663 ^a	4.606 ^a	4.544 ^a
L_{rad}^{**} (Thomas-Fermi-Moliere)	5.216	4.985	4.850	4.754	4.679	4.618	4.567
$L_{\text{rad}}(c \rightarrow 2c)$			4.742 ^b	4.715 ^b	4.680 ^b	4.631 ^b	4.576 ^b
L_{rad} (Best estimate)	5.31	4.79	4.74	4.71	4.68	4.62	4.57
$L'_{\text{rad}} \dagger\dagger$ (Thomas-Fermi-Moliere)	7.085	6.623	6.353	6.161	6.012	5.891	5.788
L'_{rad} (Best estimate)	6.144 [†]	5.621 [†]	5.805 ^c	5.924 ^c	6.012	5.891	5.788

* From Eq. (III.33).

** Using $L_{\text{rad}} = \ln(184.15 Z^{-1/3})$.

† From Eq. (III.35).

†† Using $L'_{\text{rad}} = \ln(1194 Z^{-2/3})$.

a. Using Table B.1 and Eq. (B.19).

b. Using Table B.1 and Eq. (B.19) with c replaced by 2c.

c. Interpolated between the values of He and B.

TABLE B.3

Atomic Pauli Suppression Factor S

ν	S(Thomas-Fermi)	S(Molierre)
0.00	13.8 ν	0.000
0.01	0.097	0.066
0.02	0.169	0.127
0.03	0.227	0.182
0.04	0.277	0.232
0.05	0.319	0.277
0.1	0.486	0.452
0.2	0.674	0.652
0.3	0.776	0.761
0.4	0.839	0.828
0.5	0.880	0.872
0.6	0.909	0.903
0.7	0.929	0.924
0.8	0.944	0.940
0.9	0.954	0.952
1.0	0.963	0.961

TABLE B.4

$a_{\text{H}} = 122.8/m_e$	From (B.12)
$a'_{\text{H}} = 282.4/m_e$	From (B.14)
$a_{\text{He}} = 90.8 Z^{-1/3}/m_e$	From (B.16)
$a'_{\text{He}} = 265.8 Z^{-2/3}/m_e$	From (B.17)
$a_{\text{Li}} = 100.0 Z^{-1/3}/m_e$	From Tables (B.1 and B.2)
$a'_{\text{Li}} = 418.6 Z^{-2/3}/m_e$	From linear interpolation between a'_{H} and a'_{B}
$a_{\text{Be}} = 106 Z^{-1/3}/m_e$	From Tables (B.1 and B.2)
$a'_{\text{Be}} = 571.4 Z^{-2/3}/m_e$	From linear interpolation between a'_{H} and a'_{B}
$a_{\text{B}} = 111.7 Z^{-1/3}/m_e$	Thomas-Fermi-Moliere or (Table B.1 and B.2)
$a'_{\text{B}} = 724.2 Z^{-2/3}/m_e$	Thomas-Fermi-Moliere